~~X 70 74864~~

~~CR117078~~

N71-18964

NASA CR-111853

STERILIZATION AND ENVIRONMENTAL QUALIFICATION OF A RATE-OF-TURN SENSOR FOR PLANETARY EXPLORATION MISSIONS

FINAL REPORT
AUGUST 1970

CONTRACT NO. NAS1-8885

NATIONAL AERONAUTICS AND SPACE
ADMINISTRATION
LANGLEY RESEARCH CENTER
LANGLEY STATION
HAMPTON, VIRGINIA

PREPARED BY
GENERAL ELECTRIC COMPANY
AVIONIC CONTROLS DEPARTMENT
BINGHAMTON, N.Y.

AUTHOR
J.N. RUSSELL

RESTRICTION: FOR NASA INTERNAL USE ONLY

ACD 9914

STERILIZATION AND ENVIRONMENTAL QUALIFICATION OF A RATE-OF-TURN SENSOR FOR PLANETARY EXPLORATION MISSIONS

FINAL REPORT
AUGUST 1970

CONTRACT NO. NAS1-8885

NATIONAL AERONAUTICS AND SPACE ADMINISTRATION
LANGLEY RESEARCH CENTER
LANGLEY STATION
HAMPTON, VIRGINIA

PREPARED BY
GENERAL ELECTRIC COMPANY
AVIONIC CONTROLS DEPARTMENT
BINGHAMTON, N.Y.

AUTHOR
J.N. RUSSELL

ABSTRACT

Under this contract four VYRO sensor packages were manufactured. These units were tested by a qualification test program designed to qualify the units for interplanetary probe missions. Both sterilization and environmental testing were performed on the units. This report includes discussion of each test with supporting test data, and states achievements and failures throughout the program.

TABLE OF CONTENTS

LIST OF ILLUSTRATIONS

LIST OF ILLUSTRATIONS (cont'd)

LIST OF ILLUSTRATIONS (cont'd)

LIST OF TABLES

Section I

INTRODUCTION

GENERAL DESCRIPTION

The solid-state-rate sensor (VYRO) utilizes Coriolis acceleration produced on the vibrating particles of a rectangular metal beam due to an input angular rate about the longitudinal axis of the beam to provide an output motion proportional to input angular rate. Figure 1 pictorially shows the VYRO beam as an aid in understanding its operation. The beam is supported at the nodes for the first fundamental free-free bending mode of the prizmatic beam. Through the use of piezoelectric crystals on opposite faces of the beam in the drive plane the beam is made to vibrate at its resonant frequency by using it as the frequency controlling element within an amplitude-regulated-oscillating loop. This is indicated by the drive circuits shown in the sensor functional block diagram, Figure 2. With the beam vibrating in the drive plane and with the application of an angular rate about the longitudinal axis of the beam the coriolis acceleration of the beam particles causes a small motion to occur orthoginal to the drive plane. This motion is detected by the use of a readout piezoelectric crystal mounted on the appropriate face of the beam. A fourth crystal is used on the face of the beam opposite the readout crystal for the purpose of damping the natural second-order response of the beam to a sinusoidally varying input angular rate at the separation frequency or difference between the drive and readout plane resonant frequencies.

The output from the readout crystal is amplified, demodulated and filtered to provide a d. c. output proportional to input angular rate. A canceller circuit connected to the demodulator output provides a stable null output as the sensor temperature is varied.

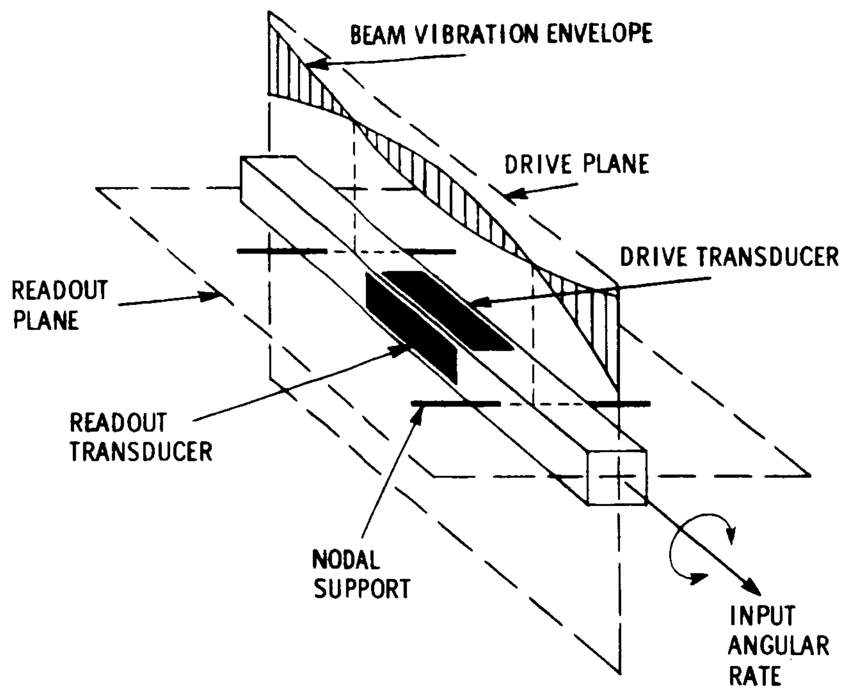

Figure 1. VYRO Principles of Operation

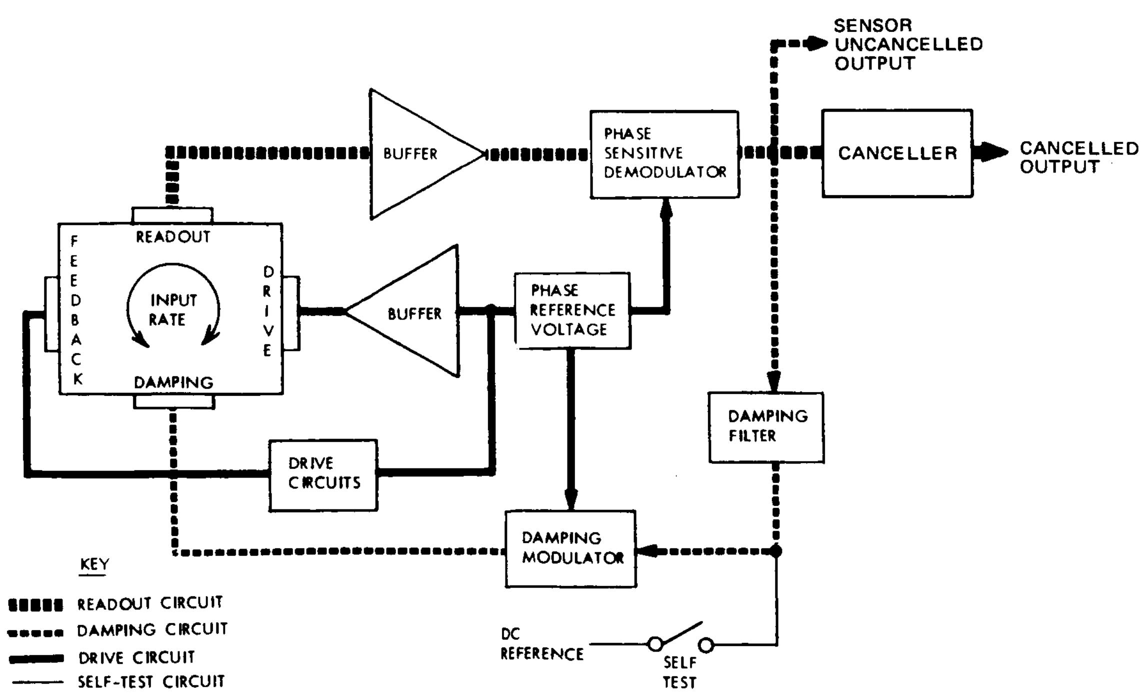

Figure 2. Sensor Functional Block Diagram

WORK SCOPE AND DESIGN GOALS

The work scope of this contract provides for the design, building and testing of four engineering model vibratory rate-of-turn sensors for the purpose of sterilization and environmental qualification for planetary exploration missions. The four units are shown in Figures 3 and 4, pages 5 and 6.

DESIGN GOALS AND ACHIEVEMENTS

The following are the goals for the four VYRO units throughout the entire test period:

		Goals	Achievements
1.	Sensor Range	$\pm 50^{o}$/sec = ± 5 vdc	$\pm 50^{o}$/sec = ± 5 vdc
2.	Threshold	0.1^{o}/sec or less	0.1^{o}/sec
3.	Hysteresis	0.1^{o}/sec or less	zero at cancelled output
4.	Drift	0.1^{o}/sec or less	0.13^{o}/sec at cancelled output*
5.	Linearity	1% full scale or better	$\ll$1% of full scale**
6.	Cross Coupling Between Axes	0.1% or less	$<$1%
7.	Operating Temperature Range	$+20^{o}$C to $+70^{o}$C	$+20^{o}$C to $+70^{o}$C
8.	Frequency Response	0.016 to 20 Hz or greater	$>$ 20 Hz
9.	Damping	0.4 to 0.8 critical	0.31 to 0.42 critical (adjustable if desired)
10.	Power	1.25 watts or less	$<$1 watt
11.	Weight and Volume	Minimum consistent with good design	
12.	Vibration	In three (3) axes	

*Excluding first set of test data on unit No. 1

**Excluding first two data points for unit No. 3 - functional test set 3

Sinusoidal: 5 Hz to 2 KHz 1g - for resonance survey
6 Hz to 14 Hz - 0.5" DA displacement
14 Hz to 2 KHz = ±5g

Sweep once from 5 Hz to 2 KHz to 5 Hz at 2 octaves per minute for each level.

	Random:	Flat spectrum 20 Hz to 2 KHz $0.5g^2/Hz = 31.5$ g rms for 2 minutes
13.	Shock	Two (2) shocks each direction in each of three (3) principal orthogonal axes. 100 g, 1.0 millisec, half sine.
14.	Steady State Acceleration	45 g for minimum of 1 minute in each direction along each of three (3) principal orthogonal axes.
15.	Acoustic Noise	Per MIL-STD-810B, Method 515, Category B (150 db overall SPL), except that the duration shall be 2 minutes minimum.
16.	Sterilization	Three of the four units shall undergo both the Ethylene oxide (ETO) decontamination and the heat sterilization procedures called for by contract NAS1-8885 and documents L12-9613A Exhibit A and the contract amendment requisition/purchase request no. P.R. 15.230.220 (Clause 2, changes, of Basic Agreement NAS12-84).

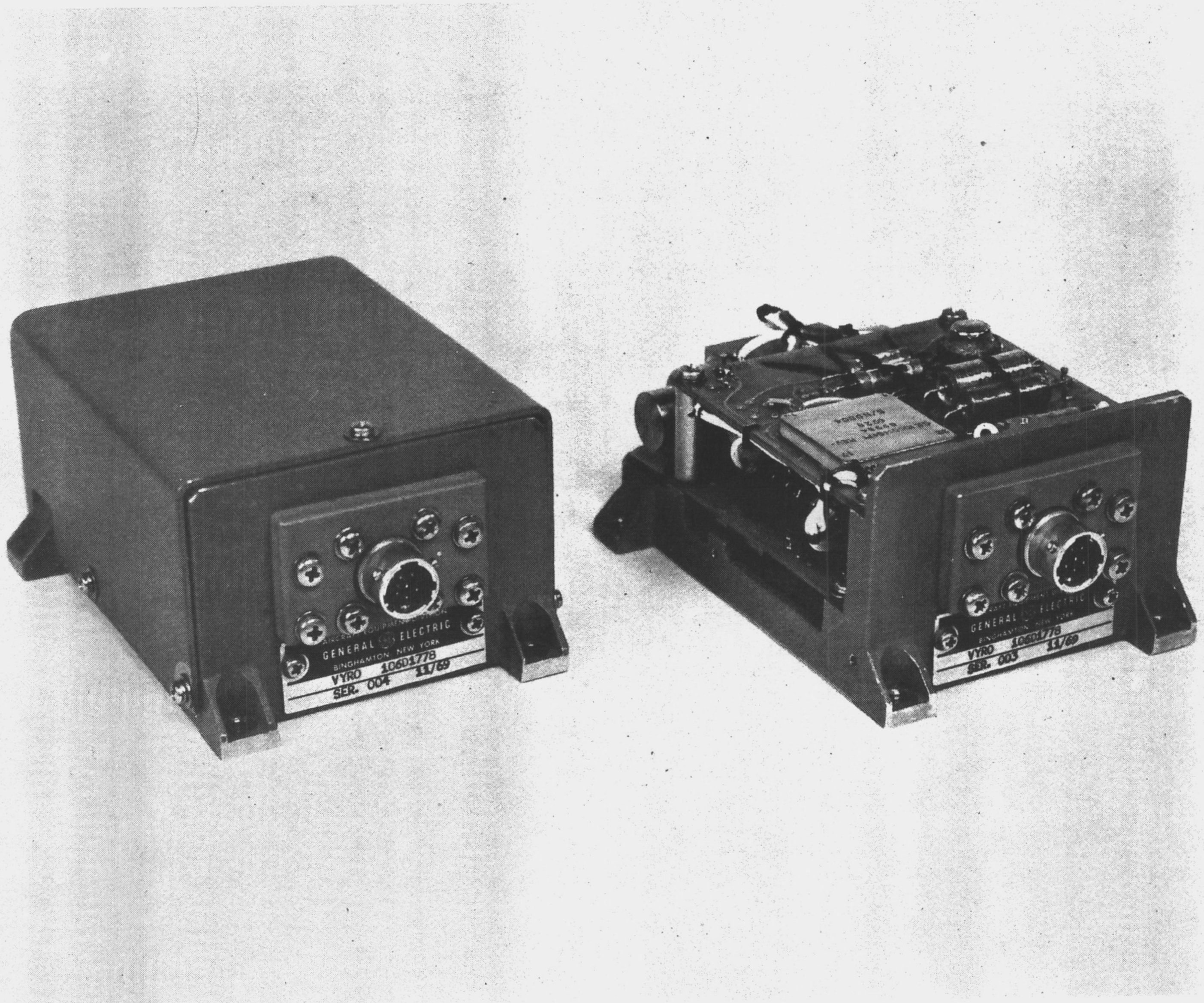

Figure 3. Completed VYRO Package

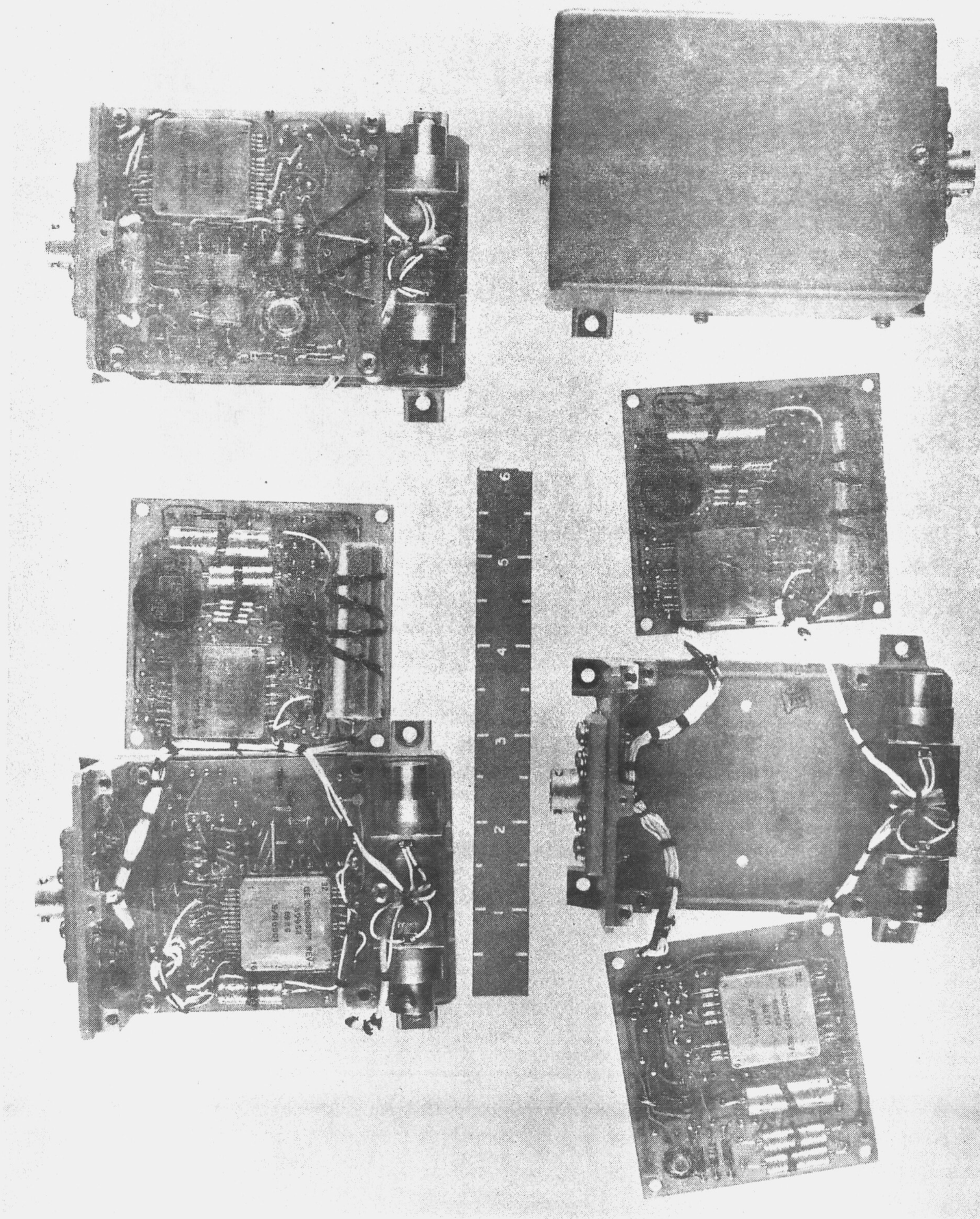

Figure 4. Assembly of VYRO Packages

Section 2

BEAM CHARACTERISTICS DATA

Data taken on beams R2, R3, R4, R1 and R5 is shown in Tables 1 through 5 respectively. In general the data taken on each beam was that of gain, bandwidth and resonant frequency in both the drive and readout planes, beam scale factor or output current from the readout crystal for 1^{o}/sec input rate to the beam, readout crystal quadrature and in-phase currents, and the beam damping rate coefficient which is the rms output current from the readout crystal for a properly phased AC signal applied to the damping crystal at the drive plane resonant frequency.

It should be noted that this data was taken prior to installation of the beams into the units. After temperature cycling of the completed sensor package between $0^{o}C$ and $+135^{o}C$ it is known that a significant beam gain reduction occurs. The reason for this is not precisely known, however, all beams presently in the units have acceptable gains. Beam R1 had to be replaced with beam R5 as a result of this gain reduction, however, as can be seen from the data for R1 (Table 4) the drive plane gain was considerably lower than for beams R2, 3 and 4 before the temperature cycling was performed. Upon disassembly of beam R1 it was noted that an excessive amount of the silver electrode had been removed during the mechanical trimming of the beam. This is most likely the reason that the beam gain for R1 dropped to an unacceptable level after temperature cycling. Beam R1 was replaced in unit 001 with a rebuilt beam labeled R5. The limited data taken on this beam is shown in Table 5. This beam has performed acceptably in sensor unit 001.

Section 3

TEST DATA AND DISCUSSION OF THE FOUR COMPLETED SENSOR PACKAGES

FUNCTIONAL TEST SETS 1, 2, 3 and 4

Prior to functional tests all four units were put through a non-operating temperature cycle shown in Figure 5. Also, prior to any functional testing the units were given a 50 hour "burn-in", that is, they were operated for 50 hours with power on. During the 50 hour "burn-in" some temperature cycling was performed.

The frequency response of each unit was measured using an oscillating rate table as a part of the calibration tests. The table pick-off voltage for these tests was held constant as the frequency of the table motion was varied. Figures 6 through 9 show the responses of units 001 through 004 respectively. Both the cancelled and uncancelled output amplitudes and phases relative to the table pick-off voltage are given.

Damping factors at the sensor uncancelled outputs ranged from 0.31 to 0.42. Actual calculated damping factors are shown on Figures 6 through 9. It will be noted that very little peaking occurs at the canceller output due to the 34 Hz lag incorporated in the canceller circuit. The 90^{o} phase points on the phase curves correspond to 270^{o} on the plot. The 90^{o} phase point for all curves is above 30 Hz.

The testing of the sensor units was done in the following sequence:

(a) Functional Test Set 1
(b) Environmental Test Set 1
(c) Functional Test Set 2
(d) ETO Decontamination and Heat Sterilization
(e) Functional Test Set 3
(f) Environmental Test Set 2
(g) Functional Test Set 4

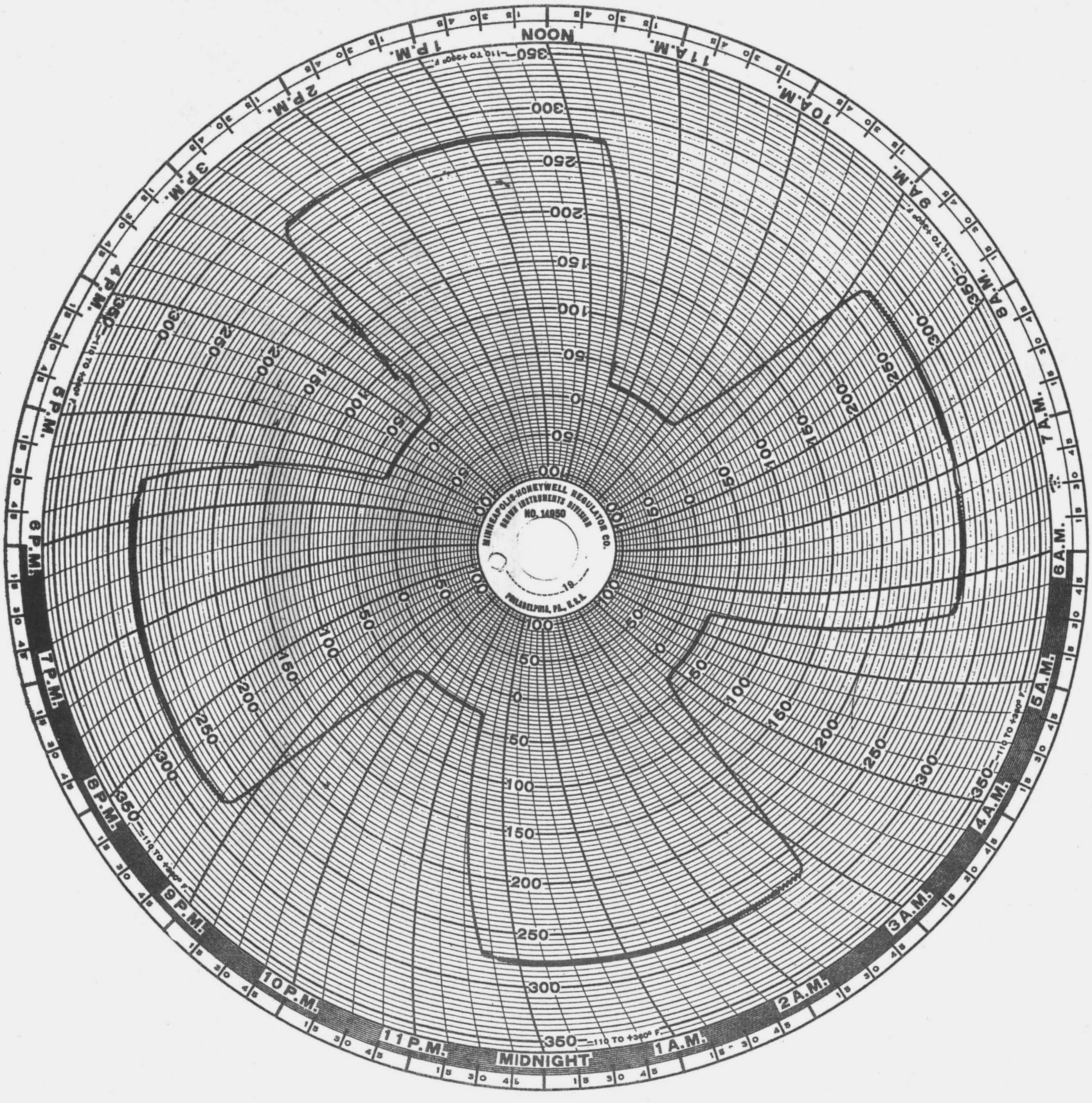

Figure 5. Non-Operating Temperature Schedule

Functional tests consist of threshold linearily and scale factor, cross axis sensitivity, temperature sensitivity, null stability and supply voltage sensitivity. The performance of each of these tests is discussed below.

THRESHOLD TEST

Figures 10 and 41 show threshold measurements on unit 1 demonstrating 0.1^{o}/sec threshold for functional test sets 1, 2 and 3, 4 respectively. These traces are of the cancelled output through a 2 Hz filter and show approximately 10 millivolt change in output for a step change of rate of 0.1^{o}/sec. Note that the canceller outputs do not always reach a full 10 millivolt deflection for 0.1^{o}/sec step input rate. This is due to the slow speed-up of the rate table to a full 0.1^{o}/sec and the fact that the canceller circuit immediately starts to charge up the 2 μf capacitor which begins to decrease the sensor output. Also, severe rate table switching transients will be noted on Figure 41 which were not present in Figure 10. Figures 11, 12, 13, 42 and 43 show similar data for units 2, 3 and 4 except that there are no data on Unit 2 for Functional Tests 3 and 4 since a beam failure occurred during heat sterilization.

Figure 42 shows excessive noise output from unit no. 3 for Functional Test Set 3. At the time of this test it was not possible to isolate this problem, but after Environmental Test Set 2 several problems were corrected on this unit and the last threshold test is much improved. These, and other problems will be discussed in Section 4.

LINEARITY AND SCALE FACTOR TESTS

Linearity and scale factor data is given in Tables 6 through 13 and 26 through 31. Tables 6 through 13 give data taken before and after Environmental Test Set 1, and 26 through 31 give data taken before and after Environmental Test Set 2. A computer program was used to compute the linearity as a percent of full scale, and scale factor from these data. The computer program used a least squares curve fitting method to compute the best straight line through the points and then computed linearity. Linearity error for all units is less than 2.3 percent and is much better for most. These data for these tests were taken using a steady state rate table and reading the uncancelled sensor output. Considerable variation of the scale factor of Unit 3 throughout the program will be noted. The reason for this is unknown, but the last three sets show only a 6 percent variation.

CROSS AXIS SENSITIVITY TEST

The cross axis sensitivity of each unit is shown in Table 14. These data were taken by placing the unit on an oscillating rate table and measuring the cancelled out put with the input rotation about each of the 3 axes of the sensor. In all cases the cross axis sensitivity was less than 1.1 percent.

TEMPERATURE SENSITIVITY

For this test a programmable oven was used to change the temperature from $+20^{\circ}C$ to $+45^{\circ}C$ to $+70^{\circ}C$ with rates of change of temperature of about $2.5^{\circ}C$/minute. Figure 14 shows the temperature schedule for this test. This cycle was run for 24 hours and both the cancelled and uncancelled outputs plotted on a recorder during the run. Tables 15 through 18 show a tabulation of the null data during the temperature cycle for each unit. Both the maximum and steady-state null for a given temperature are listed. Note that most canceller outputs had less than .25 degrees/sec equivalent null shift.

NULL STABILITY

For this test the sensor units were placed on a granite block in a temperature controlled lab. Both the cancelled and uncancelled outputs were plotted on a recorder. From this, data points were picked off every 15 minutes and long term and short term null stability calculated per the definitions given in the test plan. The null stabilities are listed in Table 19 for the uncancelled output. The shift in the cancelled output was virtually zero.

SUPPLY VOLTAGE SENSITIVITY

Table 20 shows the supply voltage sensitivity for each unit for both the cancelled and uncancelled outputs. The data shows that for these very large changes of supply voltage from ±11 vdc to ±13 vdc, about a nominal of ±12 vdc the maximum change of cancelled output was equivalent to 0.056^{o}/sec for one unit while it was 0.02^{o}/sec for most other units. The largest change of uncancelled output for these changes of supply voltage was equivalent to about 1.1^{o}/sec.

ENVIRONMENTAL TEST SET NO. 1

RESONANCE SURVEY AT 1-G PEAK SINUSOIDAL ACCELERATION LEVEL

A sine sweep at a 1-g acceleration level over a frequency from 5 Hz to 2000 Hz and back to 5 Hz was applied to each unit in each of the readout, drive and axial directions of the sensor. The cancelled and uncancelled output and the input g-level were plotted to determine any change in the dc null as the frequency of vibration was varied from 5 Hz to 2000 Hz and back again. Figures 15 through 26 show these plots for Environmental Test Set 1. Figures 27-38 show similar plots for the 5g level.

It should be noted that the instrumentation used in making these plots, for Environmental Test Set 1, records the dc output plus the average value of the rectified sine wave, if one is present out of the sensor with a frequency content of 30 Hz or less. The instrumentation utilizes a 60 Hz chopper at its input when used, as it was here, in the dc average mode. Thus, if there is any signal content much above 30 Hz out of the sensor a non-correlatable output will occur on the plot. This does not necessarily imply a non-correlatable output at shaker frequencies above 30 Hz. At a vibration frequency of 75 to 85 Hz (the beam separation frequency) a sinusoidal output from the sensor is anticipated due to a natural resonance in the sensor beam at this frequency. This mode is damped by use of the damping crystal and damping circuitry to a damping ratio between 0.3 and 0.4 as stated previously. Thus a small sinusoidal output is expected at the beam separation frequency when the vibration frequency reaches 75 to 85 Hz. However, the instrumentation will not give an output which can be correlated with the input for this condition or for any other condition causing a higher frequency output from the sensor.

For Environmental Test Set 2 the instrumentation was changed to record the AC output of the sensors instead of the DC output. In this mode, the instrumentation has a flat frequency response from about 10 Hz to 20 KHz.

As can be seen in Figures 44 through 52 a resonance occurs in the readout plane at about 40 to 50 Hz. This may be due to the damping factor of the units being somewhat low, or a rate input from extraneous table motion, or to flexing of the beam on the RTV pad.

5-G SINE SWEEP

The next vibration test was a qualification level test using sinusoidal vibration of 0.5 inch double amplitude from 6 Hz to 14 Hz and ±5 g peak from 14 Hz to 2000 Hz. This was to be run up and down in frequency with the unit not operating. Subsequent to the run the sensor uncancelled output was to be measured with and without the self test input applied. Though it was not required, the sensors were turned on and the outputs plotted as for the 1-g runs. These runs are shown in Figures 27 through 38 for Environmental Test Set 1 and in Figures 53 to 61 for Environmental Test Set 2.

Each unit displayed a peaking effect when vibrated in the readout plane between 40 and 60 Hz. This is most likely due to the fact that the frequency response plots for each unit display peaks in the cancelled and uncancelled outputs at about this frequency range. Unit 2 showed a package resonance in the readout plane between 1500 and 2000 Hz (Figure 30a). Units 3 and 4 showed point resonances in the readout plane at 310 and 200 Hz, respectively (Figures 33a and 36a). All units showed some resonance phenomenon between 1000 and 2000 Hz in the drive plane and all units showed a resonance between 300 and 400 Hz in the axial plane. All of these resonances are believed to be small package (component) resonances of a non-destructive nature and are not resonances within the beam assembly.

Table 21 lists the uncancelled null and the uncancelled output with the self test feature activated after each 5 g run in each plane. Two damping flat pack failures occurred in Unit no. 4 during Environmental Test Set 1. These will be discussed in Section 4. The data in Table 21 show that all units were operating normally at the completion of these tests.

RANDOM VIBRATION

Random vibration of 0.5 g^2/Hz with a flat spectrum from 20 Hz to 2000 Hz was run on each unit for 2 minutes in each axis. After completion of a run in each axis the uncancelled null and the uncancelled output with the self test activated were measured. Table 22 lists these data and shows that all units were working properly at the completion of the test. A short circuit occurred in a damping flat pack in Unit no. 4 during the random vibration of Environmental Test Set 1. This failure will be discussed in Section 4.

SHOCK

The shock test consisted of dropping each unit twice in each direction of the 3 principal axes (12 drops total). The shock level used was a 100 g-1 millisecond, half sine pulse. After all four drops along one axis the unit was turned on and the self test operated. These data are given in Table 23. Although large variations in the uncancelled null will be noted the units were all working properly at the completion of these tests. This change in uncancelled null will not affect the cancelled output.

STEADY STATE ACCELERATION

Each unit was given a 45 g steady state acceleration of one minute duration in each direction along each of the three principal axes of the unit. At the completion of an acceleration run along one axis the unit was turned on and the self test activated. These data appear in Table 24. All units were operating properly at the completion of these tests.

ACOUSTIC NOISE

Each unit was subjected to a non-operating acoustic noise test run to MIL-STD-810B, Method 515 - Category B with 150 db (referred to $2 \times 10^4 \frac{\text{dynes}}{\text{cm}^2}$) for 2 minutes. The units were tested, using their self test feature, both before and after the test. These data are presented in Table 25. All units were operating properly at the completion of this test.

ETO DECONTAMINATION AND HEAT STERILIZATION

Units 2, 3 and 4 were subjected to the 6 cycles of ETO decontamination and the 6 cycles of 135°C heat sterilization called for by the contract. The ETO tests were performed during the period from 1/19/70 through 2/1/70. These test were performed at Langley Research Center, Langley Station in Hampton, Va., by NASA personnel. Upon completion of the tests the units were brought back to the General Electric Company in Binghamton, N. Y. and given a nominal performance test. These tests consisted of a three point scale factor and linearity check, a null check, and a check of the operation of the self test feature. All units operated properly with the exception that units 2 and 4 had an excessive null at the canceller output (+92 mv for unit 2 and -79 mv for unit 4). Upon investigation it was determined that high resistance leakage paths existed near the canceller circuit capacitor (2 uf Teflon) and the 7 meg resistor. These leakage paths were probably caused by the 50% relative humidity content during the ETO tests. It was decided to run the units through the first heat sterilization cycle and to then re-check the canceller nulls since this test might drive the humidity out of the circuit. At the completion of the 1st heat cycle the canceller nulls of these units were back to their normal values.

After the completion of the ETO Decontamination testing and nominal performance tests, units 2, 3 and 4 were heat sterilized by applying 135°C heat to them for 6 cycles at 92 hours a cycle. After each cycle the units were given nominal performance checks to determine their condition. A considerable number of problems occurred during this sterilization. These will be summarized in Section 4. Table 32 shows self test and scale factor data taken after each heat cycle. Figure 39 shows a 2 hour null stability run taken after heat cycle no. 2, while Figure 40 shows the null stability run taken after heat cycle no. 6. The other 2 hour null stability runs were omitted to shorten the report, but they will be delivered with other data which is on long recorder plots.

The data shown in Table 32 show that the units were operable after each cycle, however, certain repairs were made whenever a failure occurred before the tests were run. These will be discussed in Section 4. As has been noted previously, unit 2 had a beam failure during sterilization testing.

Section 4

SUMMARY OF FAILURES

Unit No. 1

The canceller circuit capacitor (C16-2 uf Teflon made by Component Research Corp.) was found to be open after the completion of vibration, shock, steady state acceleration, and acoustic noise testing (Environmental Test Set 2). This is the same type of problem with this capacitor as has been found on other units. The capacitor was replaced with one of the reworked capacitors SNT3129-001. The failed capacitor was sent back to Component Research Corp. for rework.

Unit No. 2

An intermittent problem occurred with this unit during functional test set 2. This problem could not be isolated until after the first heat sterilization cycle. The unit was not operational after this cycle. A cold solder joint was found (and repaired) under the input pin (18) of the demodulator flat pack. Also, it was found that pin 32 of the damping flatpack (its output) had been broken at or close to the glass feedthrough on the pack. The broken pin of the flatpack appeared as though it had been held only by a very small area of the pin for a long time, perhaps since its manufacture. Both of these problems probably existed before the ETO tests were performed since there were indications of a problem that could not be isolated before the ETO tests were performed. A wire was soldered to the pin on this flatpack.

After completion of heat cycle no. 6, unit no. 2 was not operating properly. It was determined that the drive plane beam gain at the drive plane resonant frequency had dropped to 39 μa/volt with an increase in drive plane bandwidth to 6.2 Hz (about 3 to 1 above typical). This gain is so low that the drive regulator circuitry cannot operate properly. This appears to have been a cumulative effect over the total of 6 temperature cycles since the scale factor after each succeeding cycle was 102 millivolts/deg/sec, 108, 112, 105, and 89.5. These changes in scale factor indicate a change in amplitude of drive plane motion which is just what will occur with such a low beam gain. The regulator no longer holds a constant beam motion.

The beam from this unit has been removed from its frame and visually inspected under a microscope. It was determined that the solder bond under all crystals had degraded extensively. Cracks in the bond can be seen as well as some whiskers growing mostly out of the edge of the crystal and a few out of the solder bond. The whiskers are about 5 mils in length and appear to be metallic, but this has not been determined for sure. The cracking of the solder bond is no doubt the cause of the loss of beam Q and gain. Reasons for this deterioration of the bond are unknown at this time. This beam has been sent to Schenectady for analysis of the whiskers.

A complete beam in an open frame was run through both the ETO and heat sterilization cycles at the beginning of the program. No evidence of this type of failure was noted.

Unit No. 3

Three broken wires have occurred on this unit during Environmental Test Set 1. A wire connected to pin 4 of the beam broke during random vibration test. This was repaired and the lacing changed slightly and then the test repeated with no recurrence of the problem. Wires connected to the connector pins 1 and 5 were found to be broken after the replacement of C16 which was found to be intermittently open after performance of all environmental tests. It is believed that excessive handling was the cause of the broken connector wires.

Capacitor C16 is a high reliability Teflon capacitor made by Component Research Co. in California (catalog no. 05TC205GSN-125). This capacitor has been replaced in the unit and the bad component sent to Component Research for analysis and rework. The connection between the foil and the lead had broken. It is believed that this problem has been solved by a redesign of the foil mount by the Component Research Co. The redesign consisted of placing two silicon rubber washers, larger in diameter than the case, so that they cup over the ends of the capacitor winding. This prevents the winding from rotating inside the case during vibration. Two reworked capacitors have been given two complete sets of 5 g sine and .5 g^2/Hz random vibration, and 100 g-1 millisec shock with no failure.

After the first heat sterilization cycle this unit was not operating properly. A cold solder joint was found and repaired under the pins of the choke in the drive circuitry.

After heat cycle no. 4, unit no. 3 exhibited a high frequency oscillation ($\approx$9700 Hz) in the readout circuits. This problem has occurred on our product design units and has been solved by a component value change in the electronics. The problem occurs because the beam and its nodal wire mounts act like a second order spring-mass system with a resonant frequency of about 9700 Hz in the readout direction. If a signal is applied to the damping crystal and the output of the readout crystal observed as the frequency is varied about 9700 Hz a second order gain curve may be plotted at this wire resonant frequency. The gain at 9700 Hz is affected considerably by the torque applied to the mounting screws holding the beam frame. A slight change of mounting torque stopped the oscillation. The same problem reoccurred after heat cycle no. 5 and was stopped in the same manner. In order to complete testing on this unit without interruption due to these intermittent oscillations a .022 μf capacitor was added to the circuit in parallel with C7. This extra capacitor was left in this unit, but will not be added to units 1 and 4 since the problem has not occurred with these units. This increase in the capacitance of C7 reduces the loop gain through the beam, the readout circuits and the damping circuit at 9700 Hz such that the loop cannot oscillate at the beam-node wire resonance in the readout direction. Future designs would use a 0.027 μf capacitor for C7. This change has no adverse affect on the sensor operation.

Another poor solder joint has been found under the choke on this unit. This occurred after or during the last set of vibration, shock, acceleration and acoustic noise testing (Environmental Test Set 2). Also, a poor solder joint was found under pin 28 of the readout flatpack A3-(106D1483). These joints were resoldered and the unit is now working properly.

Unit No. 4

This unit has had 2 damping flatpacks fail during Environmental Test Set 1. The first damping flatpack was noted to be defective after a random vibration in the drive plane. However, there was an indication of a problem with this unit during a previous temperature test in that several times during a change of temperature the uncancelled null shifted suddenly by about 300 millivolts dc. This effect could not be repeated and thus it was not possible to isolate it at this time. Therefore, vibration testing was started on the unit. After the random vibration it was possible to cause the problem to occur by applying pressure to the top of the damping flatpack. This flatpack was then removed and the cover taken off. It was found that there was a bad bond under one end of a chip capacitor.

A new flatpack was put into the unit and the vibration testing repeated. After the first 5 g sine sweep in the drive plane a short circuit occurred in the new damping flatpack between the +12 volt dc input (pin 26) and the case of the flatpack (pin 1). This flatpack was then replaced with another damping flatpack and all 5 g and random vibration tests re-run with no failure. This unit has now been through all environmental tests with no further damping flatpack failures.

On this unit there was a failure in capacitor C16 which appears to be identical to the failure of C16 in unit no. 1 and no. 3.

The flatpack failures encountered in the program are covered in the Appendix which contains two trip reports, one trip to NASA Langley Research Center in Hampton, Virginia to deliver three of the sensor units for ETO decontamination and to discuss the flatpack failures. The second trip report covers a trip to Mepco, the vendor of the flatpacks, to inspect and analyze these failures.

Section 5

CONCLUSIONS AND RECOMMENDATIONS

The problems that have occurred throughout this test program are listed below:

1. Crystal-beam bond failure
2. Problems with the thick film flatpacks
3. Canceller circuit leakage problems after the ETO decontamination
4. Readout plane wire resonance problem
5. Broken wires and cold solder joints.

Each of these is discussed below:

1. Crystal - beam bond failure

This is the most serious problem encountered throughout the program. The General Electric Company is now persuing better methods of attaching the crystals to the beam. It should be noted that only one beam out of three failed and this may indicate a process control problem although all beams were built by the same person. All beams exhibited a reduction in gain and Q after their first hot-cold stabilization cycle just before functional test set 1 was performed. Further investigation into this area is required.

It is recommended that the remaining three beams at some point be disassembled and the crystal bonds be examined to determine if there has been any degradation. They should be examined under a microscope to see if there are any whiskers present.

Figure 63 shows a photograph of the crack in the solder bond under one of the crystals of beam R2. At the end of this report is an electron microprobe analysis performed on a piece of crystal broken off the failed beam. Some discussion of the analysis is also included, as well as photographs of the whiskers. An indium solder was used to bond the crystals to the beam.

2. Problems with the thick film flatpacks

Two distinct problems occurred with the thick film flatpacks throughout the program. A failure of a capacitor chip bond occurred in one unit and a piece of the solder preform from the lid sealing operation fell into the circuitry causing a short circuit. A trip report to Mepco Inc. discussing these problems is included in the appendix. The samples of chip capacitors bonded to substrates mentioned in the trip report were received and inspected by our microcircuits people. They were thought to be of excellent quality. These samples have been forwarded to NASA representatives for their investigation.

The flatpack lid sealing problem has been solved by welding the cover to the pack instead of attempting to solder seal.

3. Canceller circuit leakage problems after ETO decontamination

After the ETO decontamination it was found that two of the units had large offsets at the canceller outputs. It was determined that this was due to high resistance leakage paths around the canceller circuit capacitor (C16). This was probably caused by the 50% relative humidity during the ETO test. After the first heat sterilization cycle at $+135^{\circ}C$ for 92 hours this problem disappeared and has not occurred again throughout the rest of the program. It is necessary that the units be dried thoroughly after the ETO test in order that this problem can be eliminated or, if this is not possible a design change might be required to guard against high resistance leakage paths.

4. Readout plane wire resonance problem

This problem, discussed previously, would be corrected by a circuit design change to change the value of C7. (See schematic in Figure 62.)

5. Broken wires and cold solder joints

Numerous broken wires and cold solder joints have been found throughout the program. These problems can be eliminated by better quality control and less handling of the units. Some of these problems were probably caused by handling of the units in tracking down problems. The cold solder joints found under the pins of the drive circuit choke require a circuit board design change to give a proper mount.

In general, all of the above failures, with the exception of the beam-crystal bond failure, are easily correctable. Investigation of the bond failure and new bonding techniques is continuing. Units 3 and 4 have survived all testing including ETO and heat sterilization and are now in working condition. Unit 1 is also in working condition, but it was not run through ETO and heat sterilization.

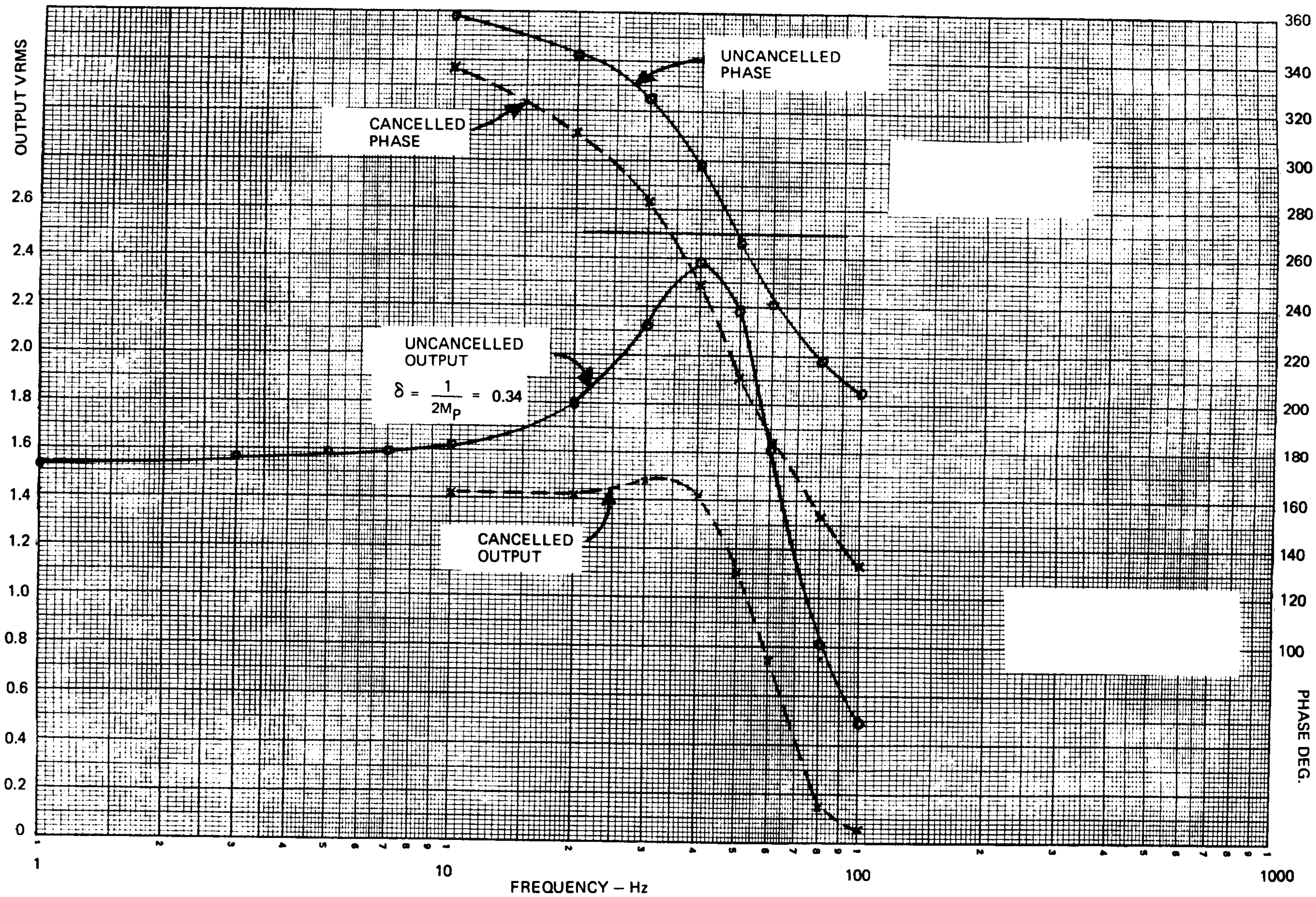

Figure 6. Frequency Response Unit No. 1

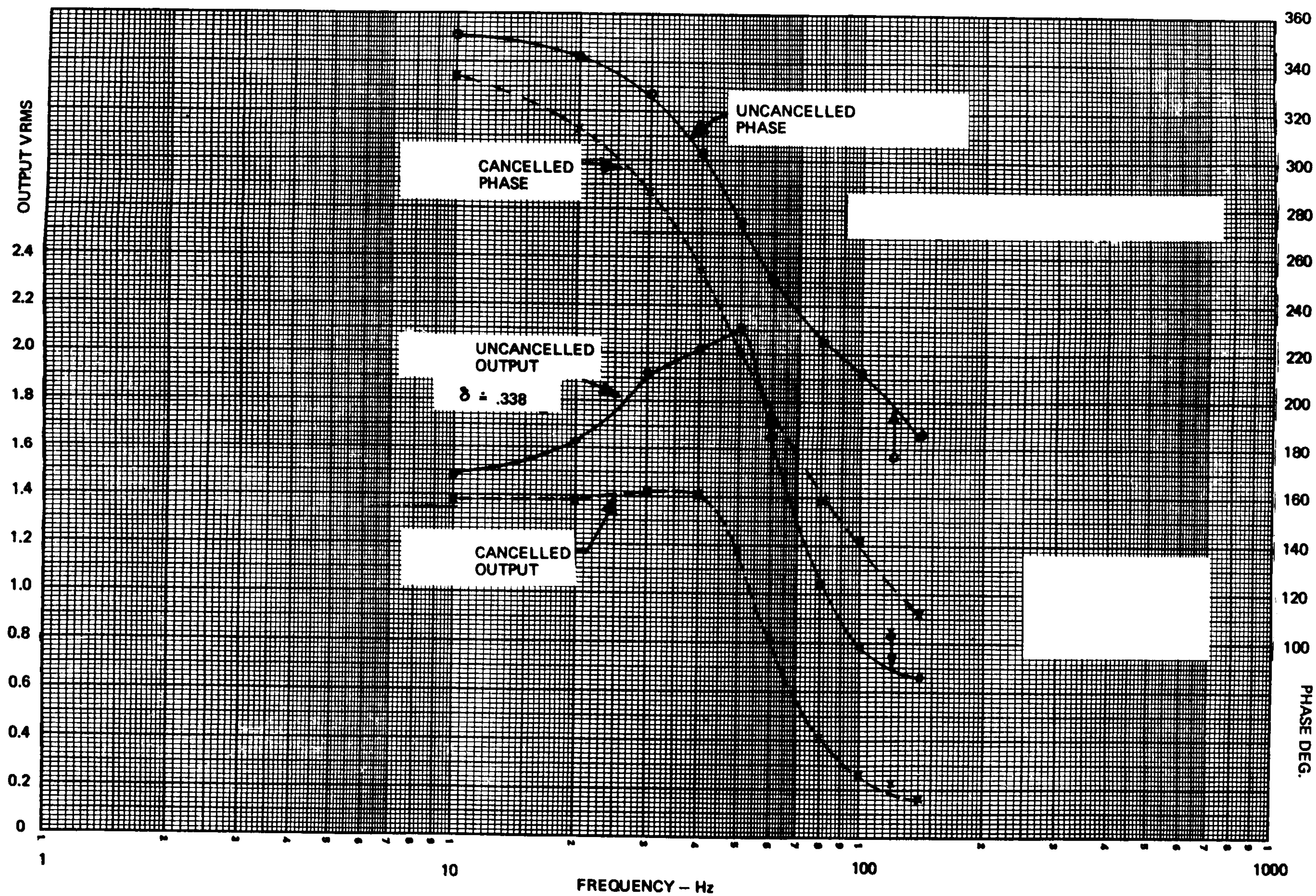

Figure 7. Frequency Response Unit No. 2

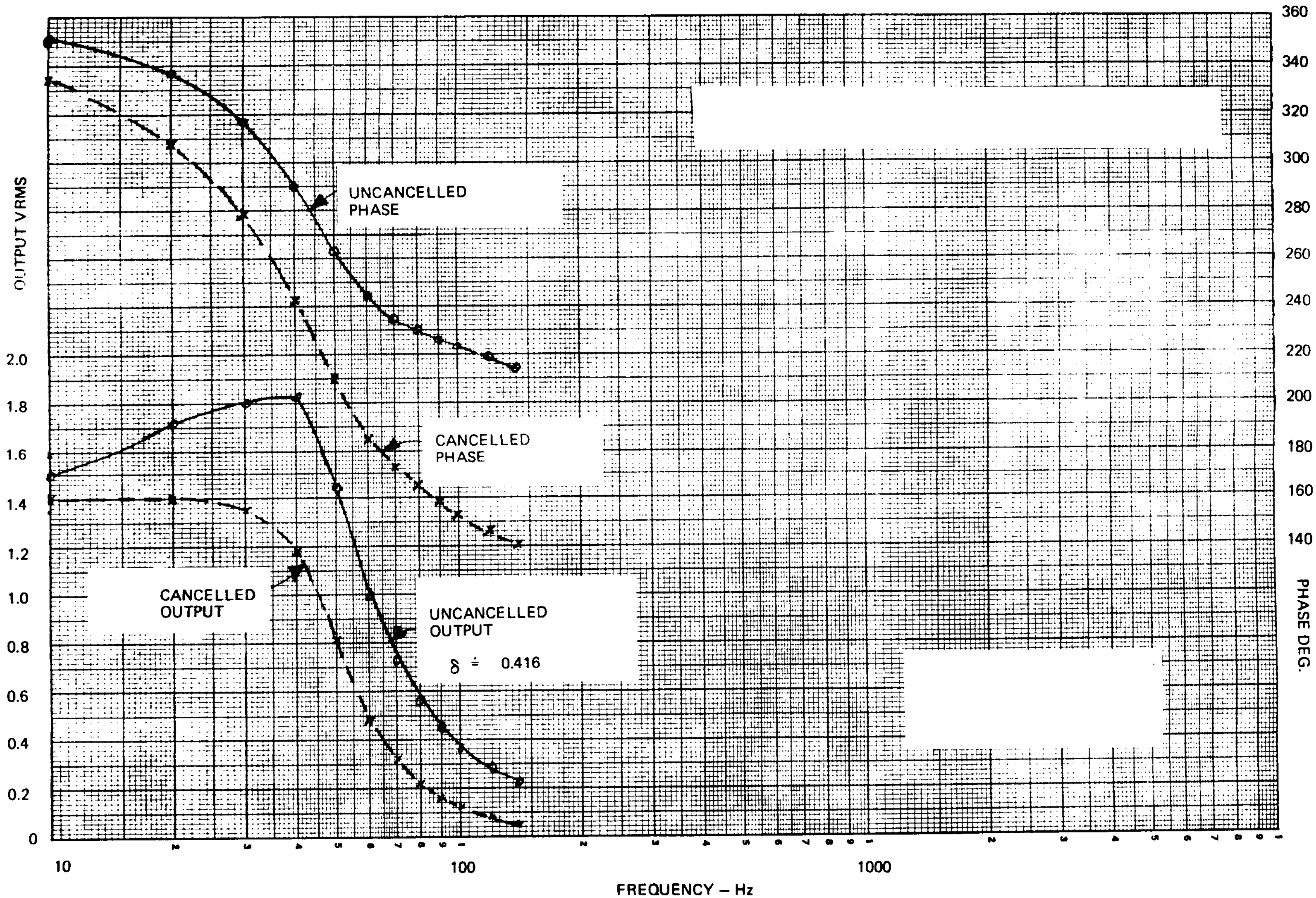

Figure 8. Frequency Response Unit No. 3

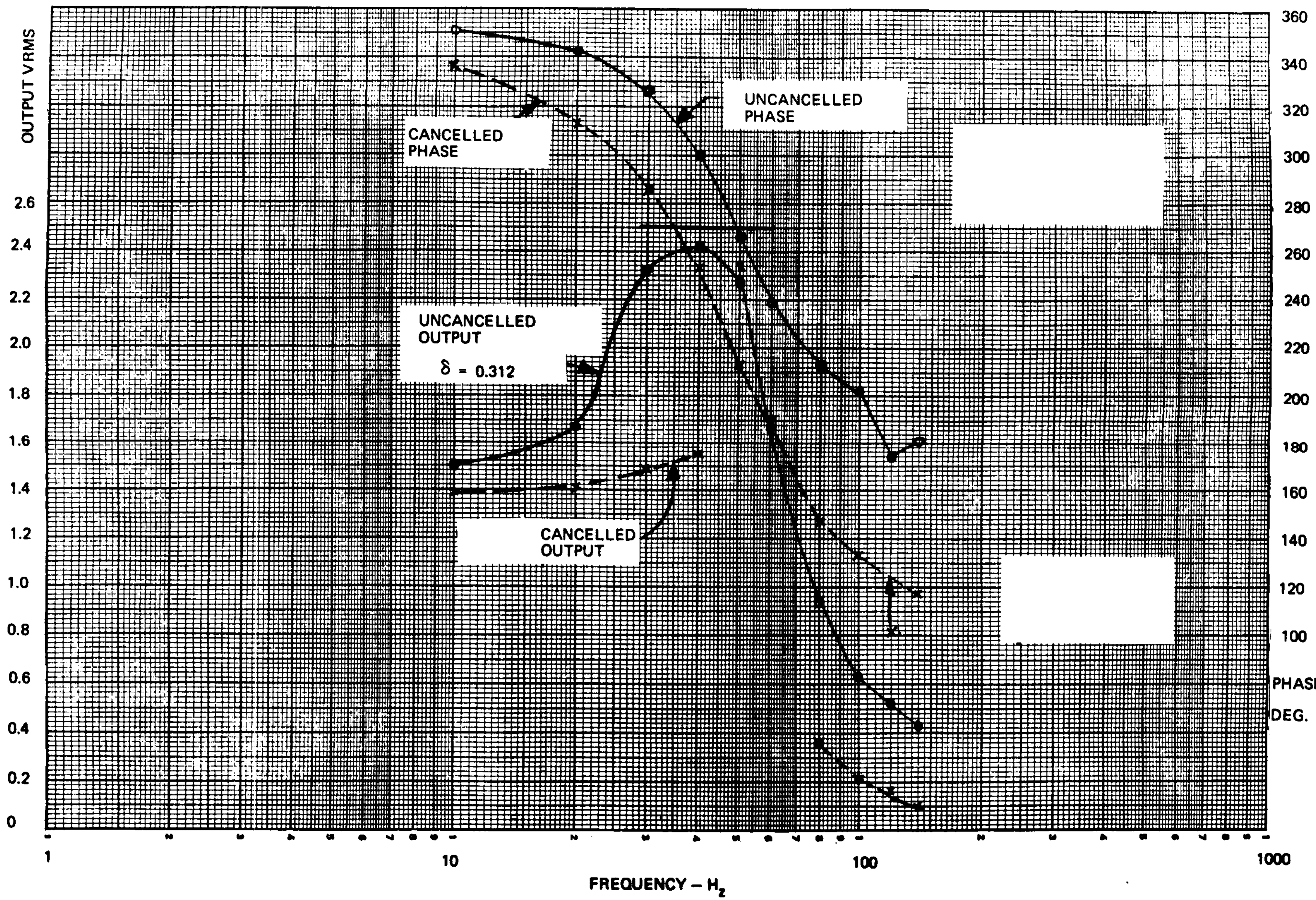

Figure 9. Frequency Response Unit No. 4

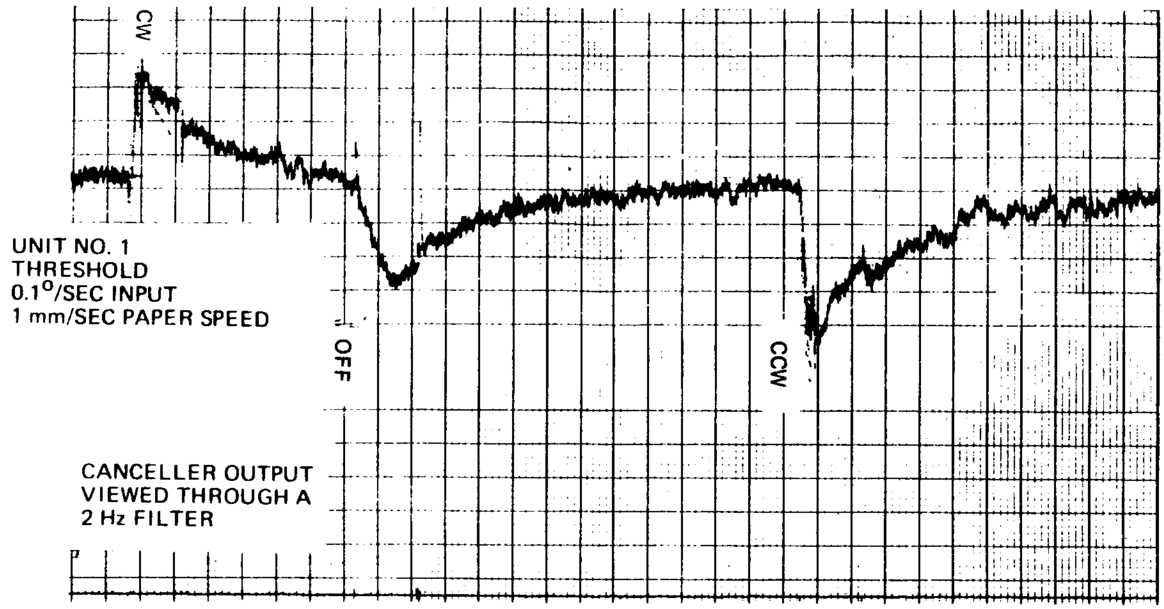

FUNCTIONAL TEST SET 1

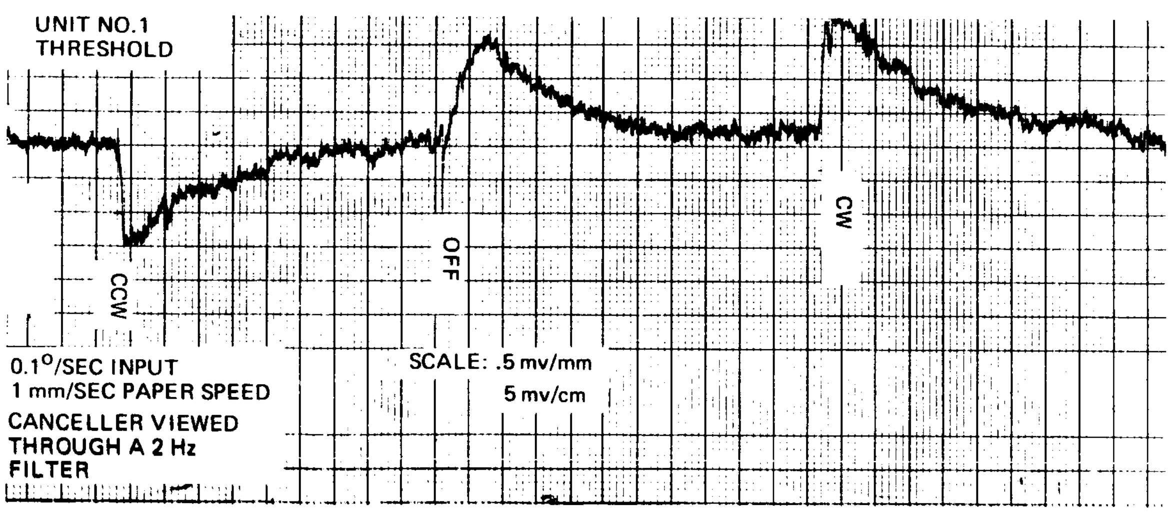

FUNCTIONAL TEST SET 2

Figure 10. Threshold Test-Unit No. 1

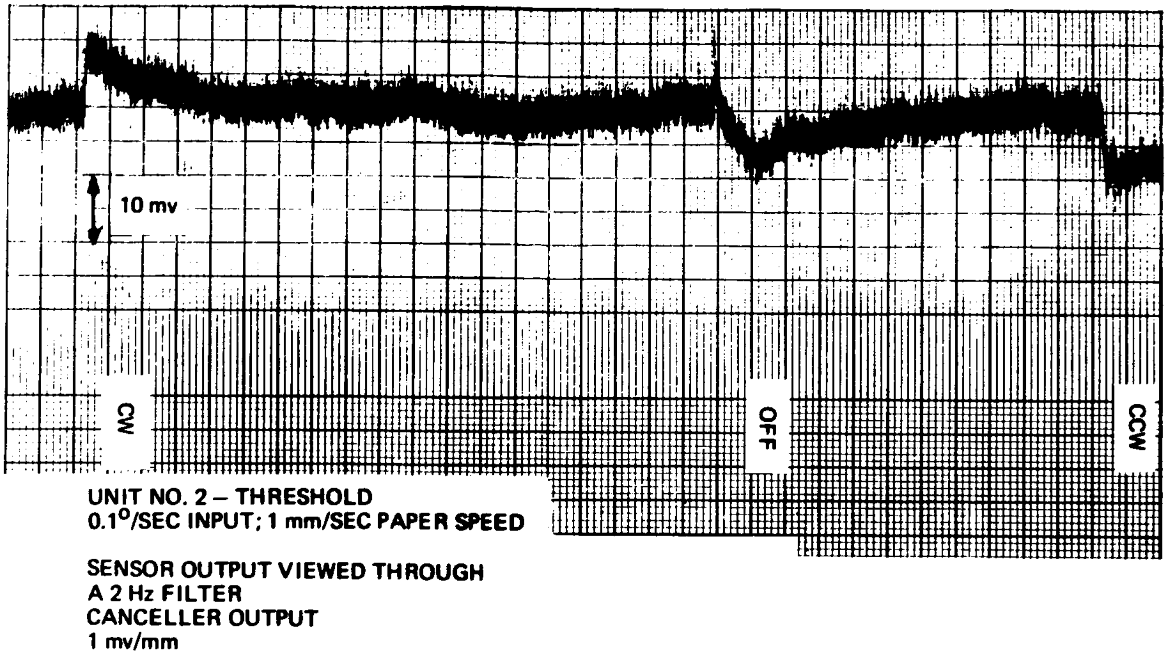

FUNCTIONAL TEST SET 1

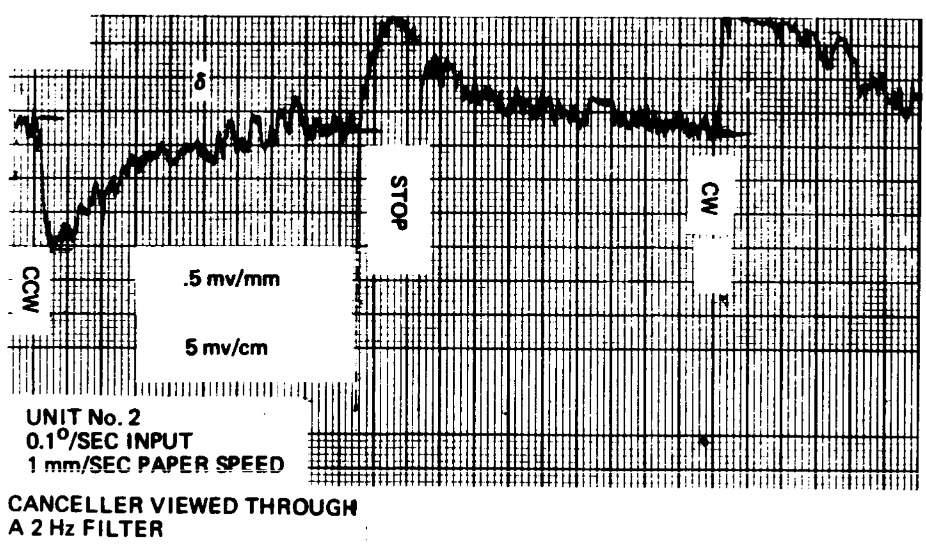

FUNCTIONAL TEST SET 2

Figure 11. Threshold Test-Unit No. 2

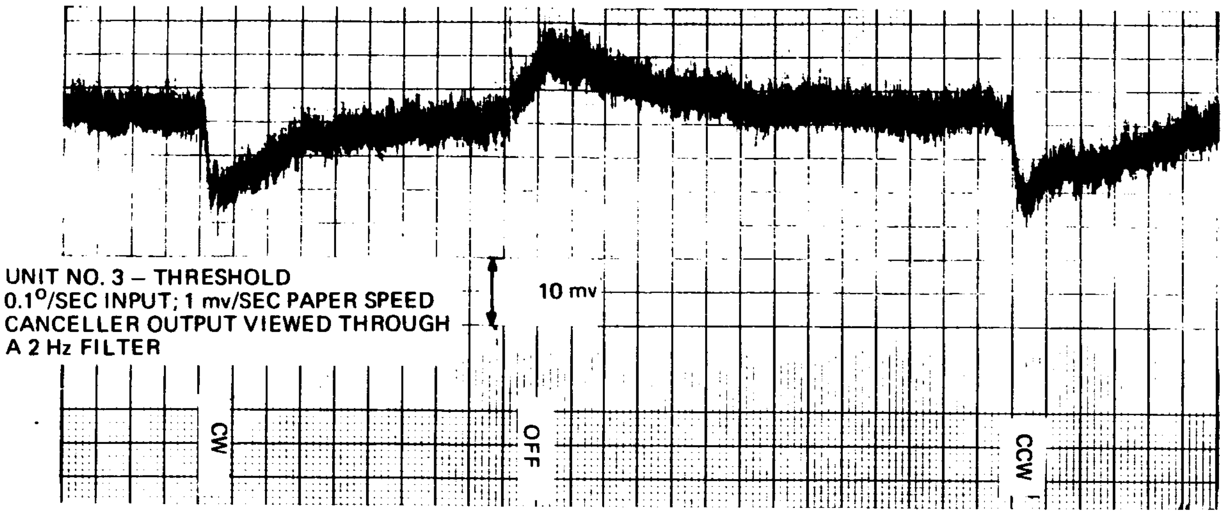

FUNCTIONAL TEST SET 1

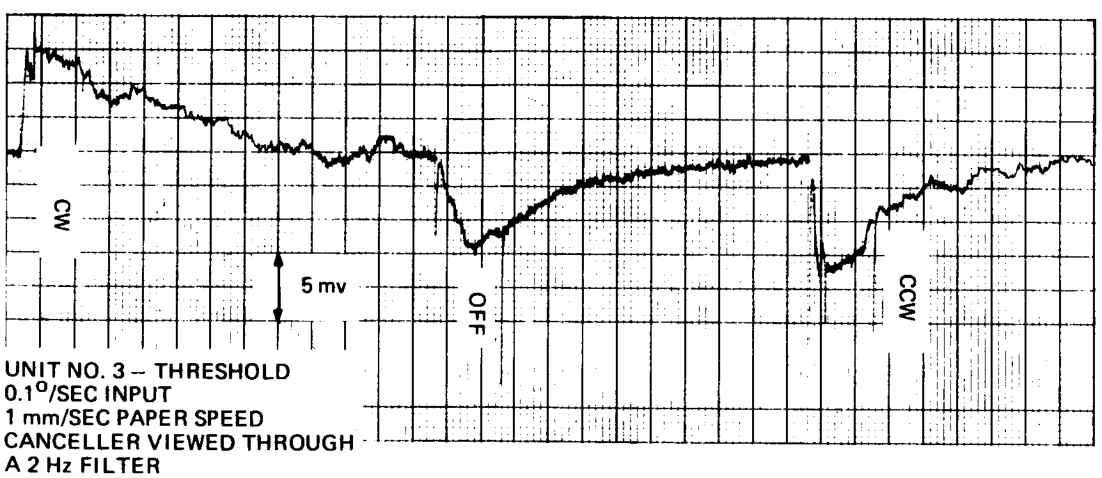

FUNCTIONAL TEST SET 2

Figure 12. Threshold Test-Unit No. 3

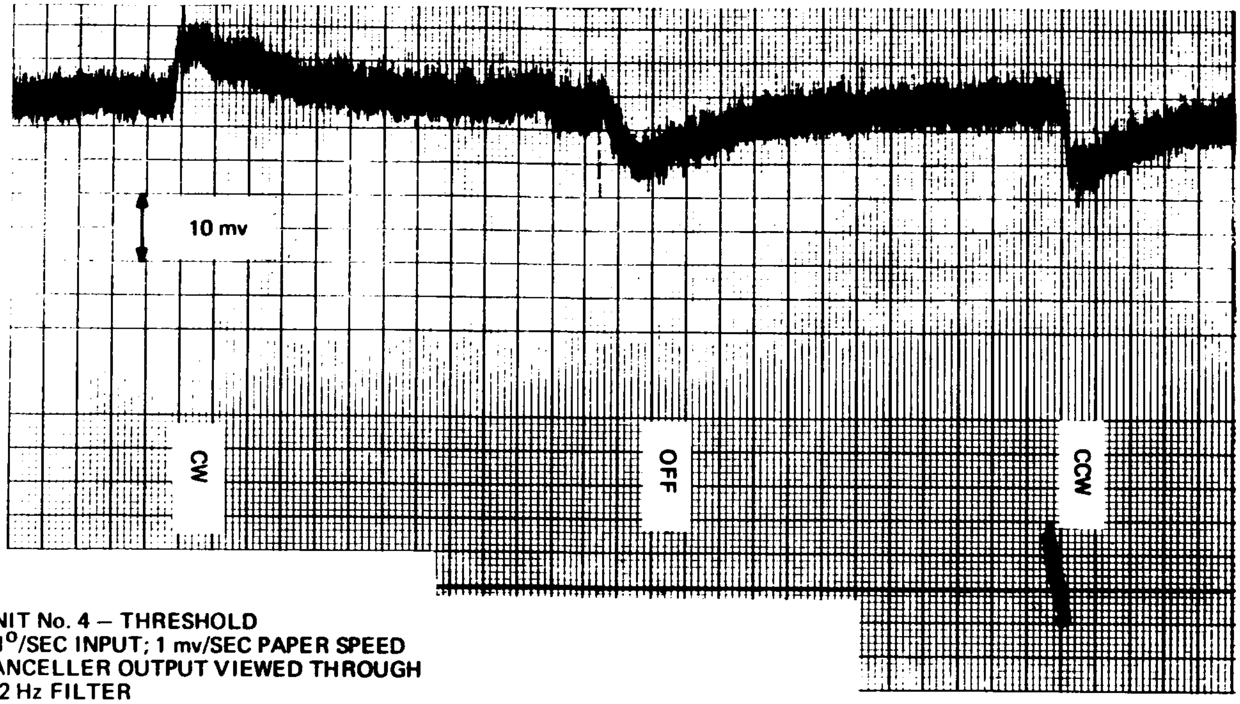

UNIT No. 4 – THRESHOLD
0.1°/SEC INPUT; 1 mv/SEC PAPER SPEED
CANCELLER OUTPUT VIEWED THROUGH
A 2 Hz FILTER

FUNCTIONAL TEST SET 1

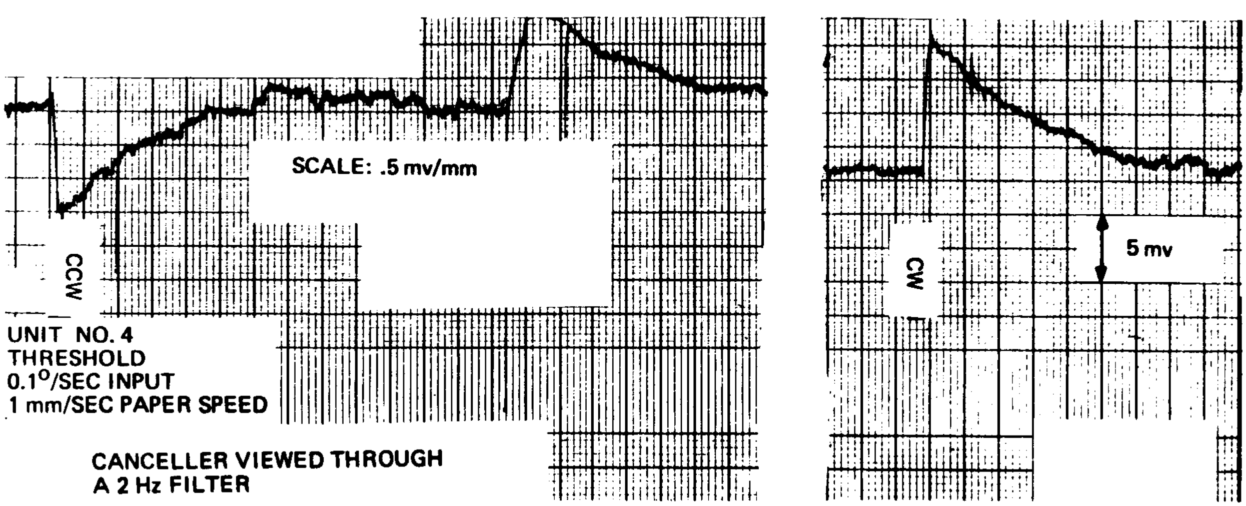

UNIT NO. 4
THRESHOLD
0.1°/SEC INPUT
1 mm/SEC PAPER SPEED

CANCELLER VIEWED THROUGH
A 2 Hz FILTER

FUNCTIONAL TEST SET 2

Figure 13. Threshold Test-Unit No. 4

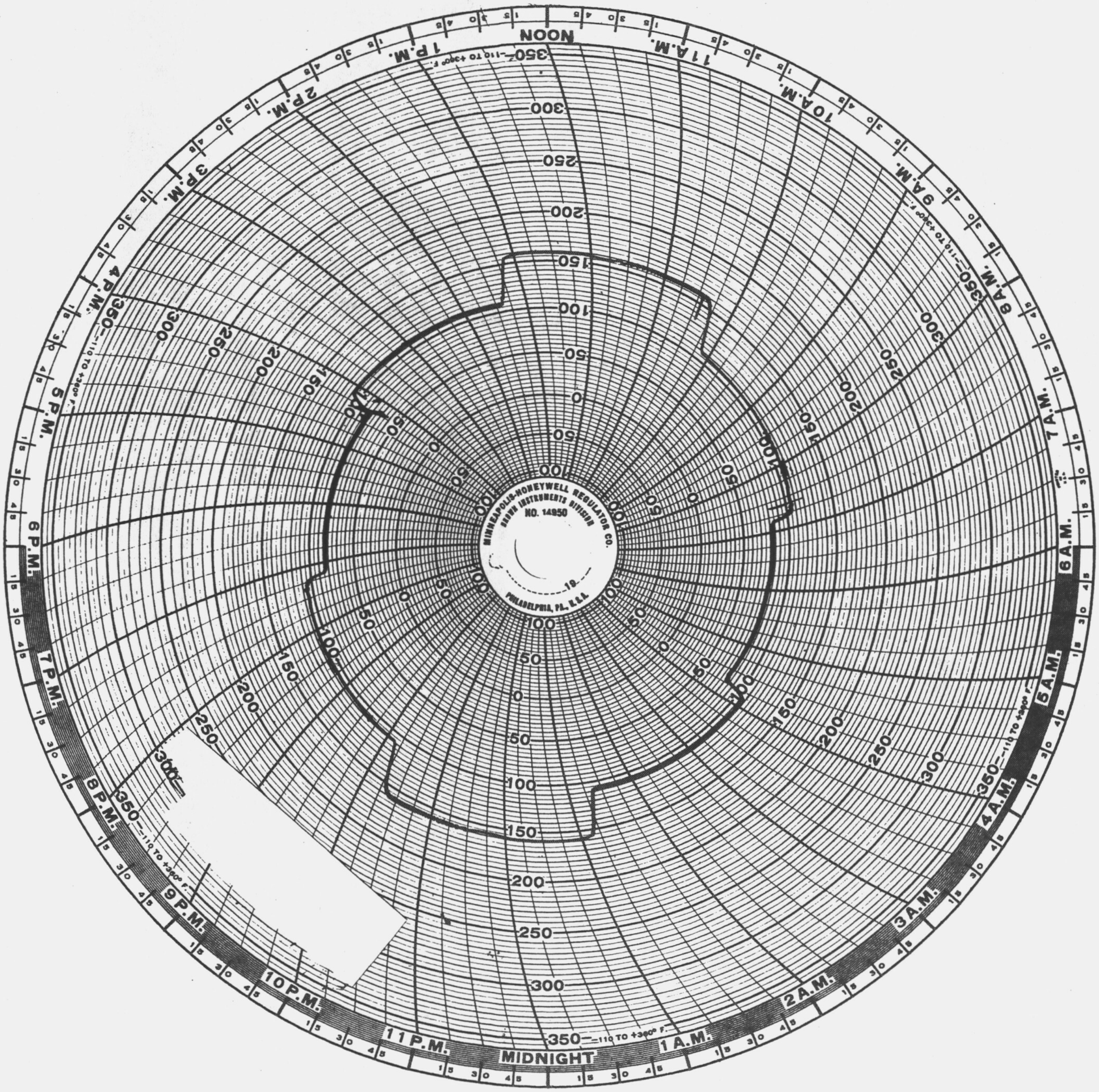

Figure 14. Temperature Schedule

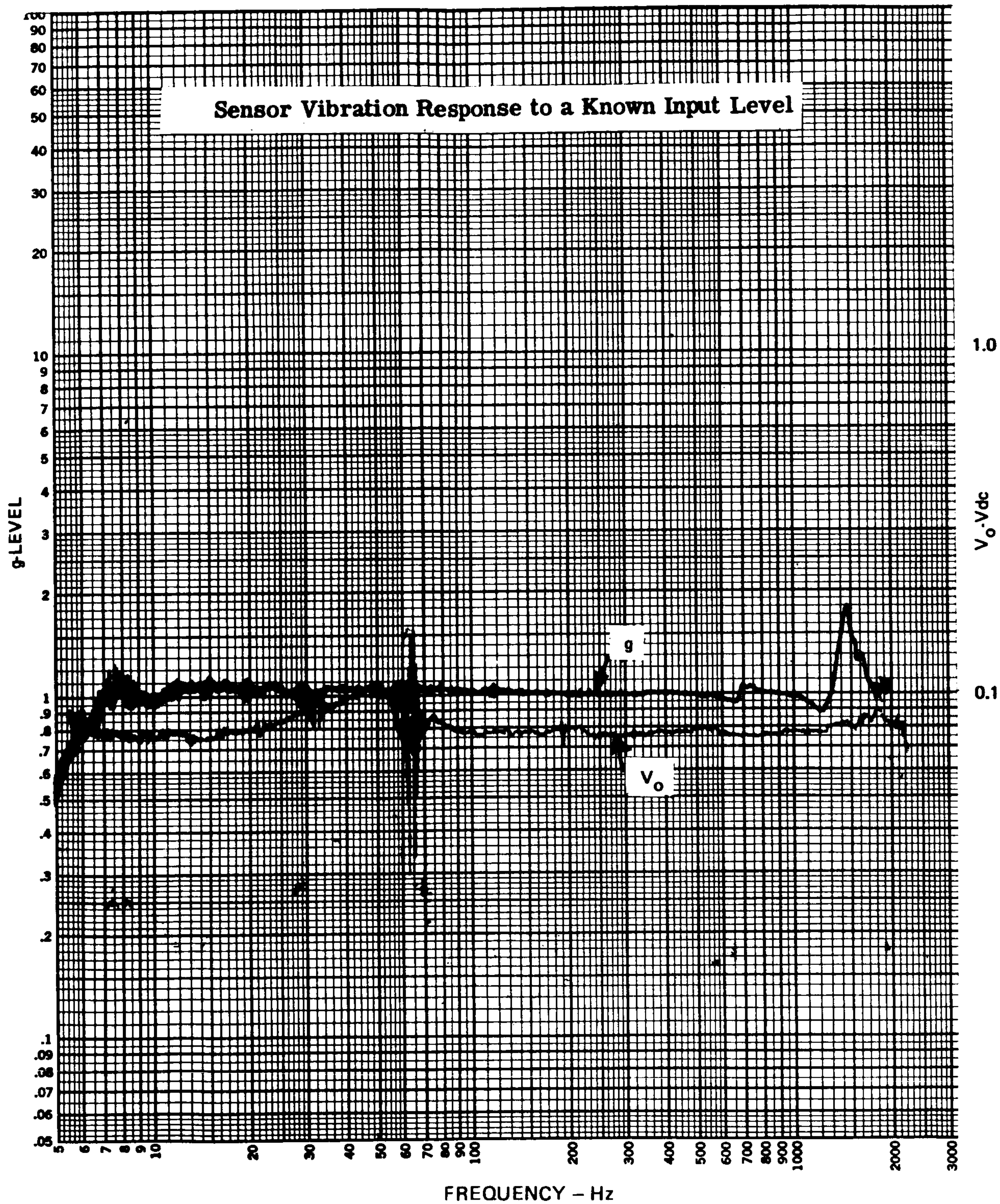

Figure 15a. Unit 1 Readout Plane (Uncancelled) - Environmental Test Set 1

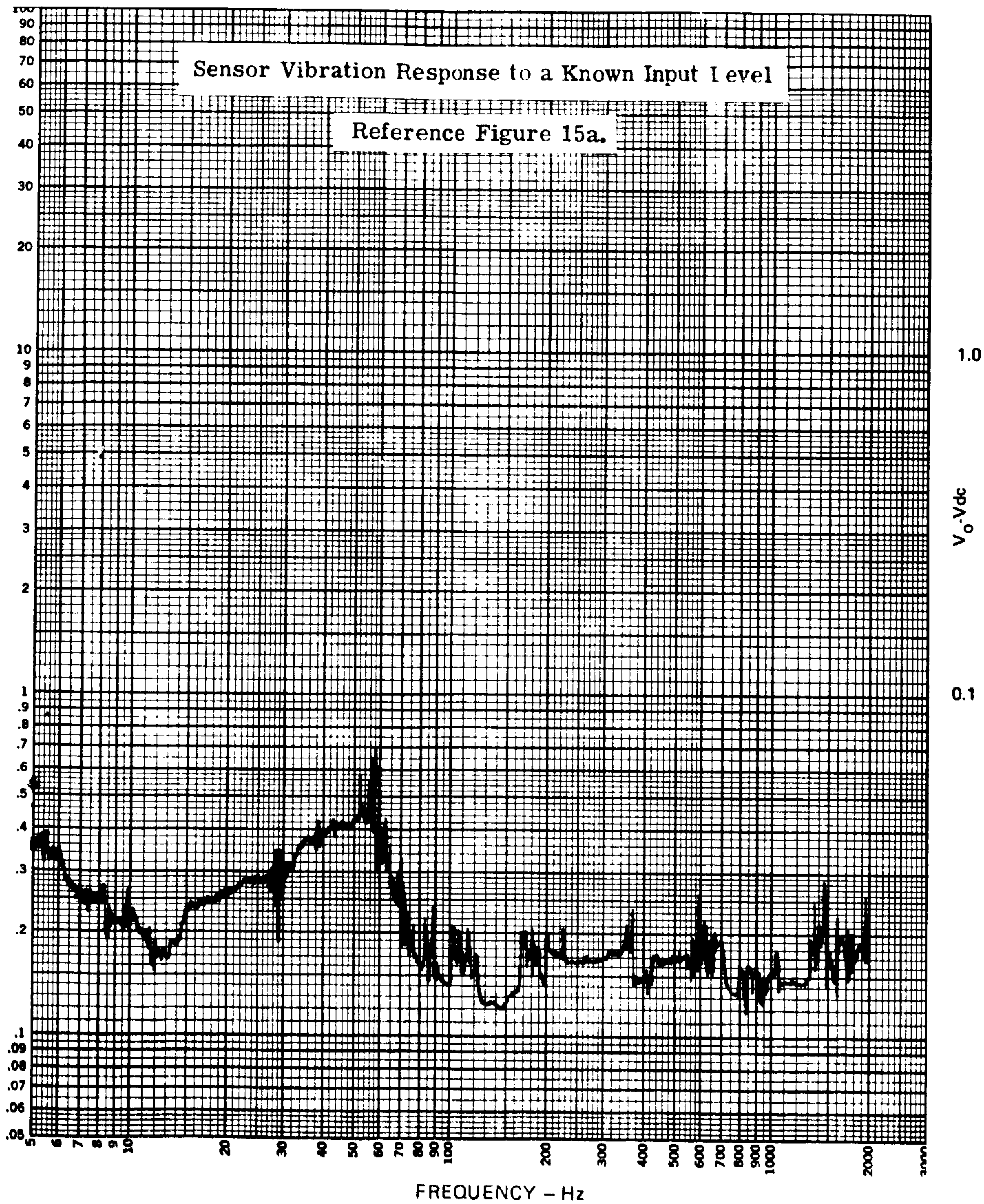

Figure 15b. Unit 1 Readout Plane (Cancelled) - Environmental Test Set 1

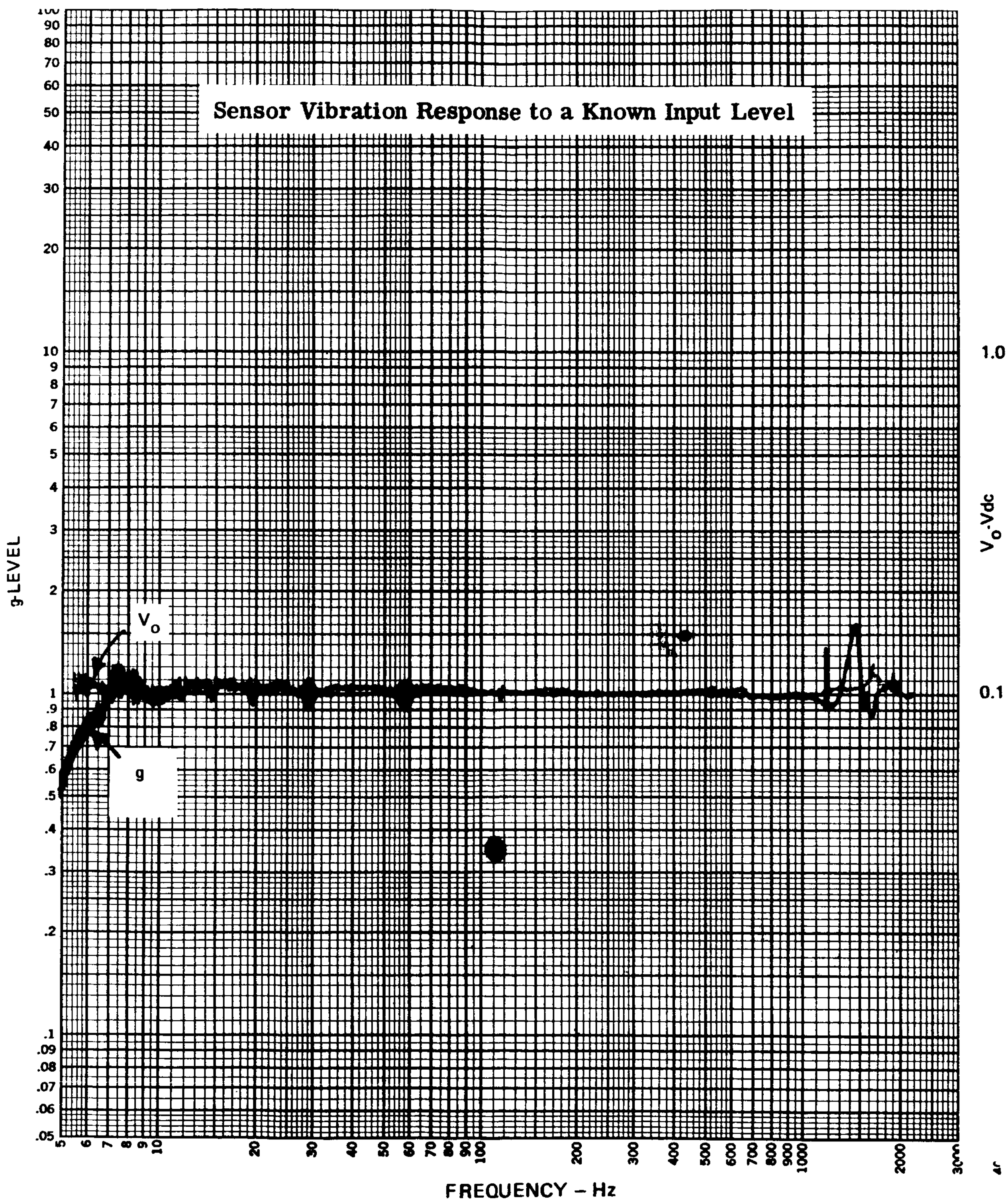

Figure 16a. Unit 1 Drive Plane (Uncancelled) - Environmental Test Set 1

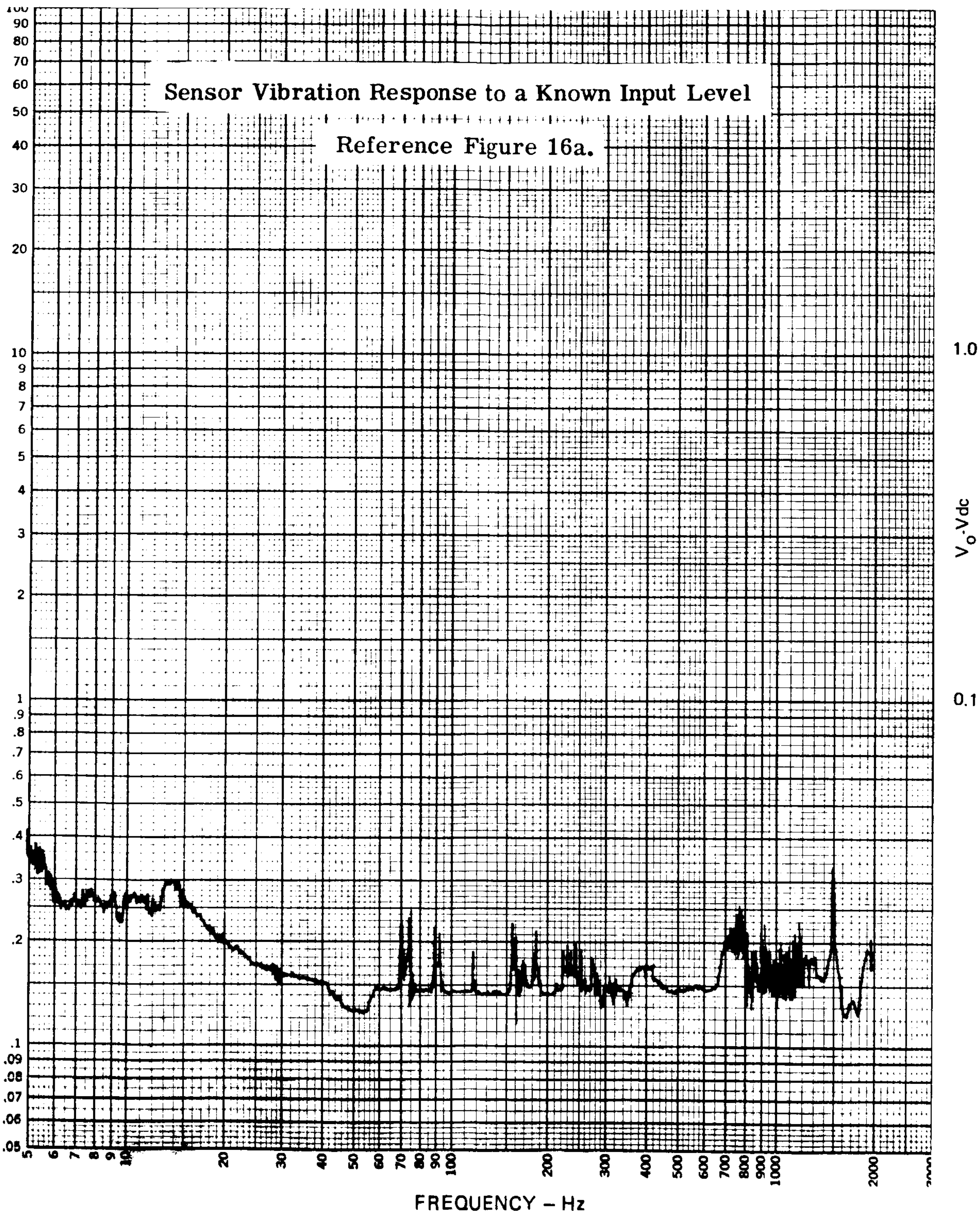

Figure 16b. Unit 1 Drive Plane (Cancelled) - Environmental Test Set 1

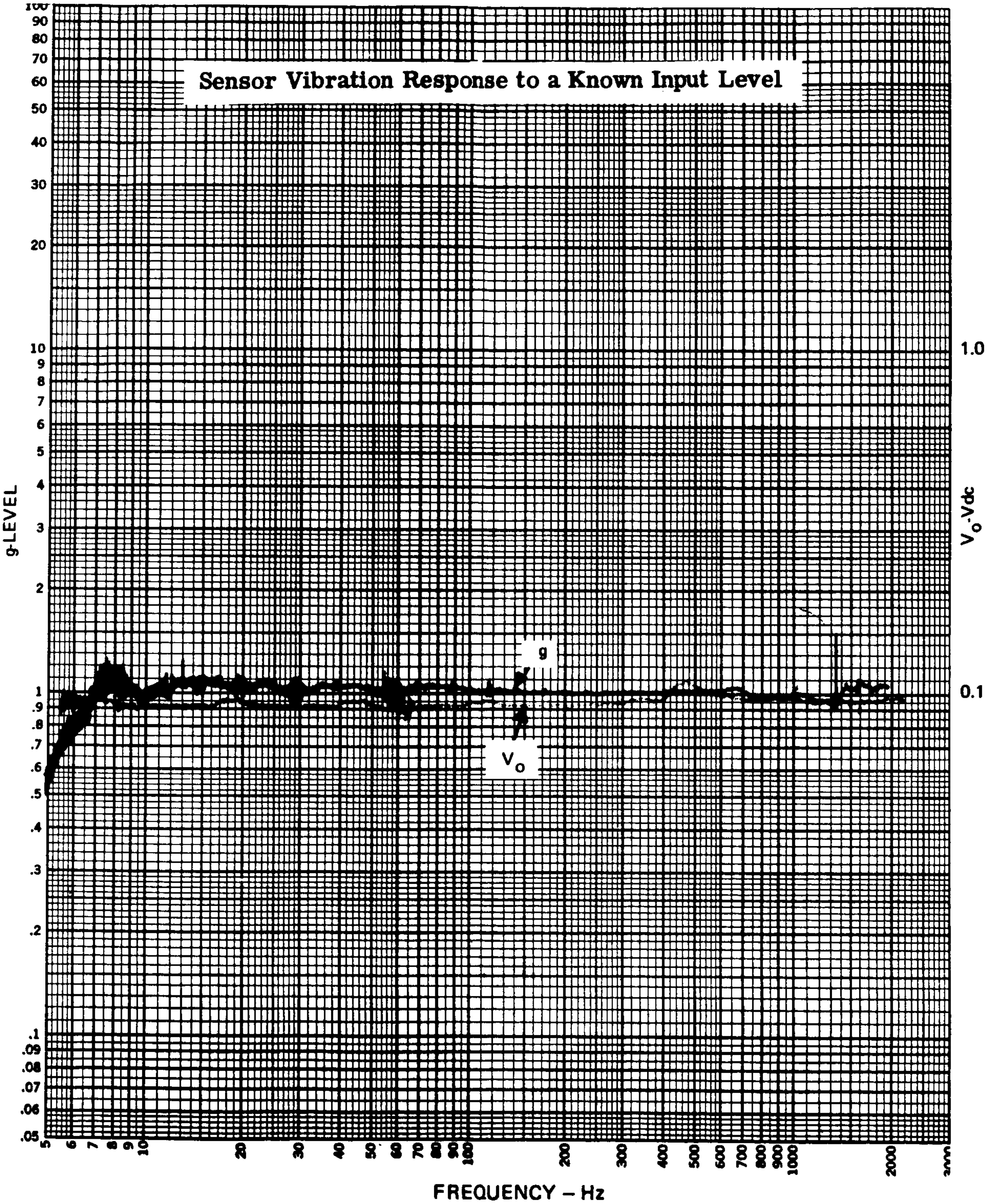

Figure 17a. Unit 1 Axial Plane (Uncancelled) - Environmental Test Set 1

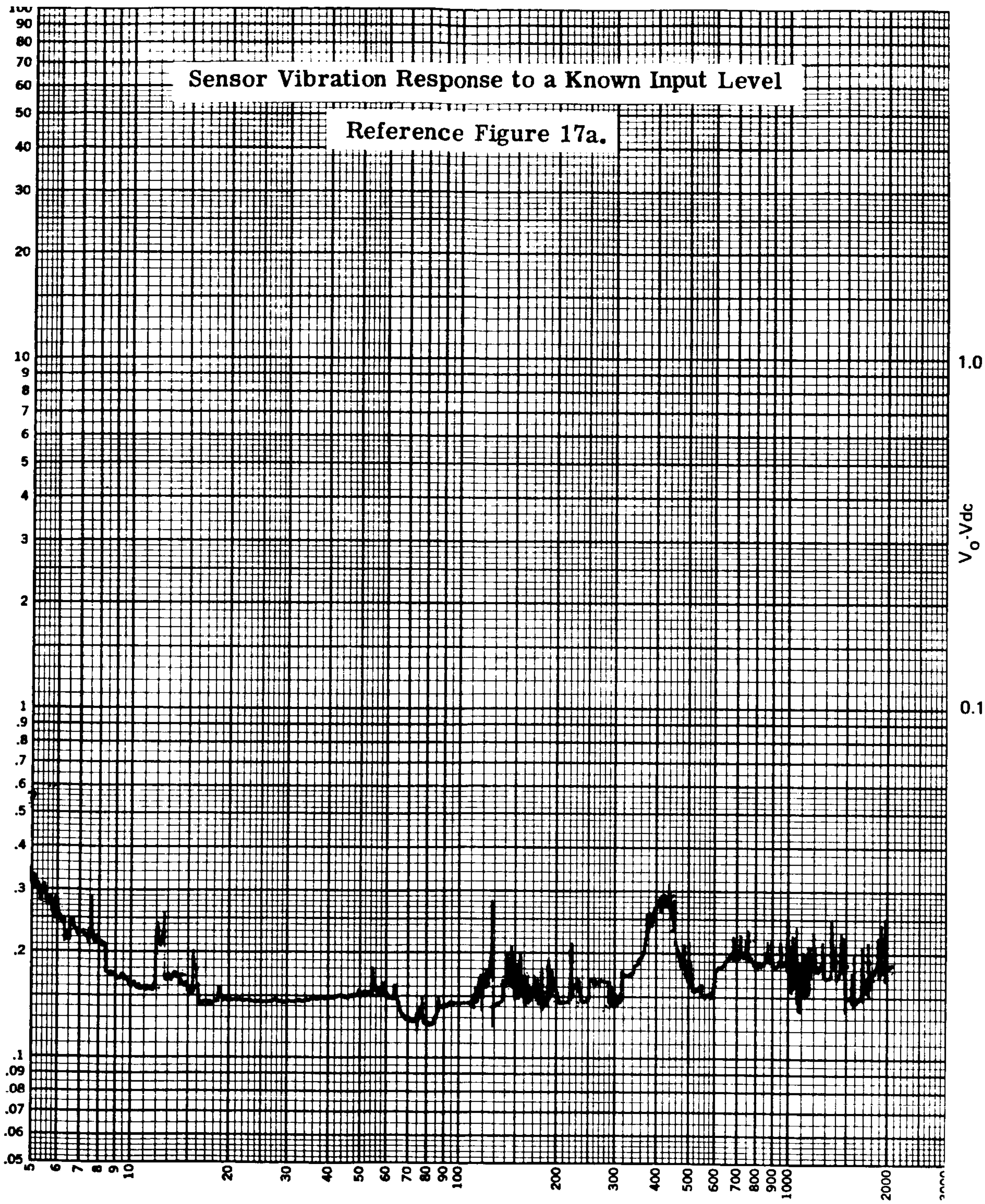

Figure 17b. Unit 1 Axial Plane (Cancelled) - Environmental Test Set 1

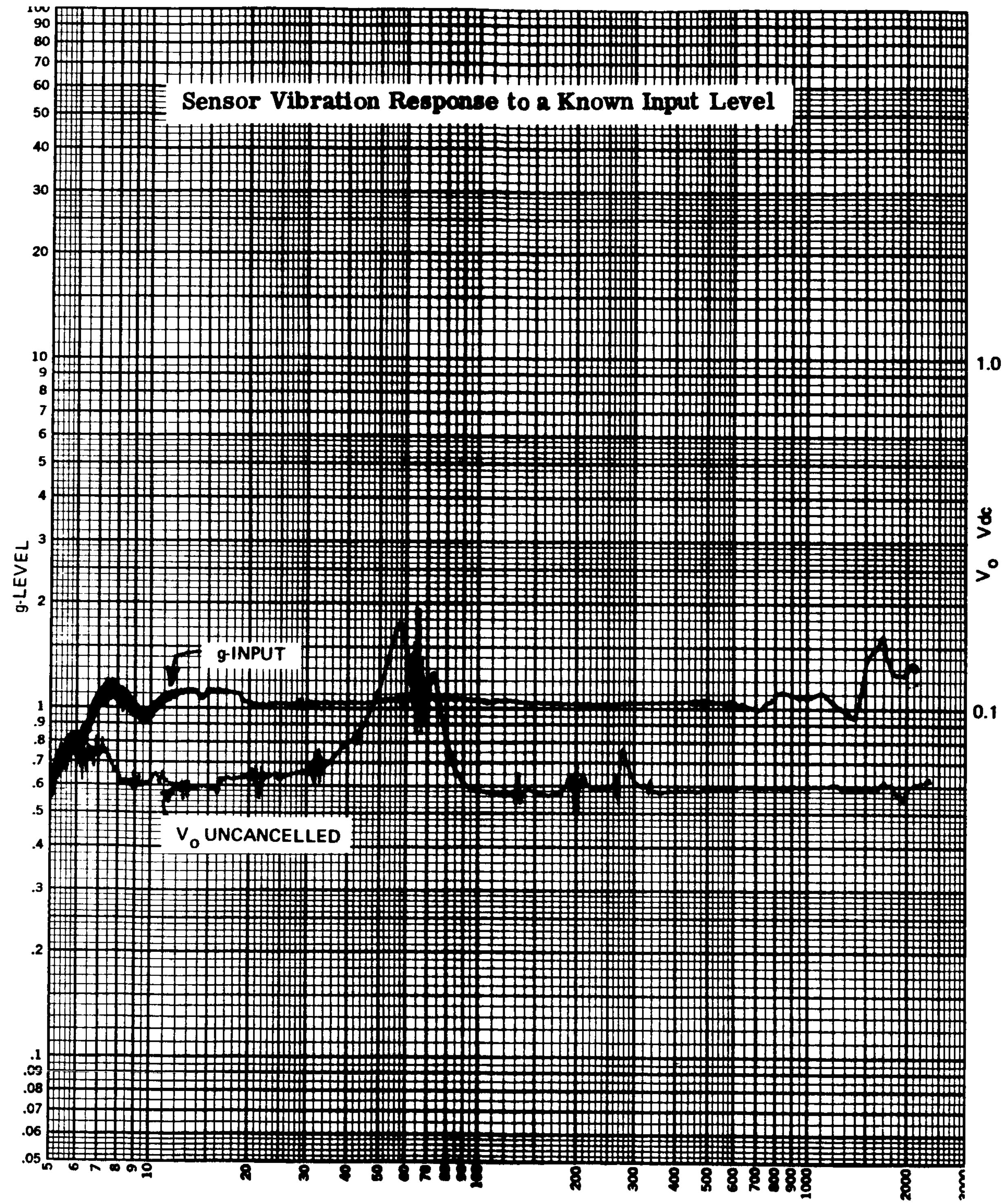

Figure 18a. **Unit 2 Readout Plane (Uncancelled) - Environmental Test Set 1**

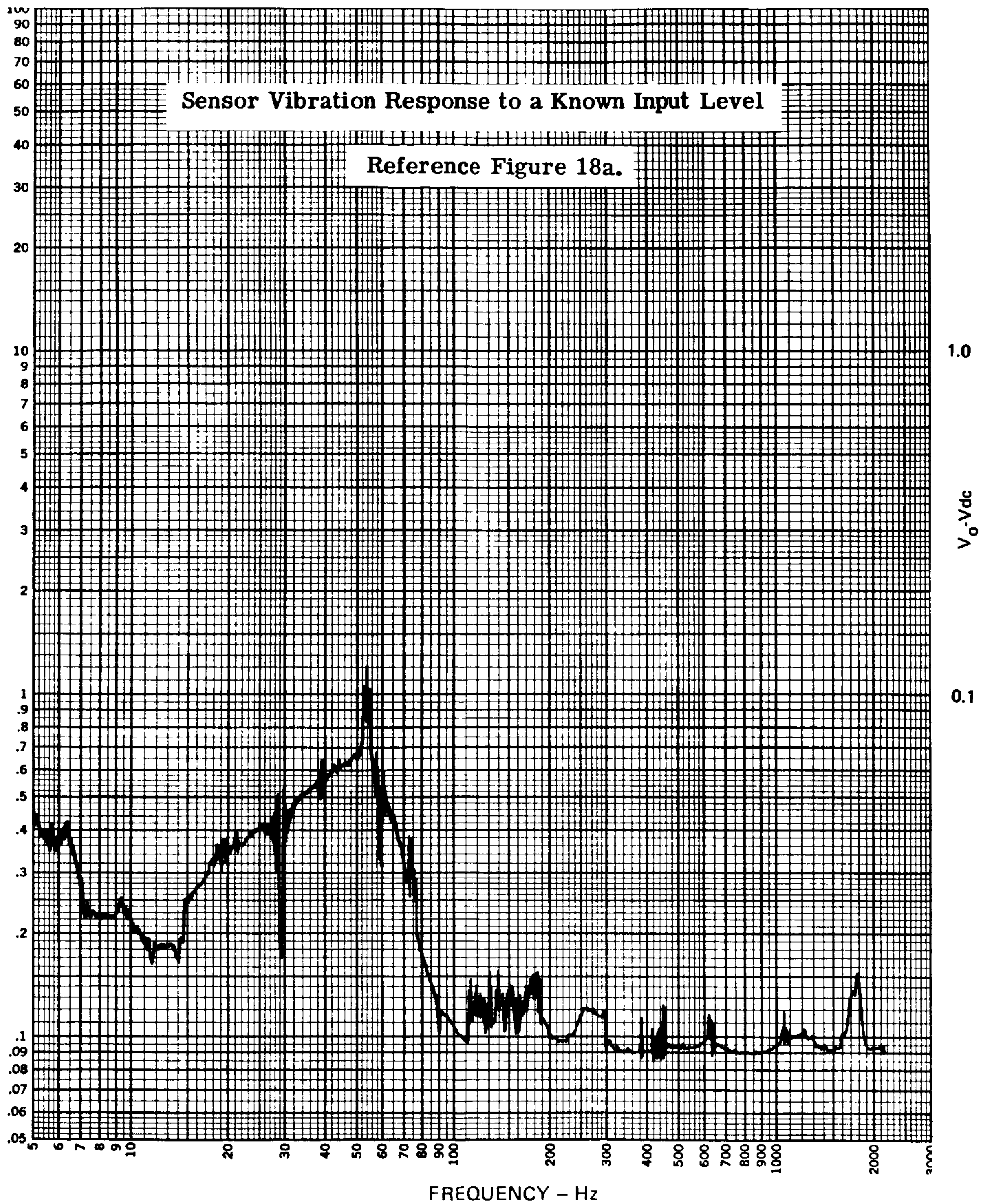

Figure 18b. Unit 2 Readout Plane (Cancelled) - Environmental Test Set 1

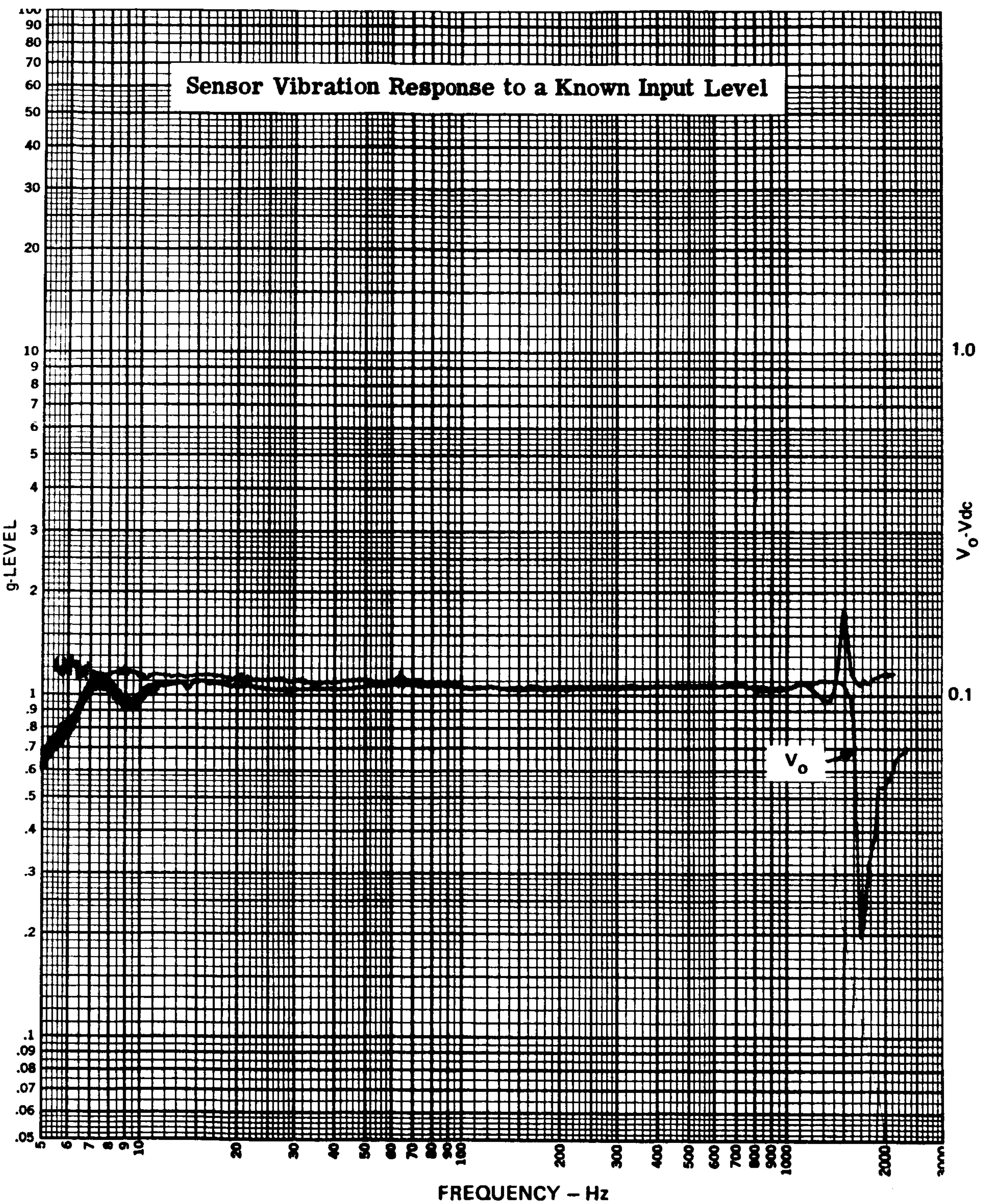

Figure 19a. Unit 2 Drive Plane (Uncancelled) - Environmental Test Set 1

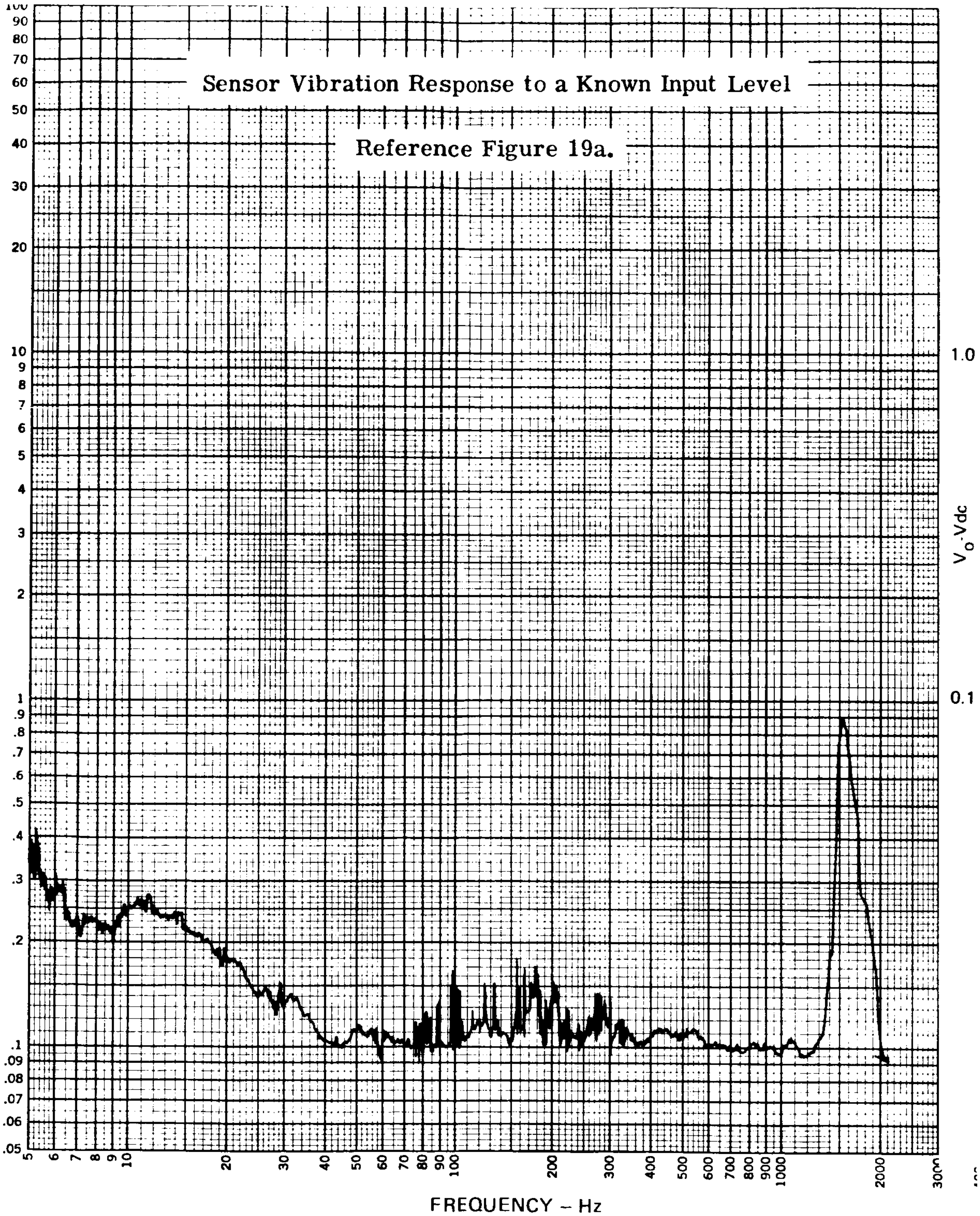

Figure 19b. Unit 2 Drive Plane (Cancelled) - Environmental Test Set 1

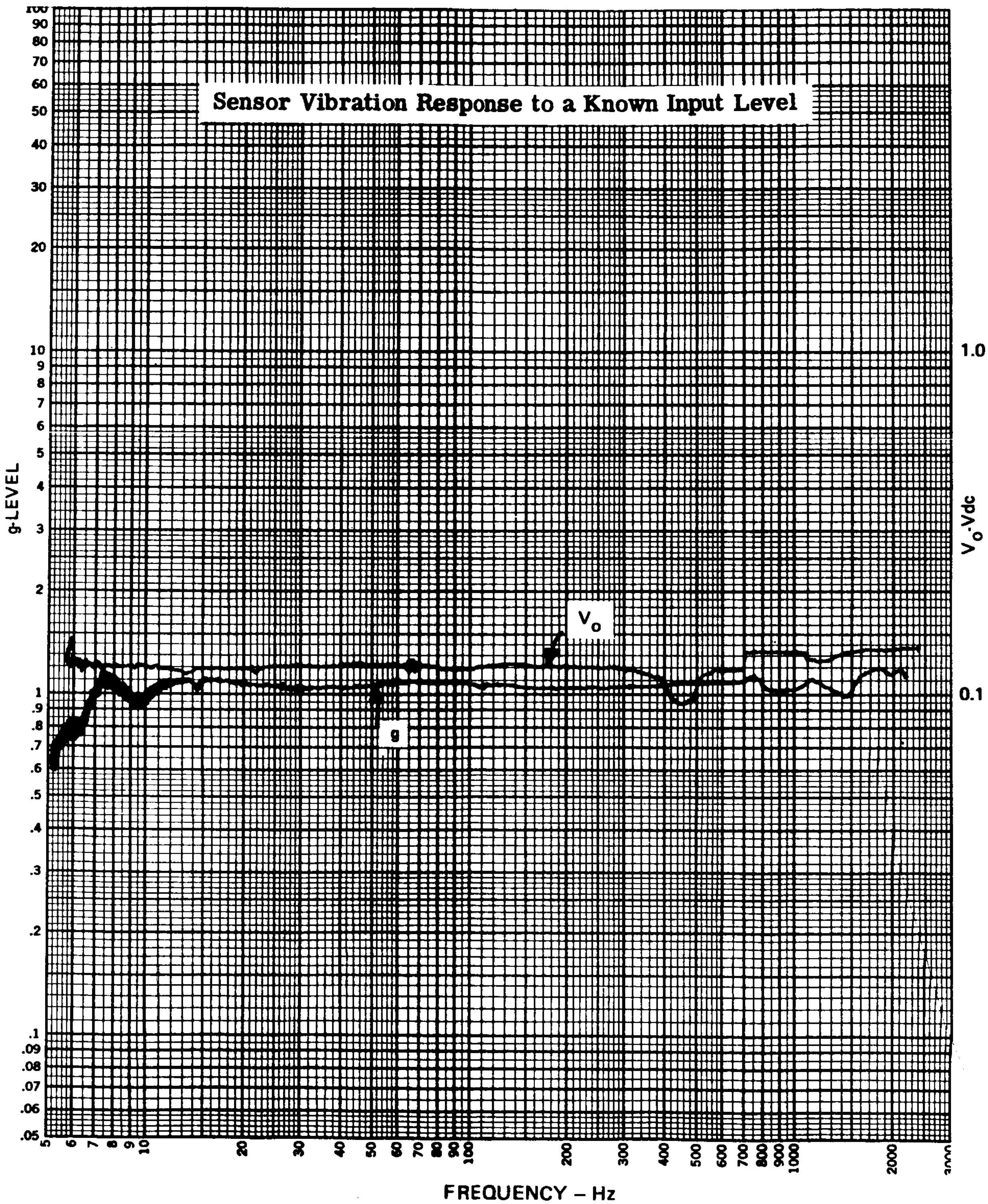

Figure 20a. Unit 2 Axial Plane (Uncancelled) - Environmental Test Set 1

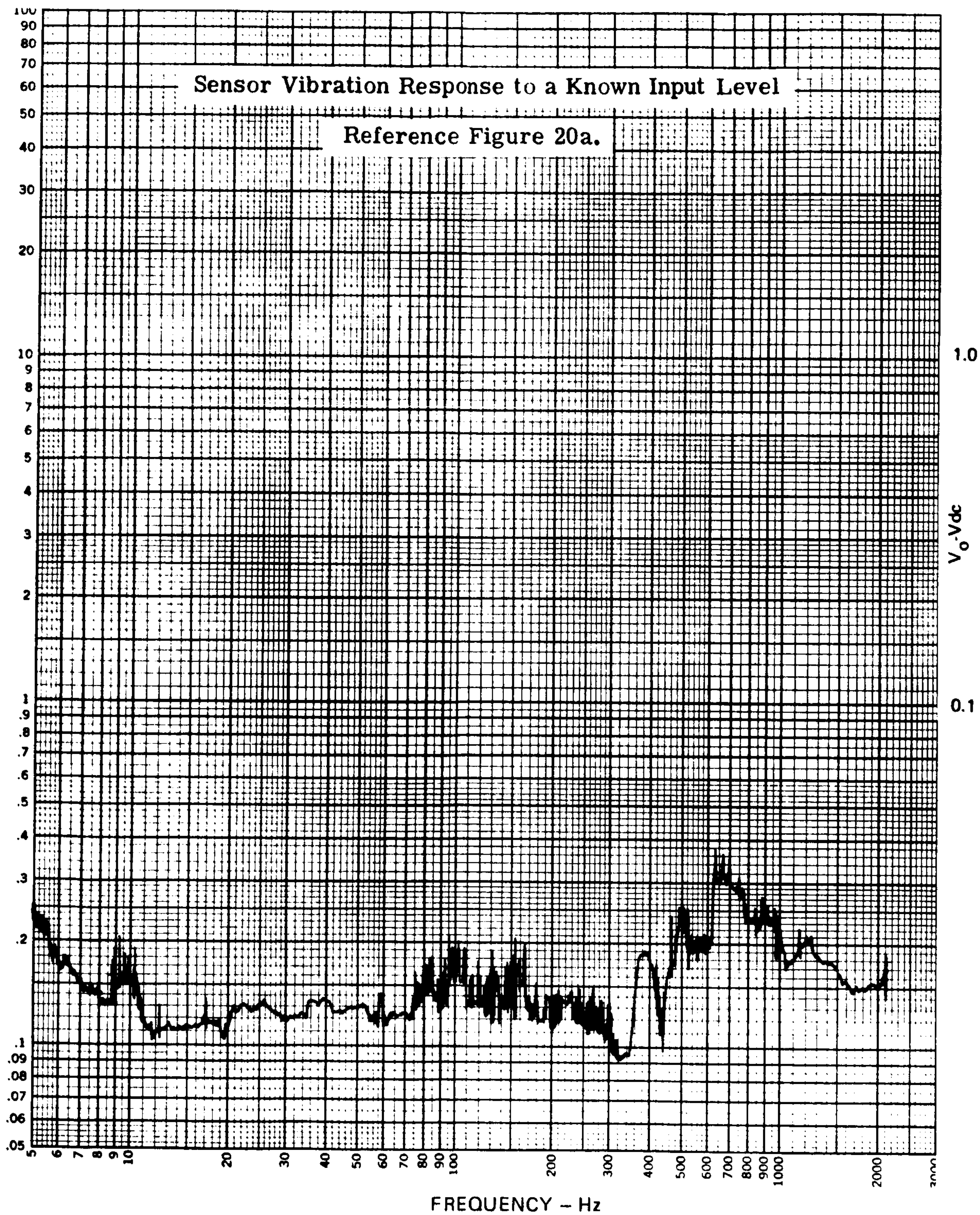

Figure 20b. Unit 2 Axial Plane (Cancelled) - Environmental Test Set 1

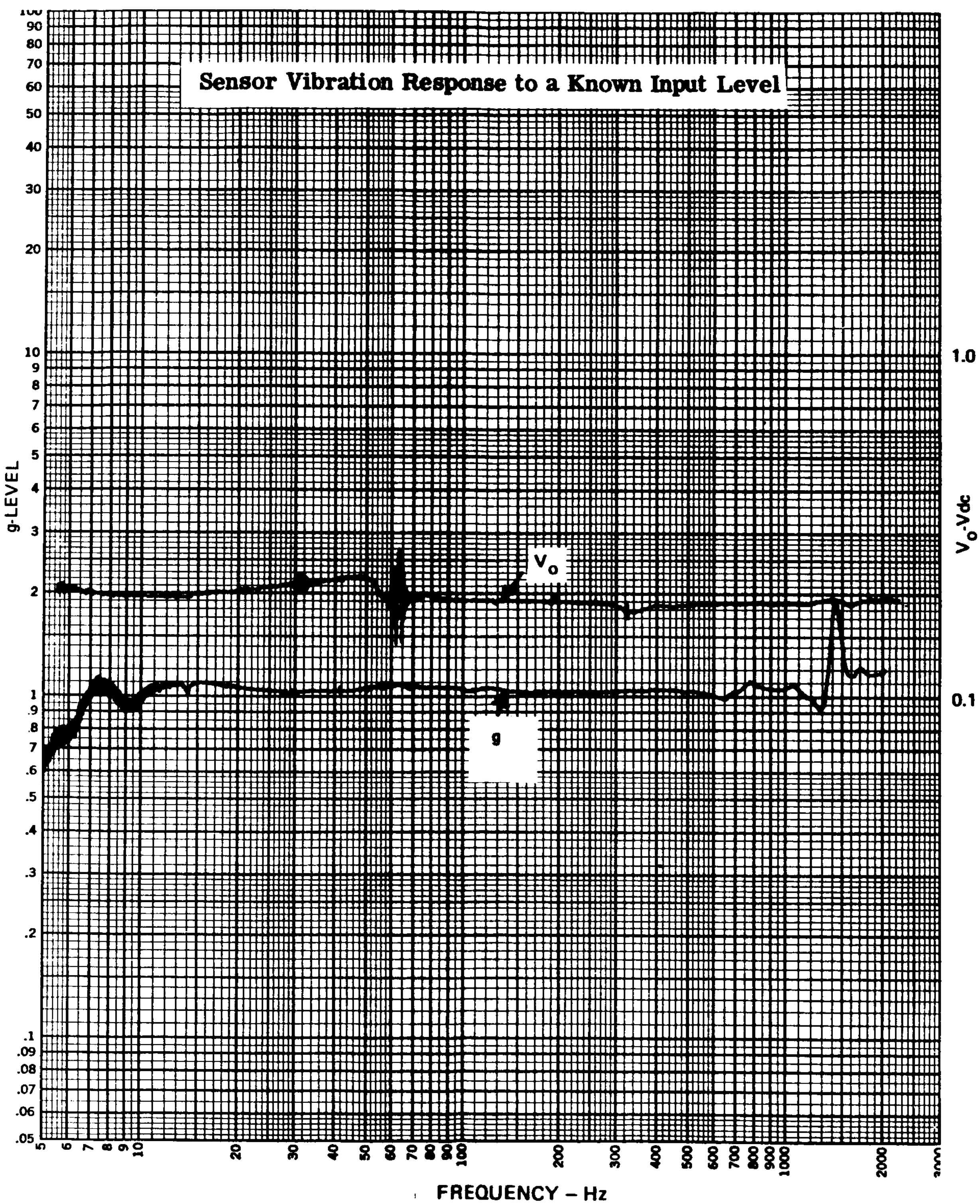

Figure 21a. **Unit 3 Readout Plane (Uncancelled) - Environmental Test Set 1**

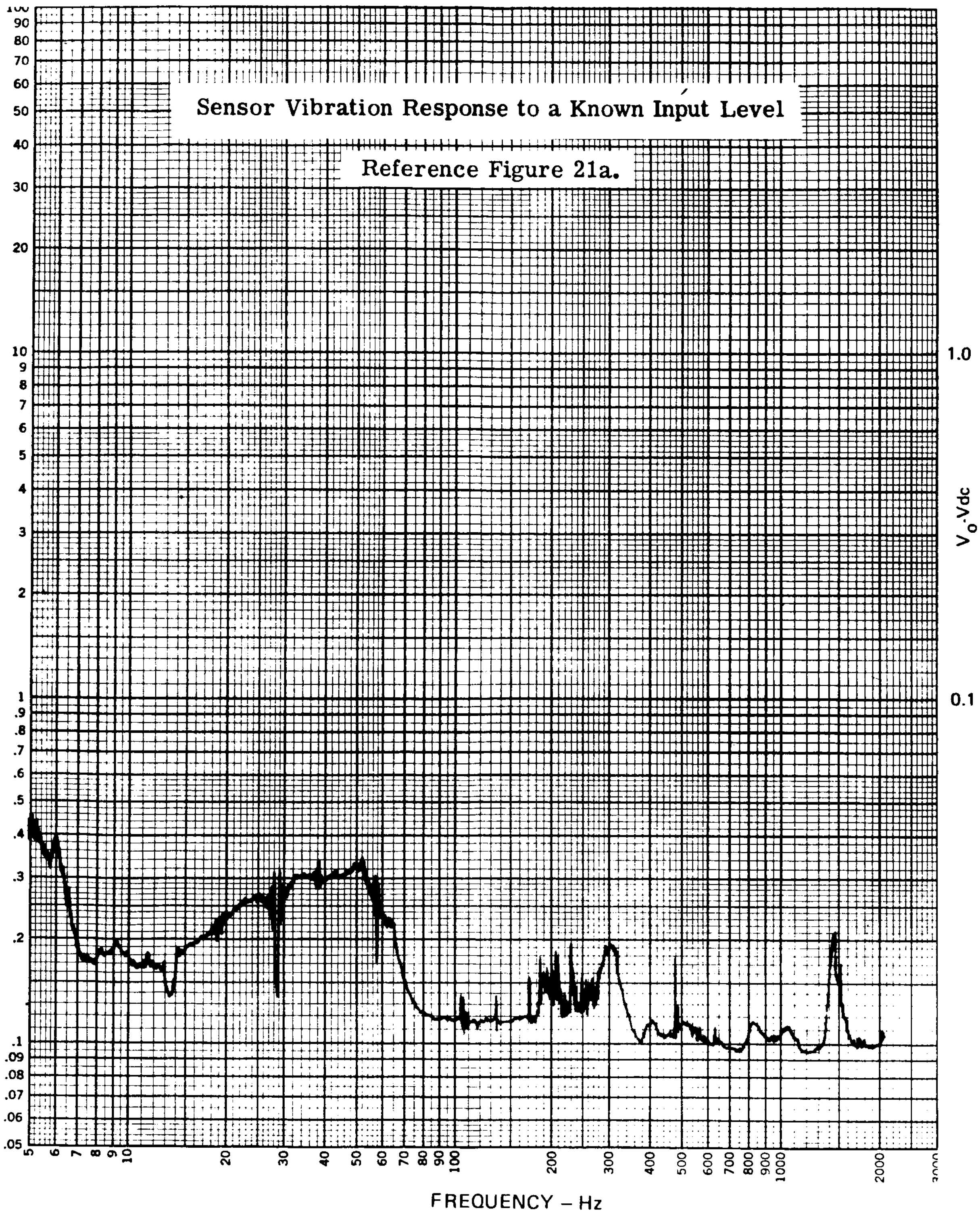

Figure 21b. Unit 3 Readout Plane (Cancelled) - Environmental Test Set 1

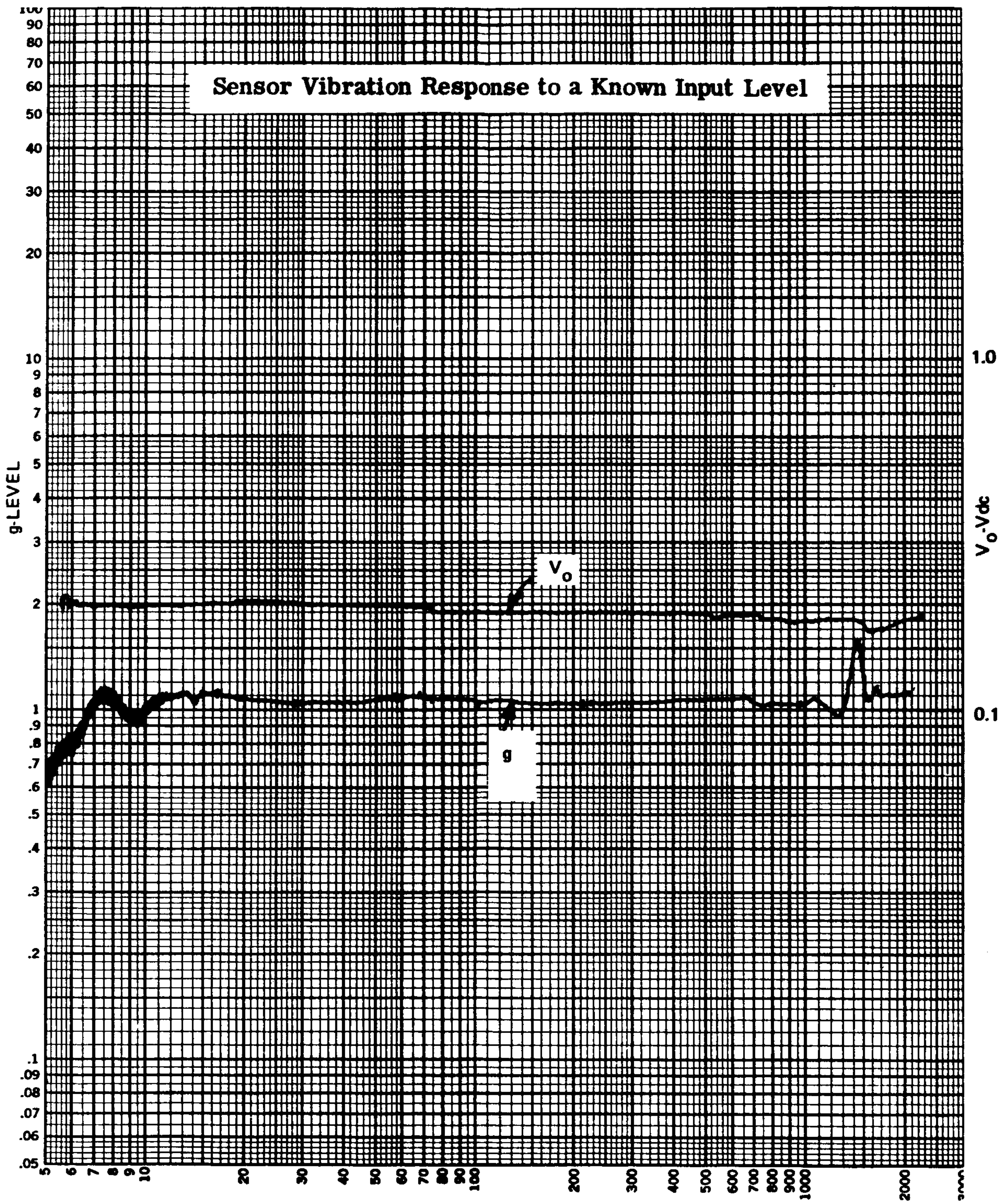

Figure 22a. Unit 3 Drive Plane (Uncancelled) - Environmental Test Set 1

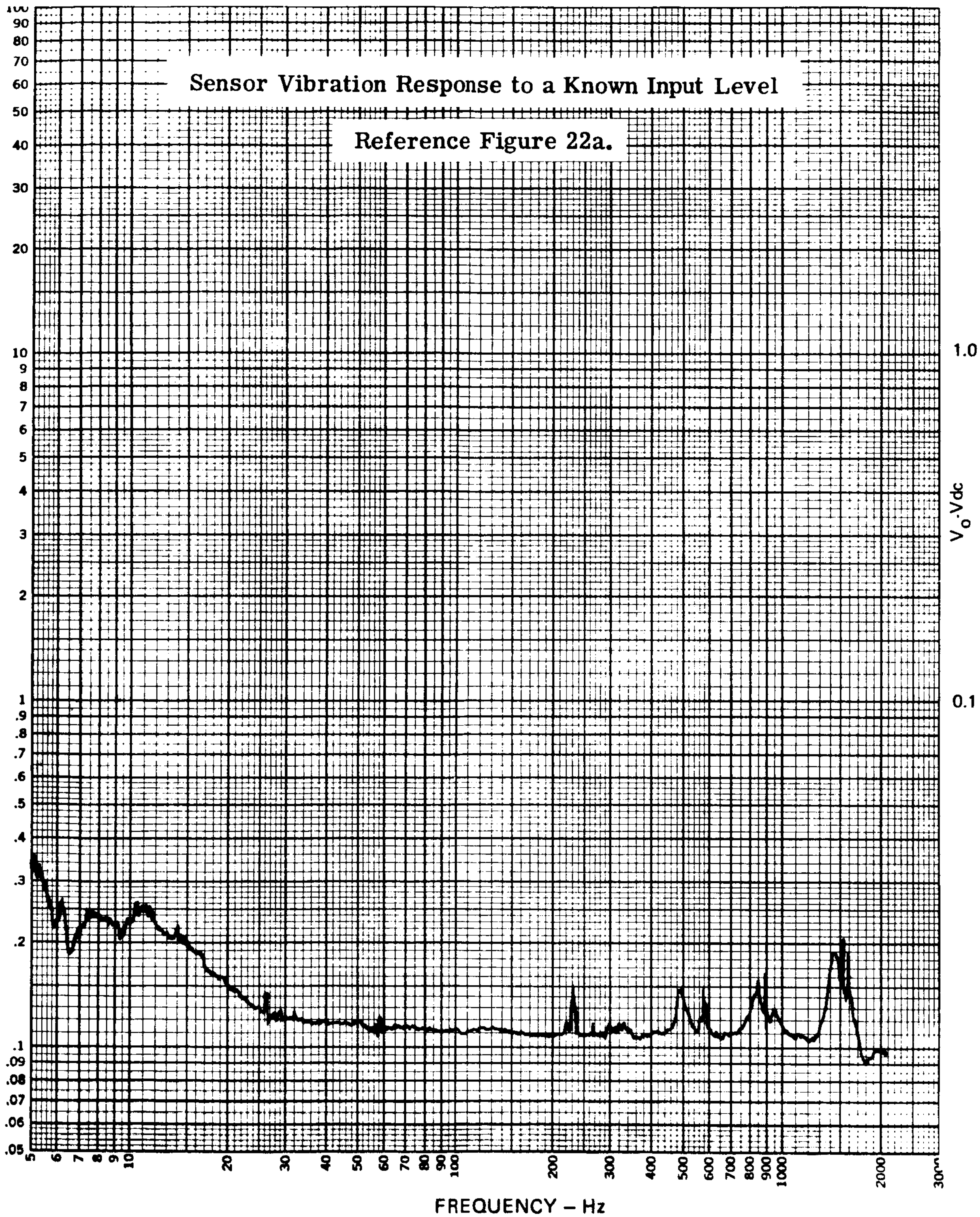

Figure 22b. Unit 3 Drive Plane (Cancelled) - Environmental Test Set 1

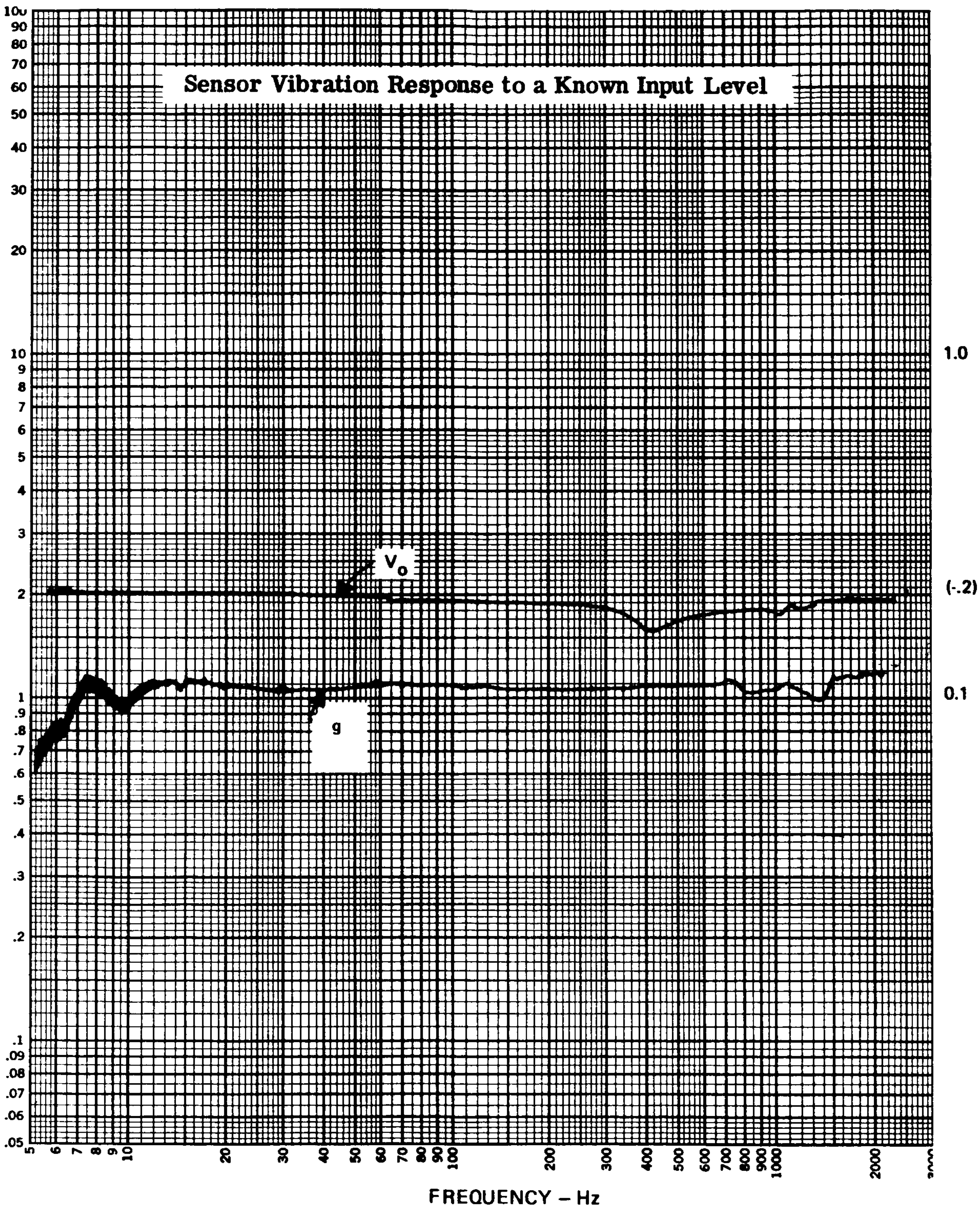

Figure 23a. Unit 3 Axial Plane (Uncancelled) - Environmental Test Set 1

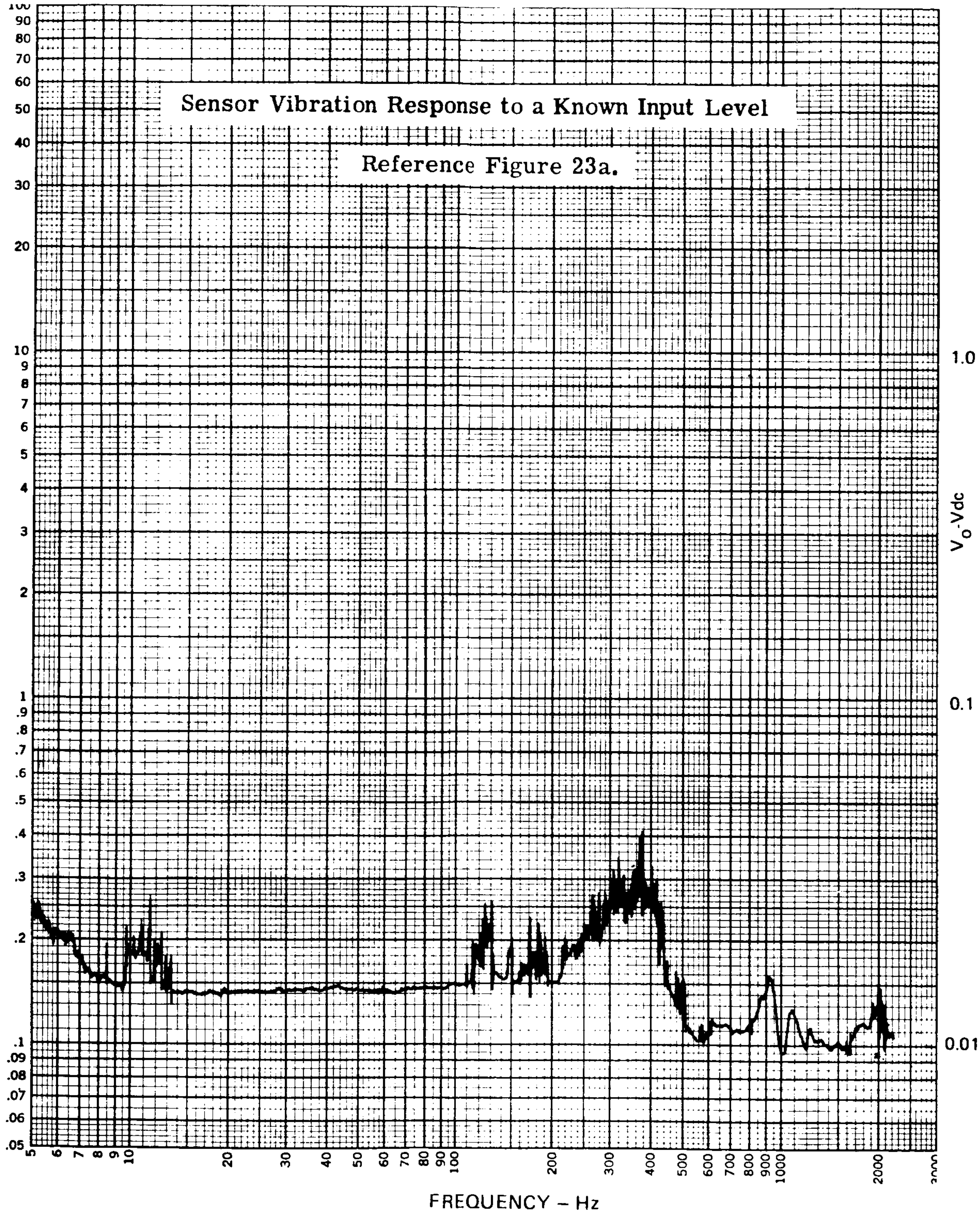

Figure 23b. Unit 3 Axial Plane (Cancelled) - Environmental Test Set 1

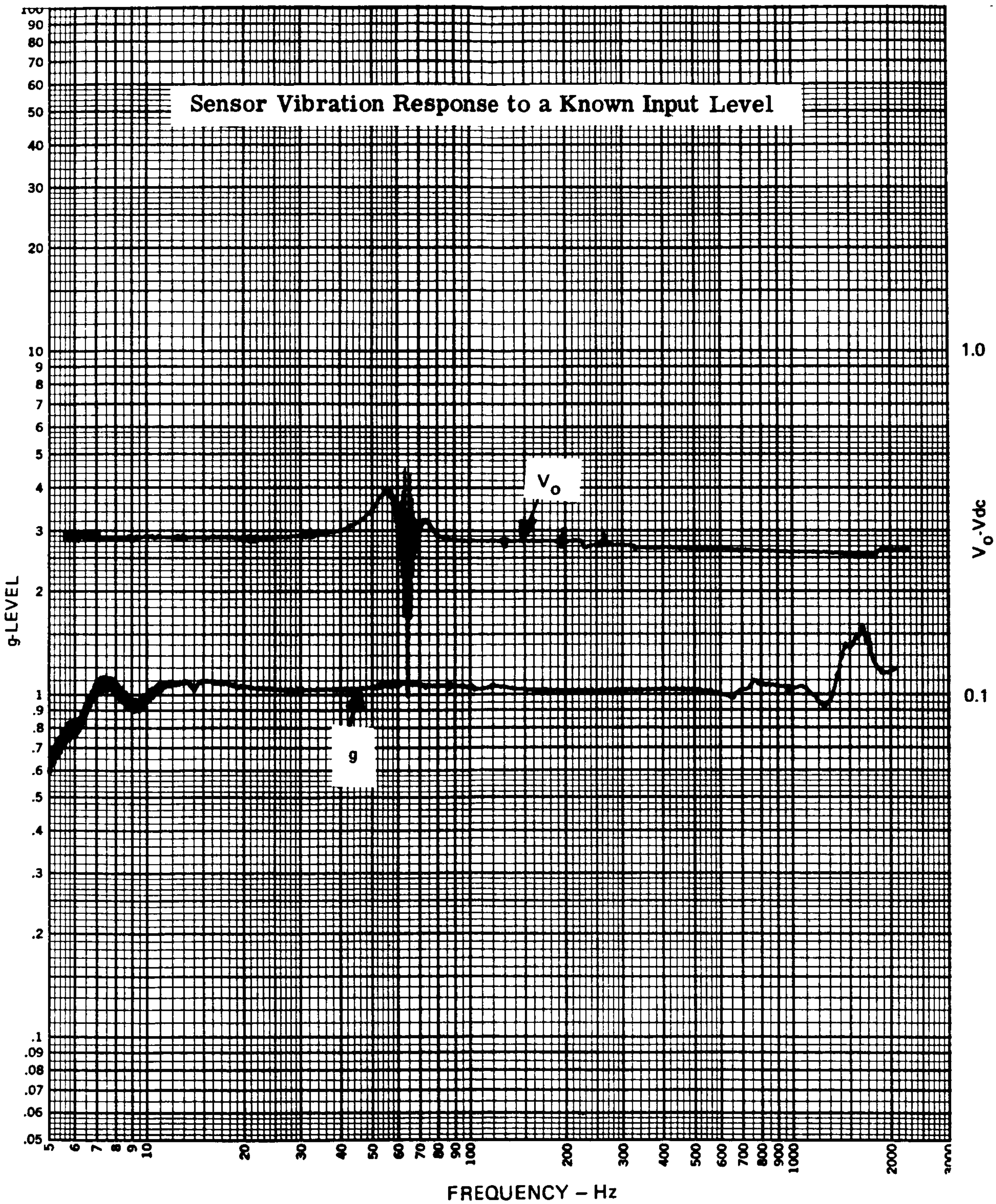

Figure 24a. Unit 4 Readout Plane (Uncancelled) - Environmental Test Set 1

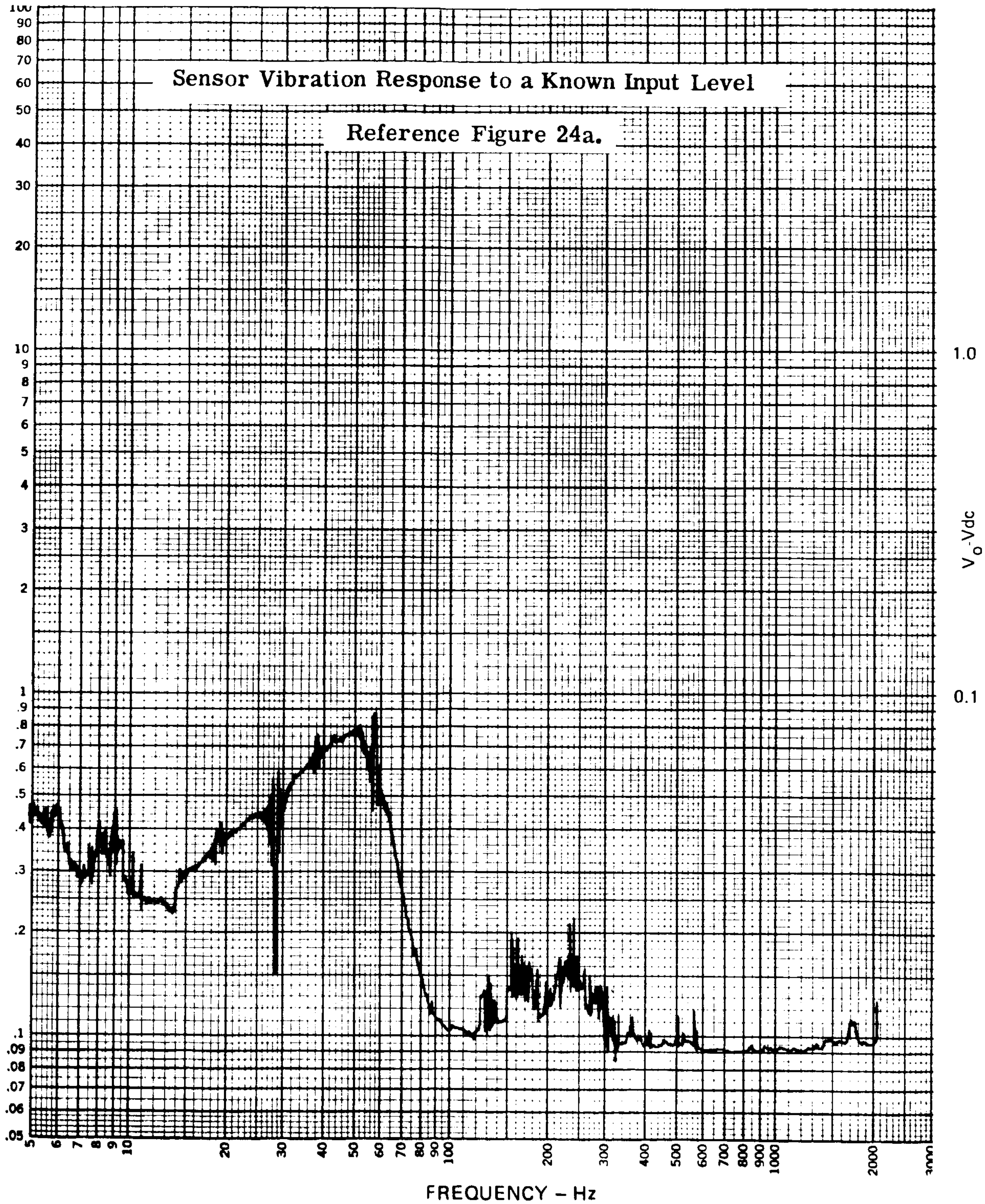

Figure 24b. Unit 4 Readout Plane (Cancelled) - Environmental Test Set 1

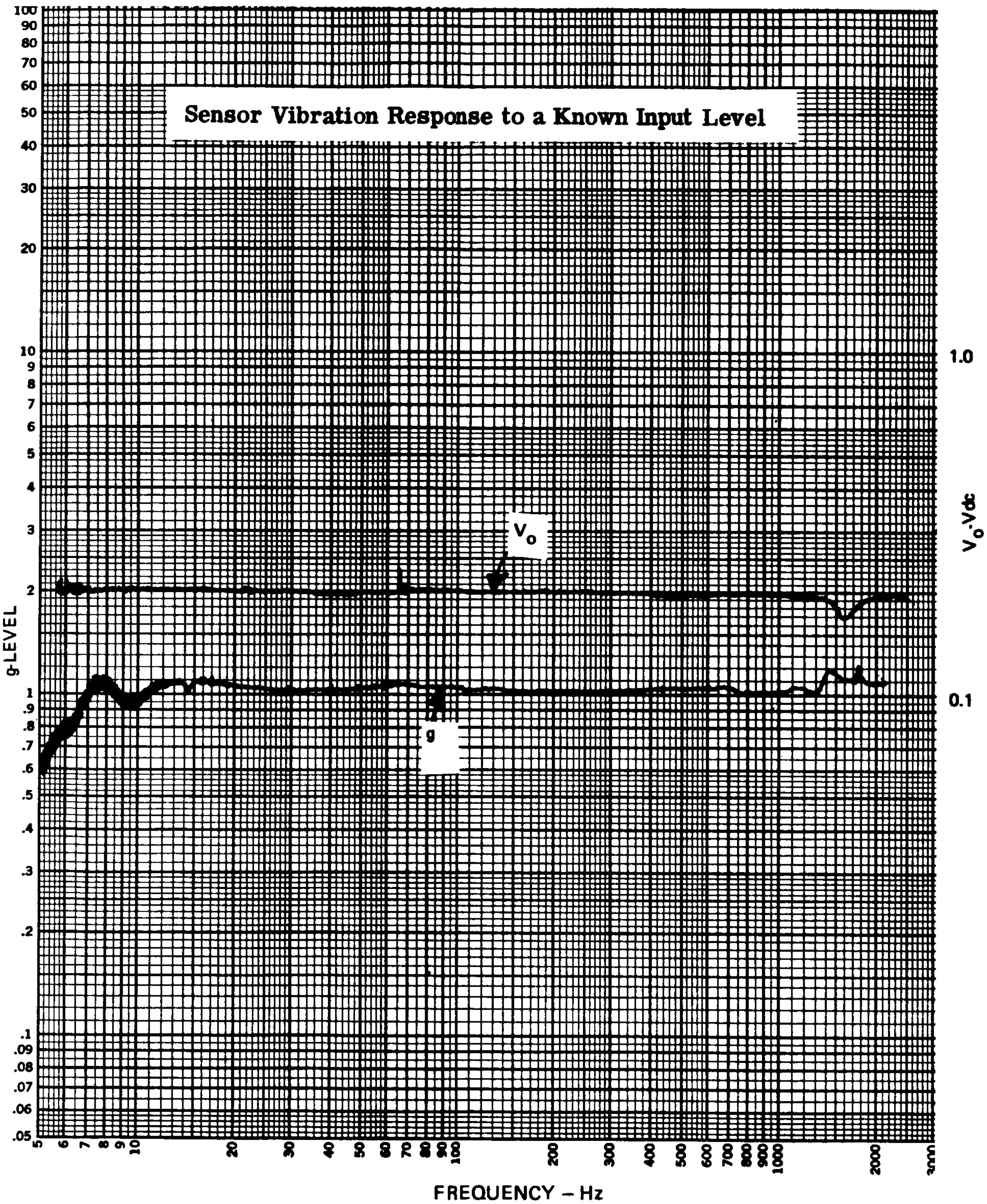

Figure 25a. Unit 4 Drive Plane (Uncancelled) - Environmental Test Set 1

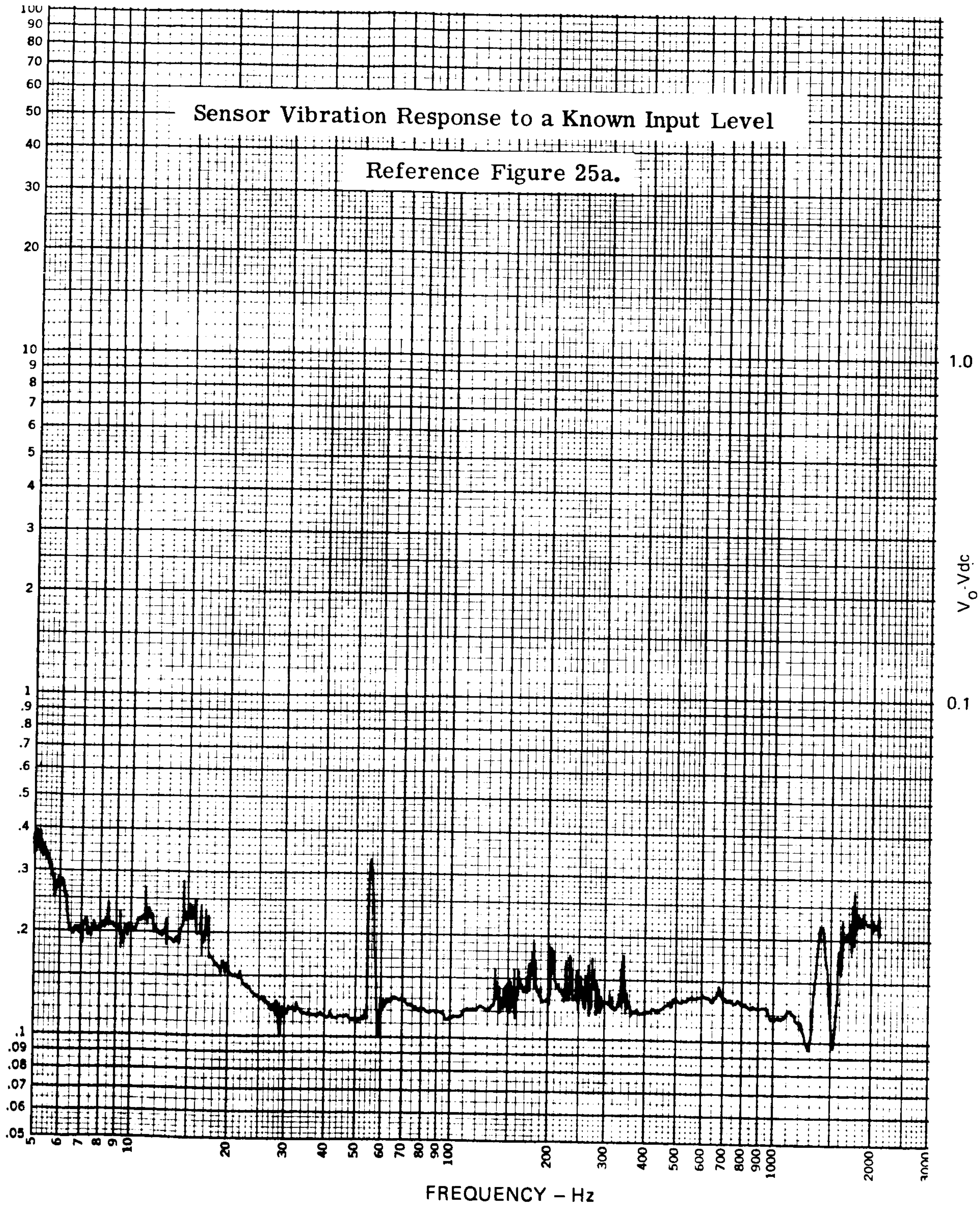

Figure 25b. Unit 4 Drive Plane (Cancelled) - Environmental Test Set 1

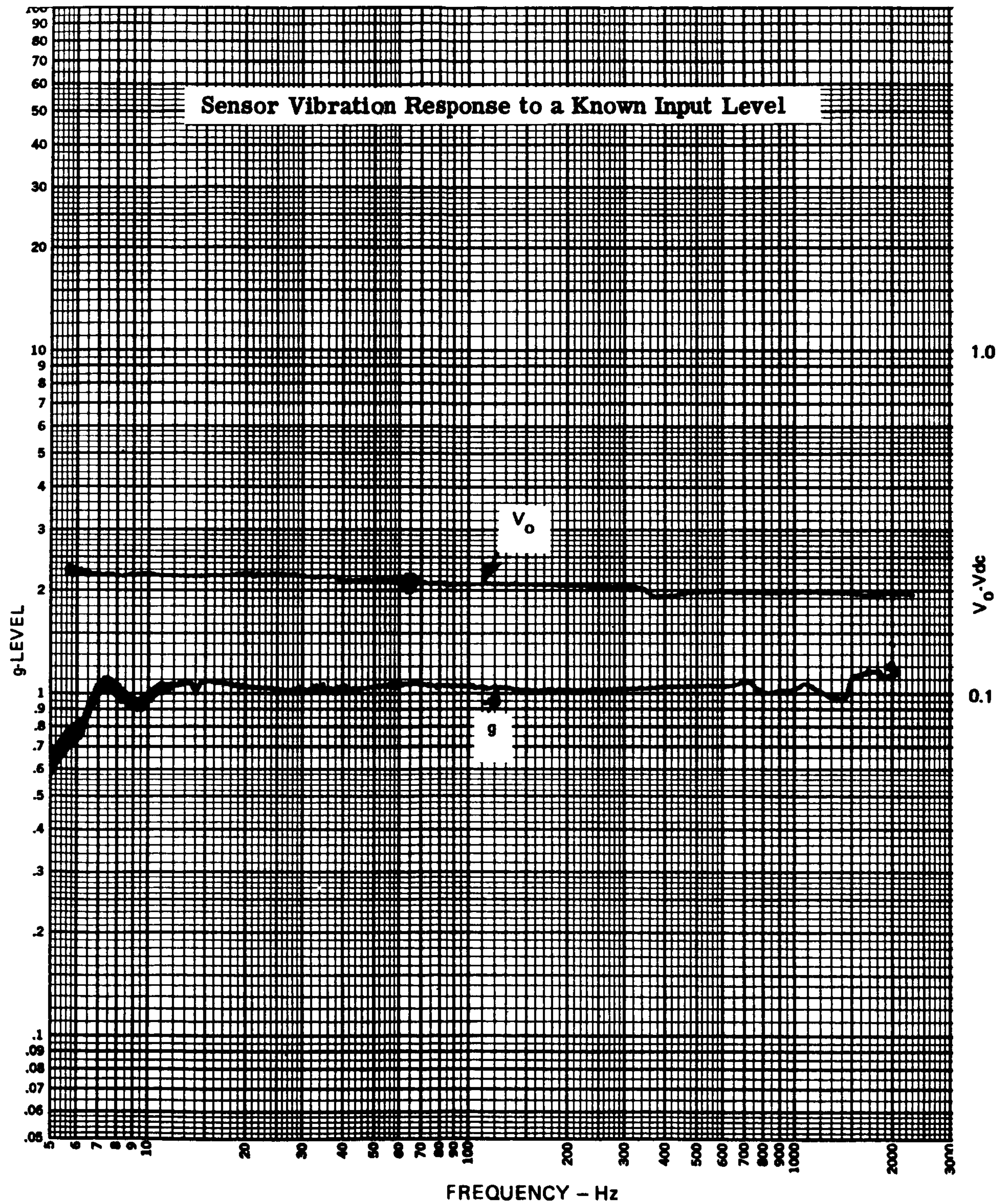

Figure 26a. Unit 4 Axial Plane (Uncancelled) - Environmental Test Set 1

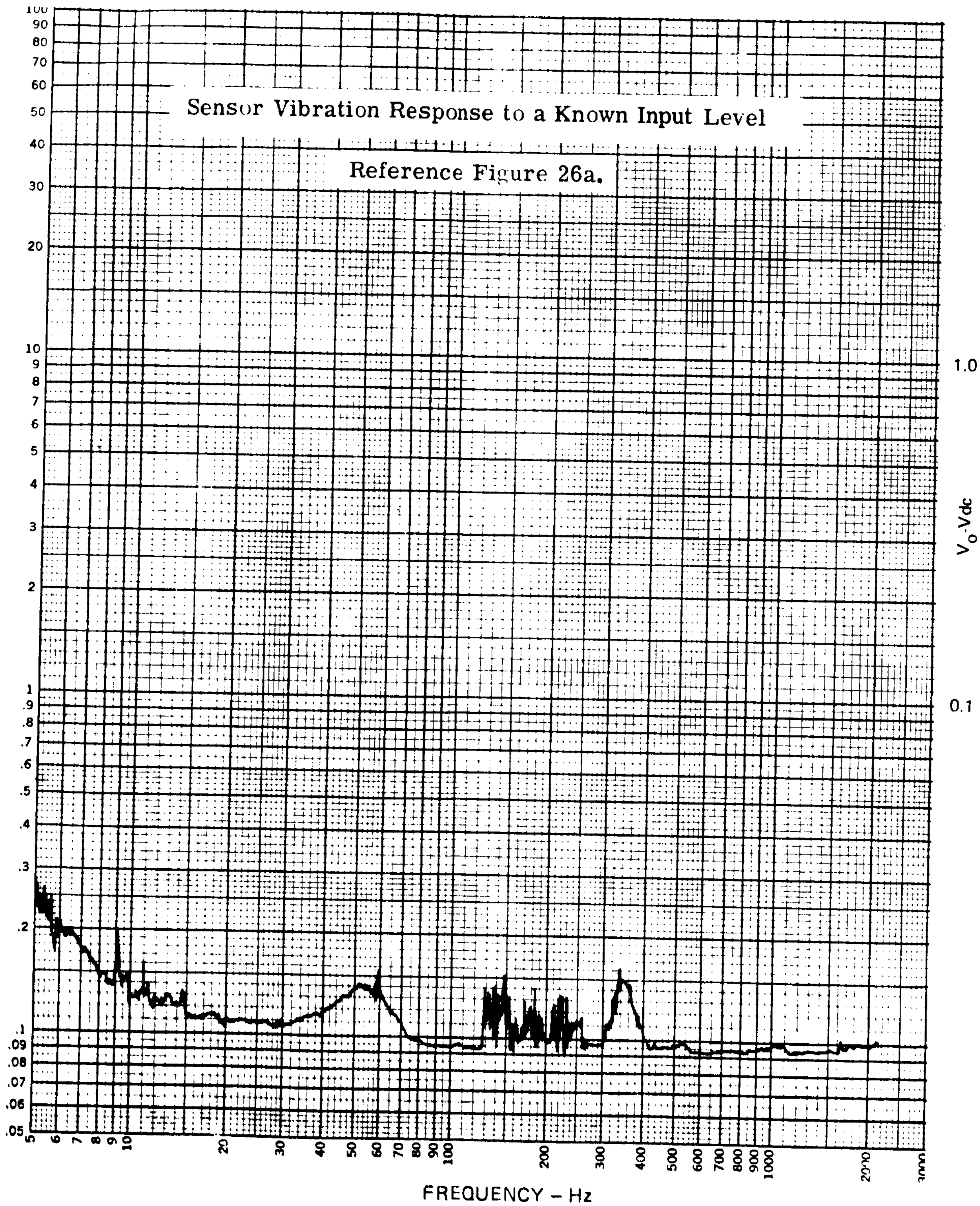

Figure 26b. Unit 4 Axial Plane (Cancelled) - Environmental Test Set 1

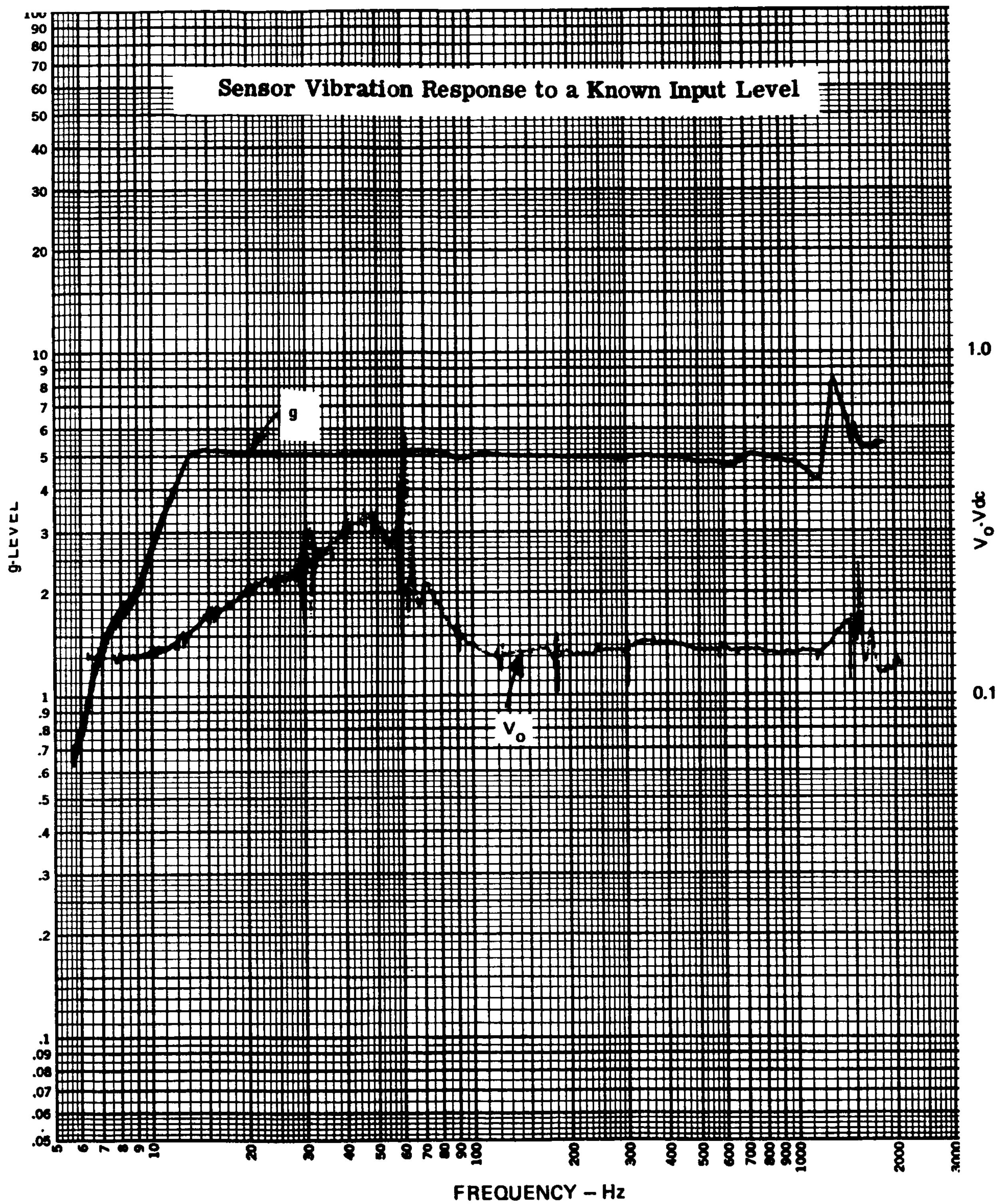

Figure 27a. Unit 1 Readout Plane (Uncancelled) - Environmental Test Set 1

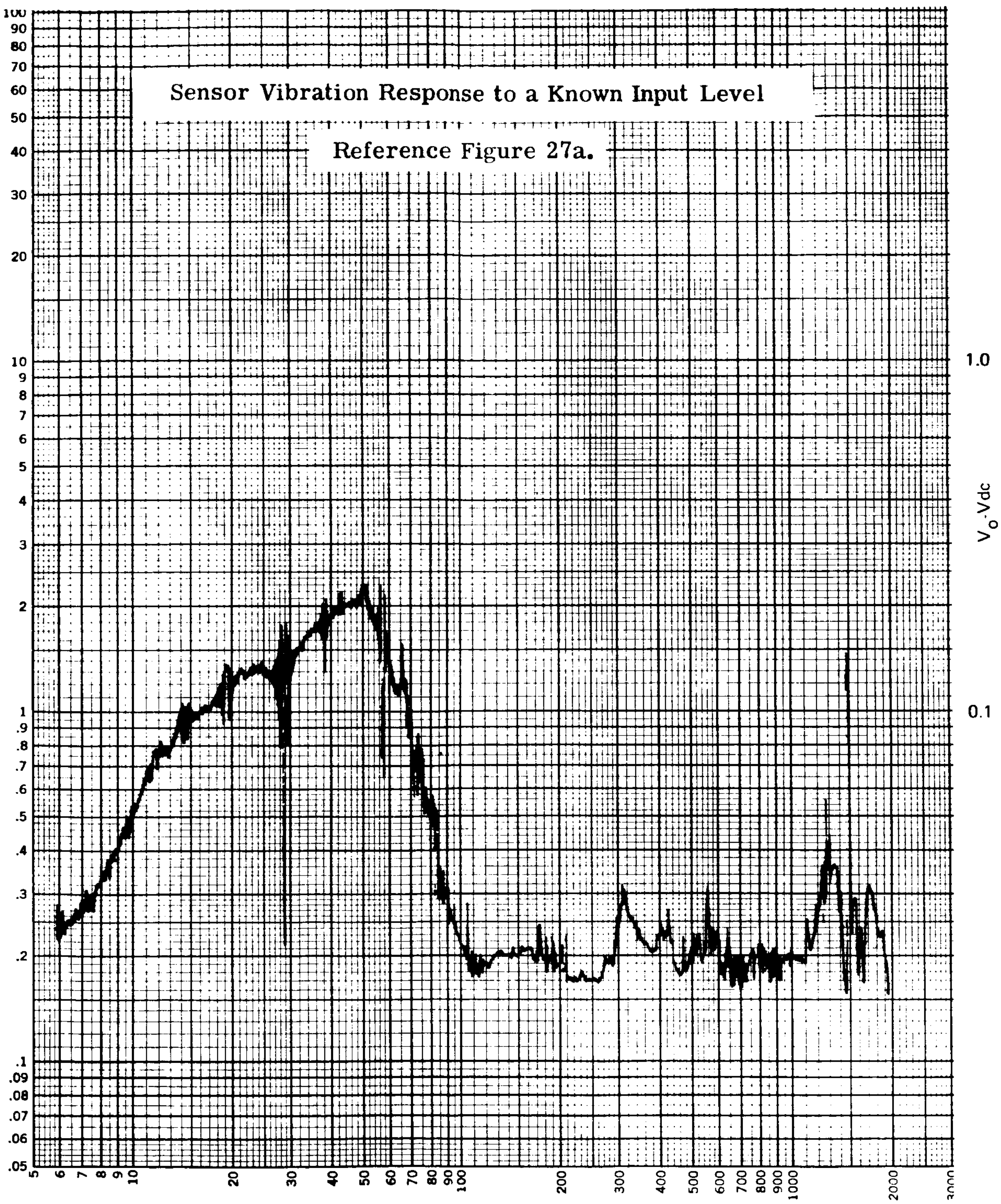

Figure 27b. Unit 1 Readout Plane (Cancelled) - Environmental Test Set 1

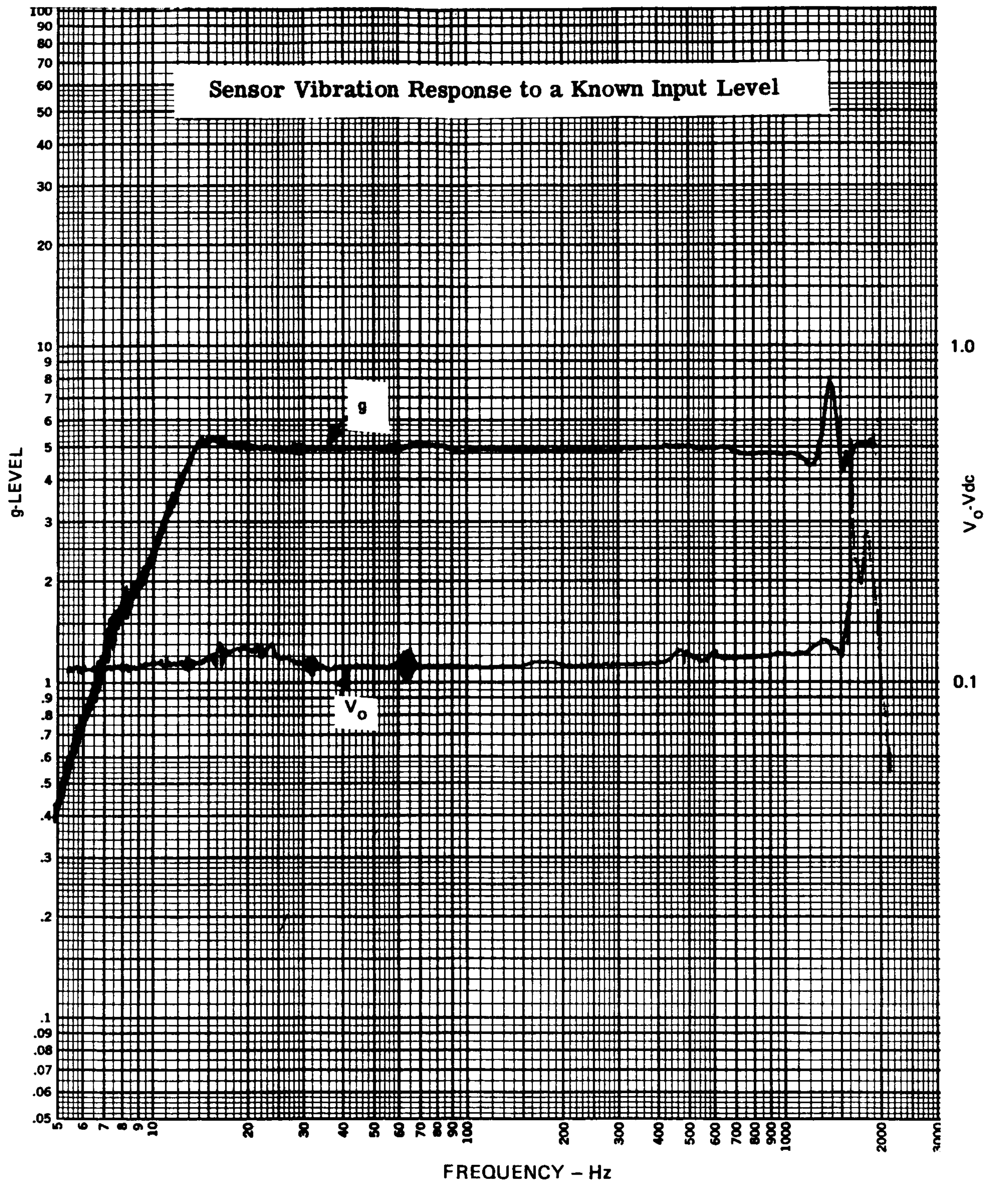

Figure 28a. Unit 1 Drive Plane (Uncancelled) - Environmental Test Set 1

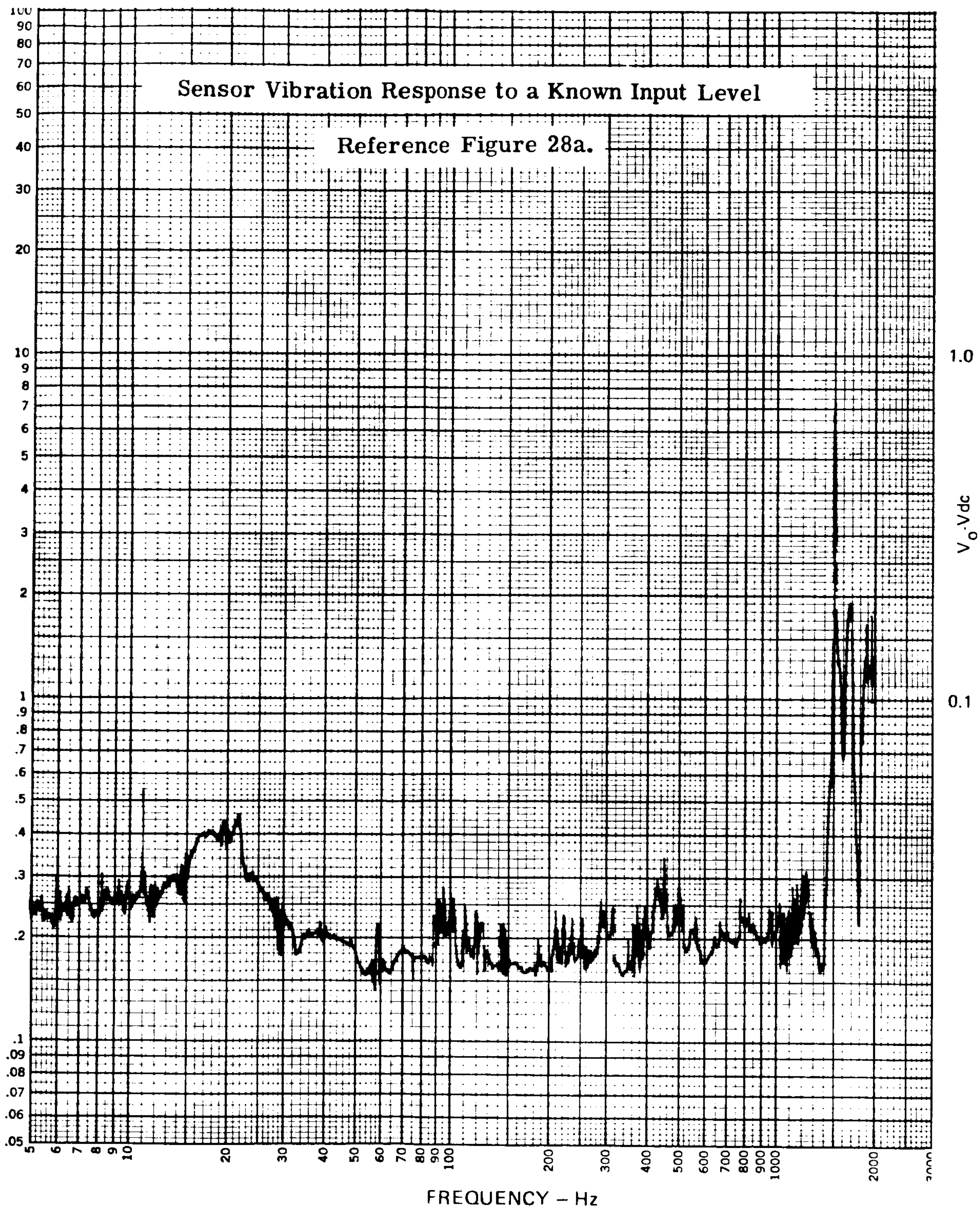

Figure 28b. Unit 1 Drive Plane (Cancelled) - Environmental Test Set 1

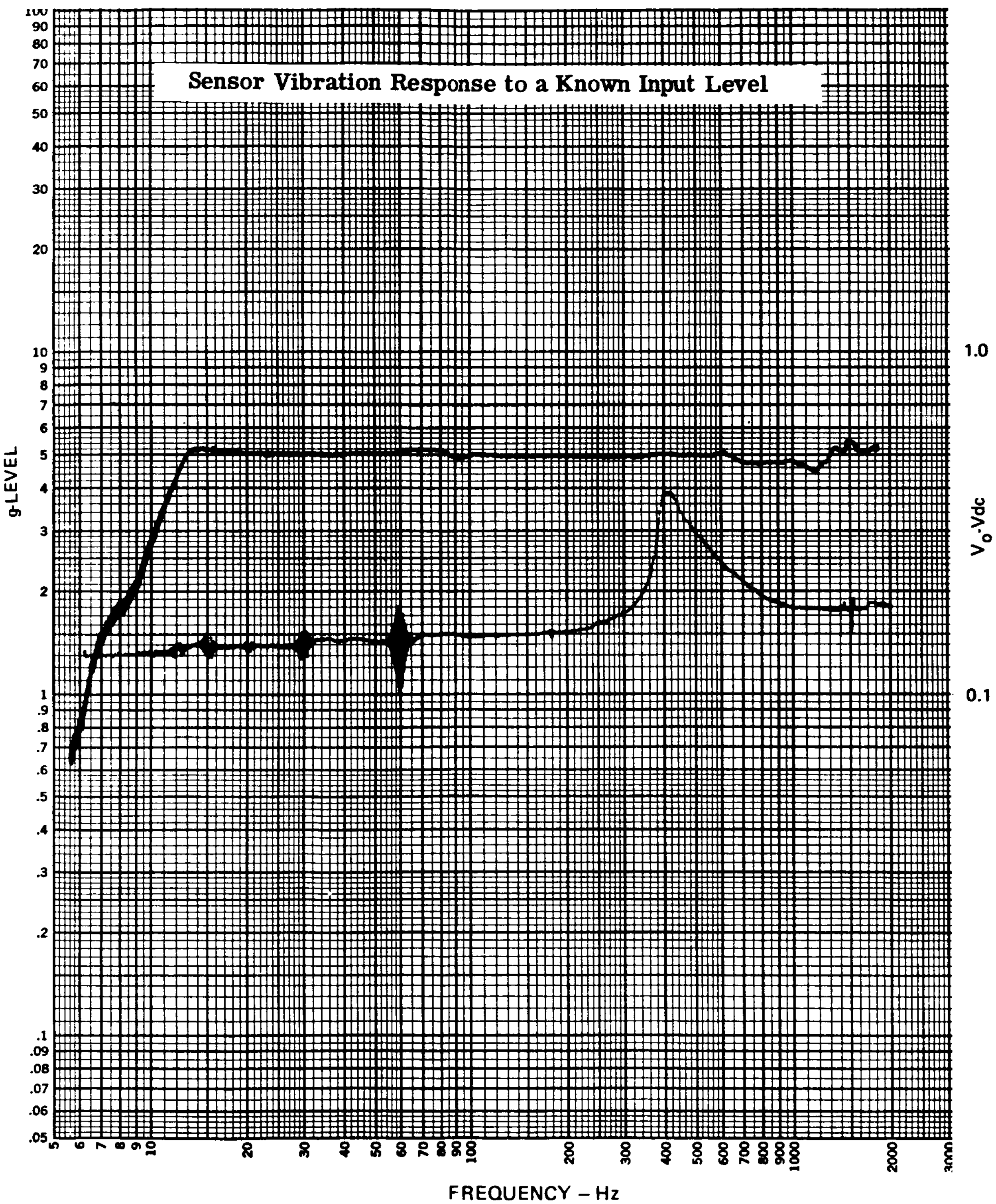

Figure 29a. Unit 1 Axial Plane (Uncancelled) - Environmental Test Set 1

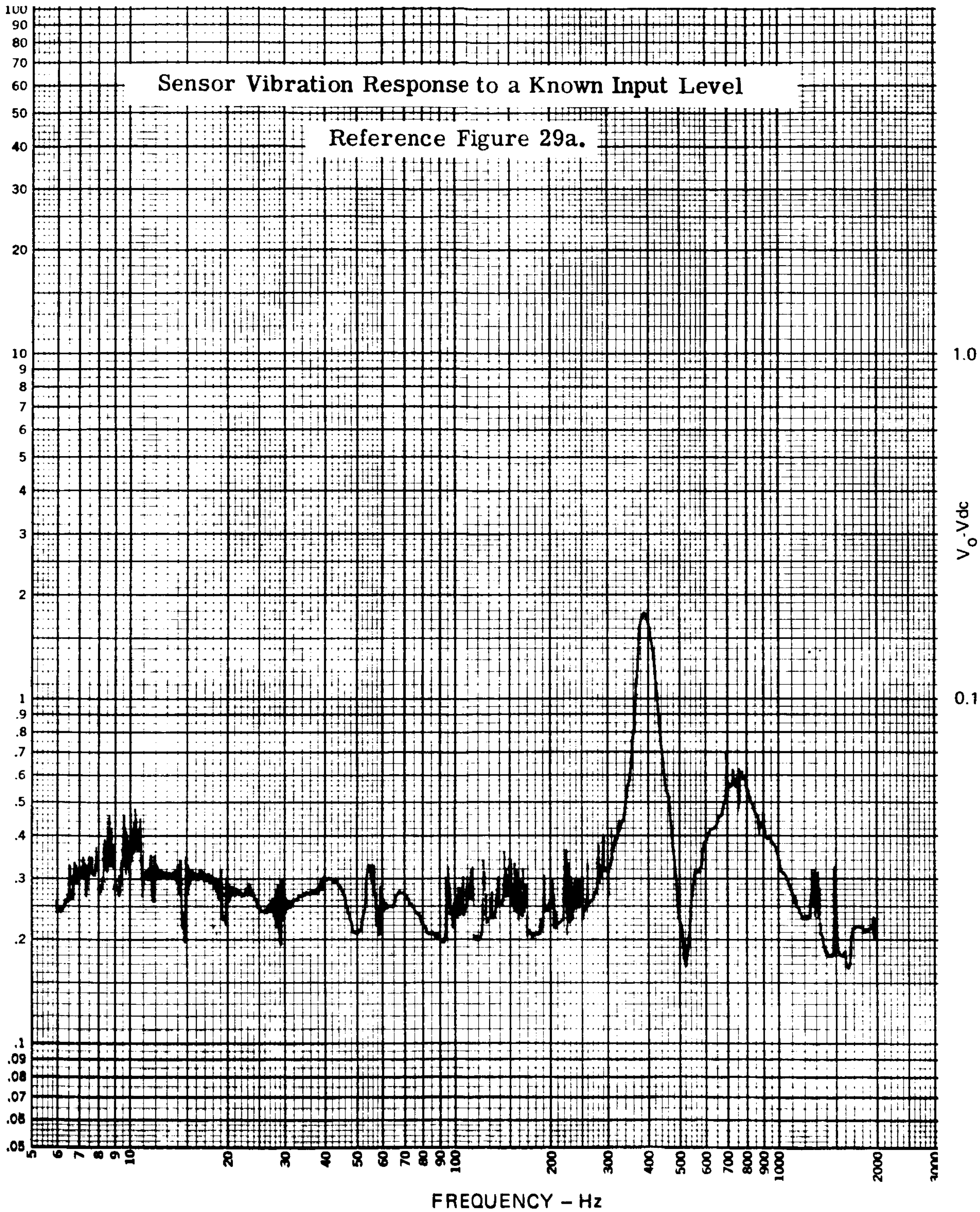

Figure 29b. Unit 1 Axial Plane (Cancelled) - Environmental Test Set 1

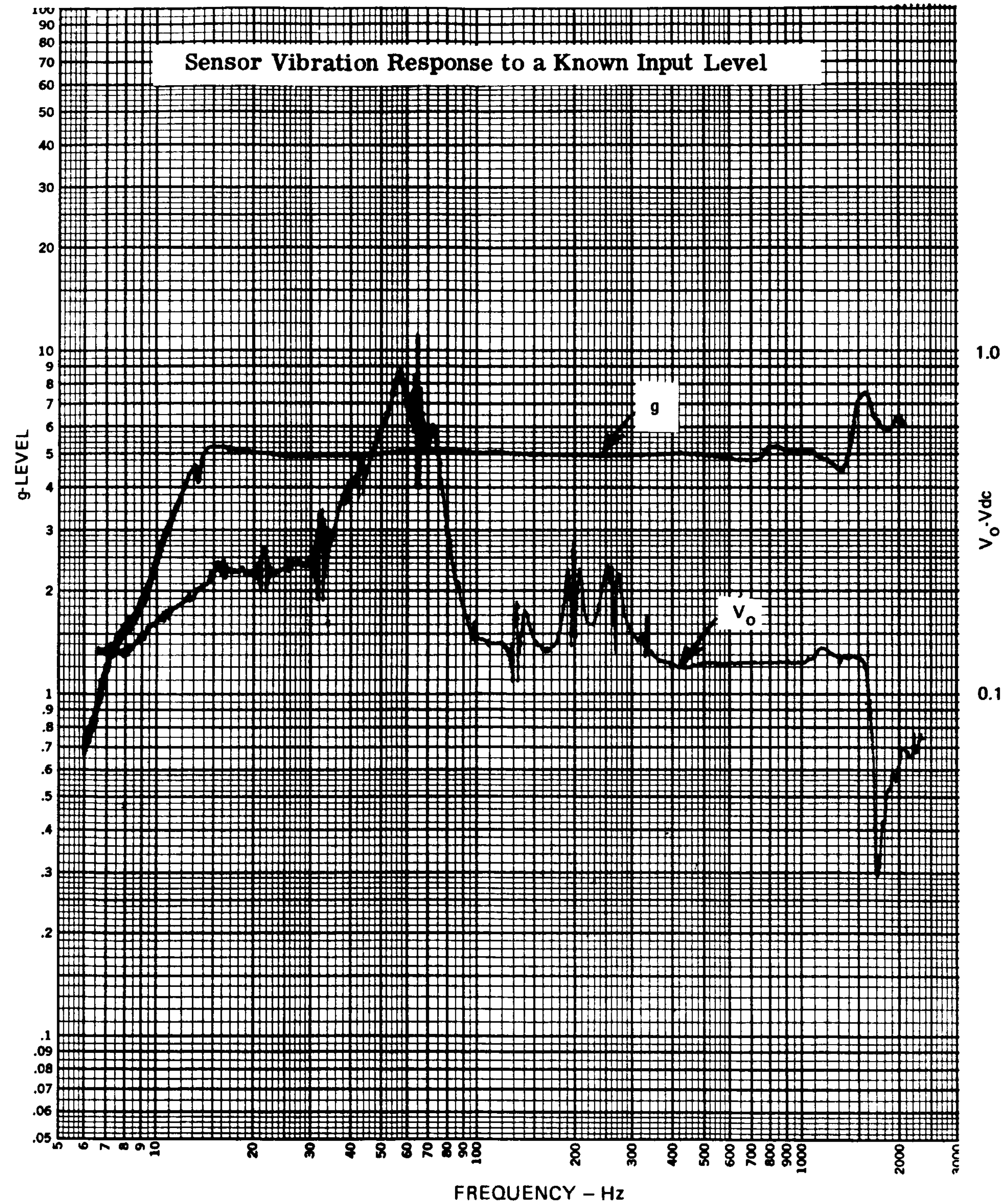

Figure 30a. Unit 2 Readout Plane (Uncancelled) - Environmental Test Set 1

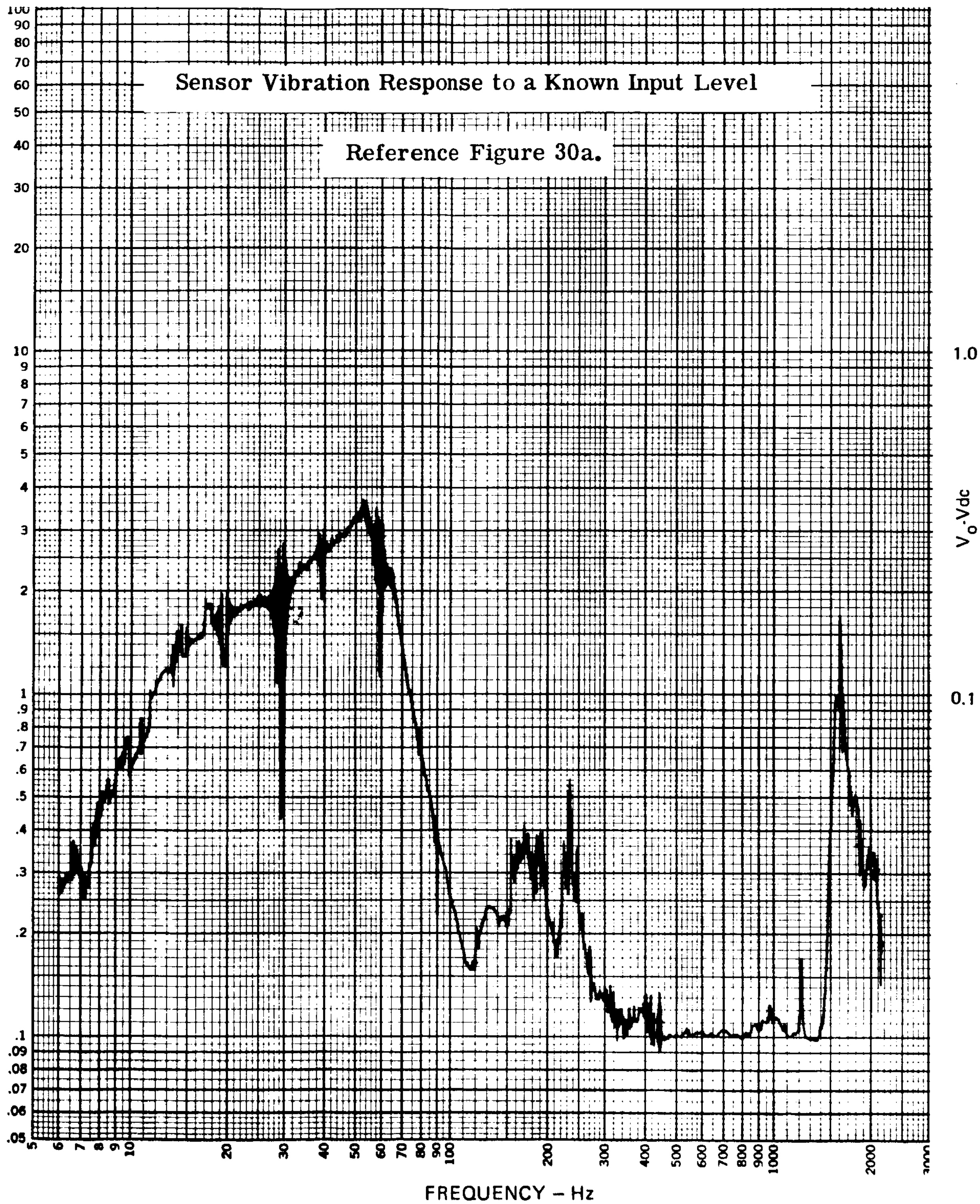

Figure 30b. Unit 2 Readout Plane (Cancelled) - Environmental Test Set 1

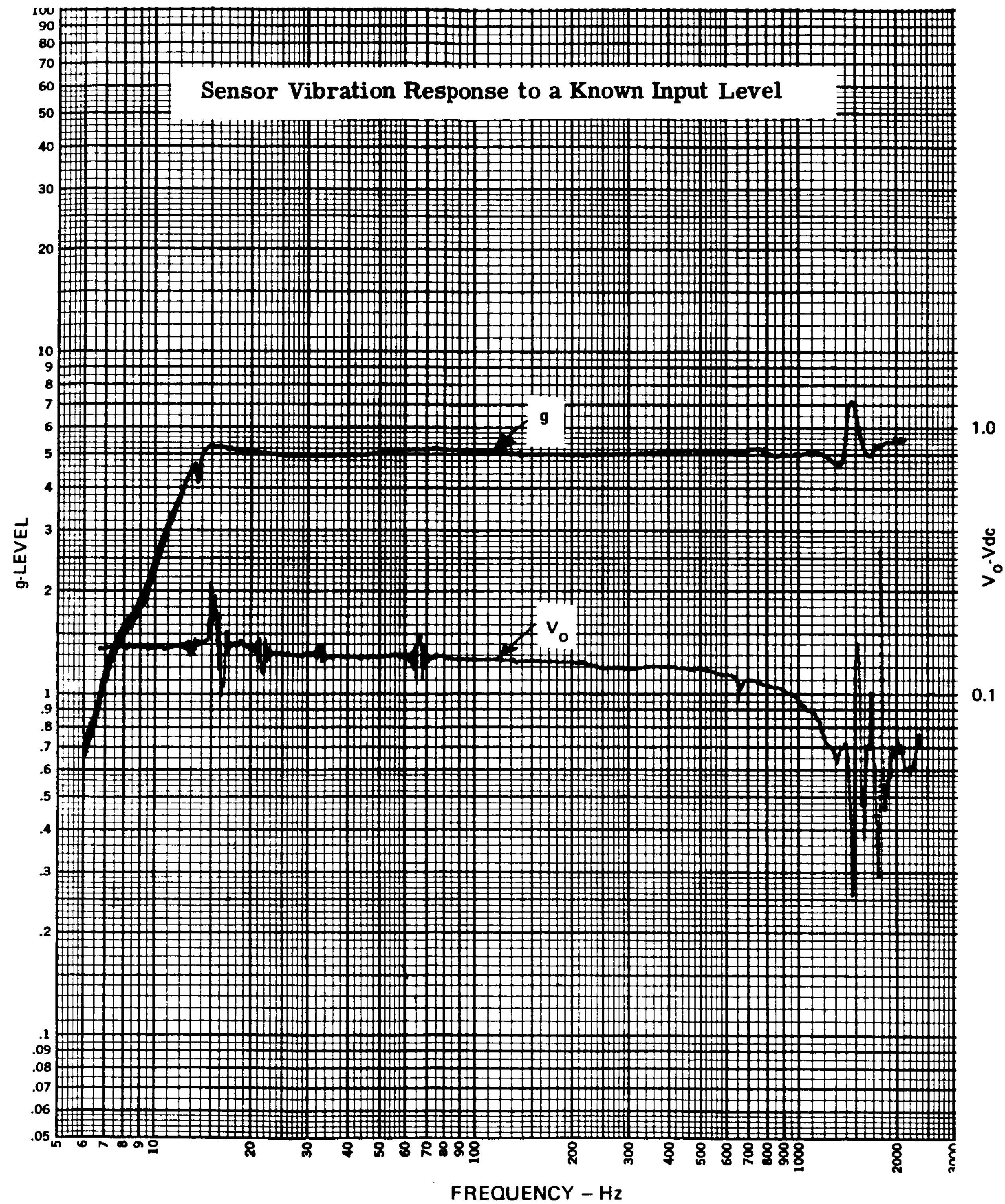

Figure 31a. Unit 2 Drive Plane (Uncancelled) - Environmental Test Set 1

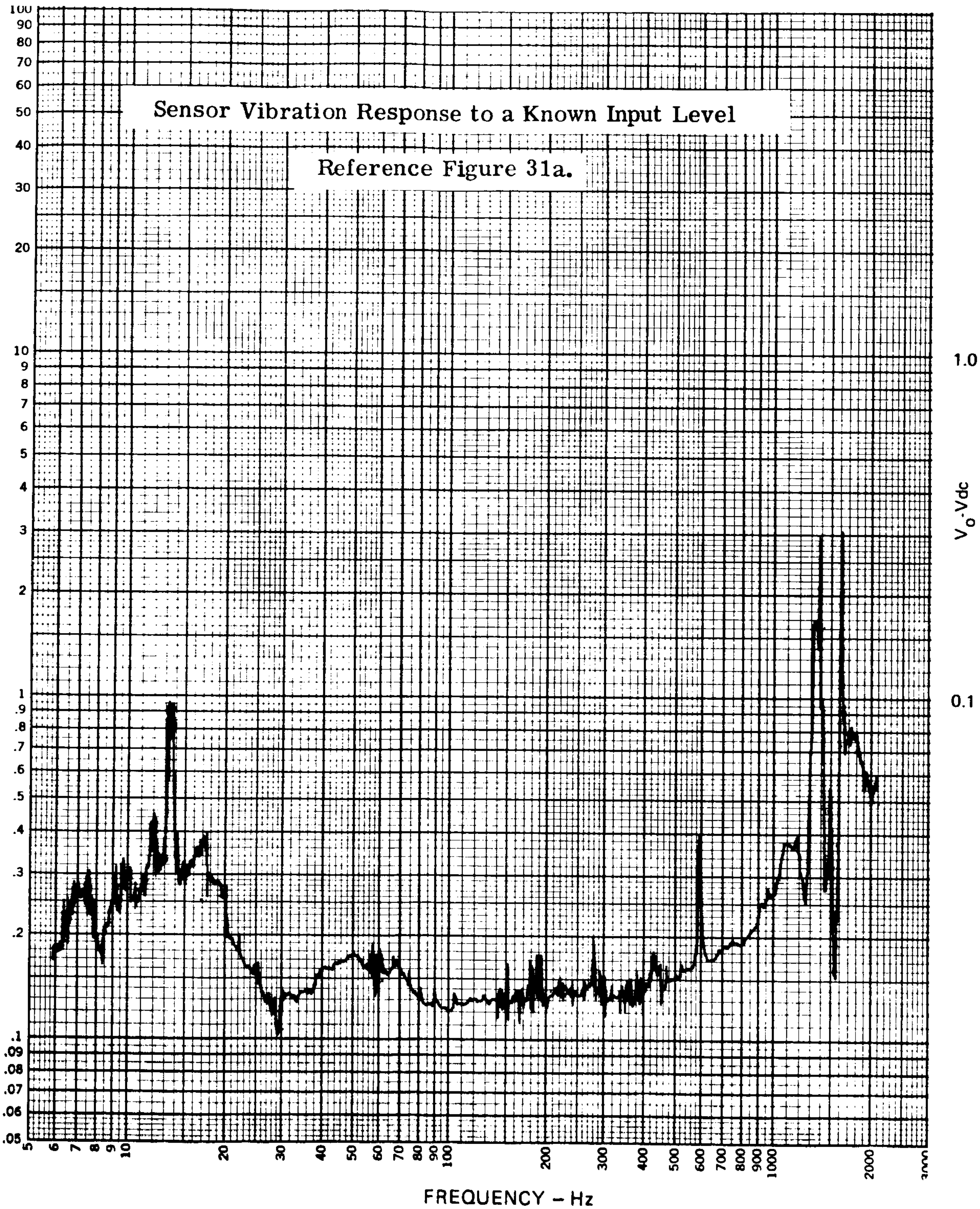

Figure 31b. Unit 2 Drive Plane (Cancelled) - Environmental Test Set 1

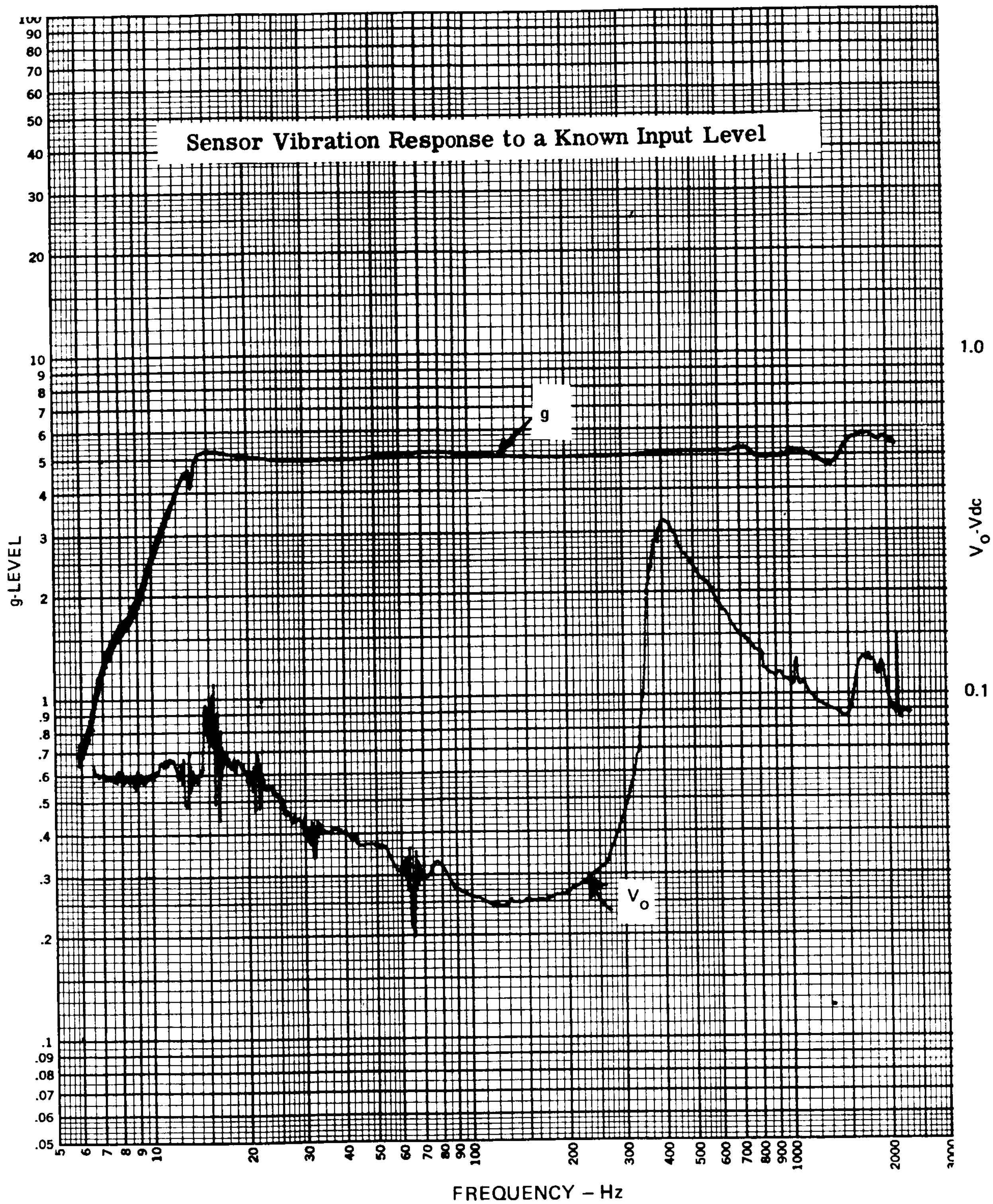

Figure 32a. Unit 2 Axial Plane (Uncancelled) - Environmental Test Set 1

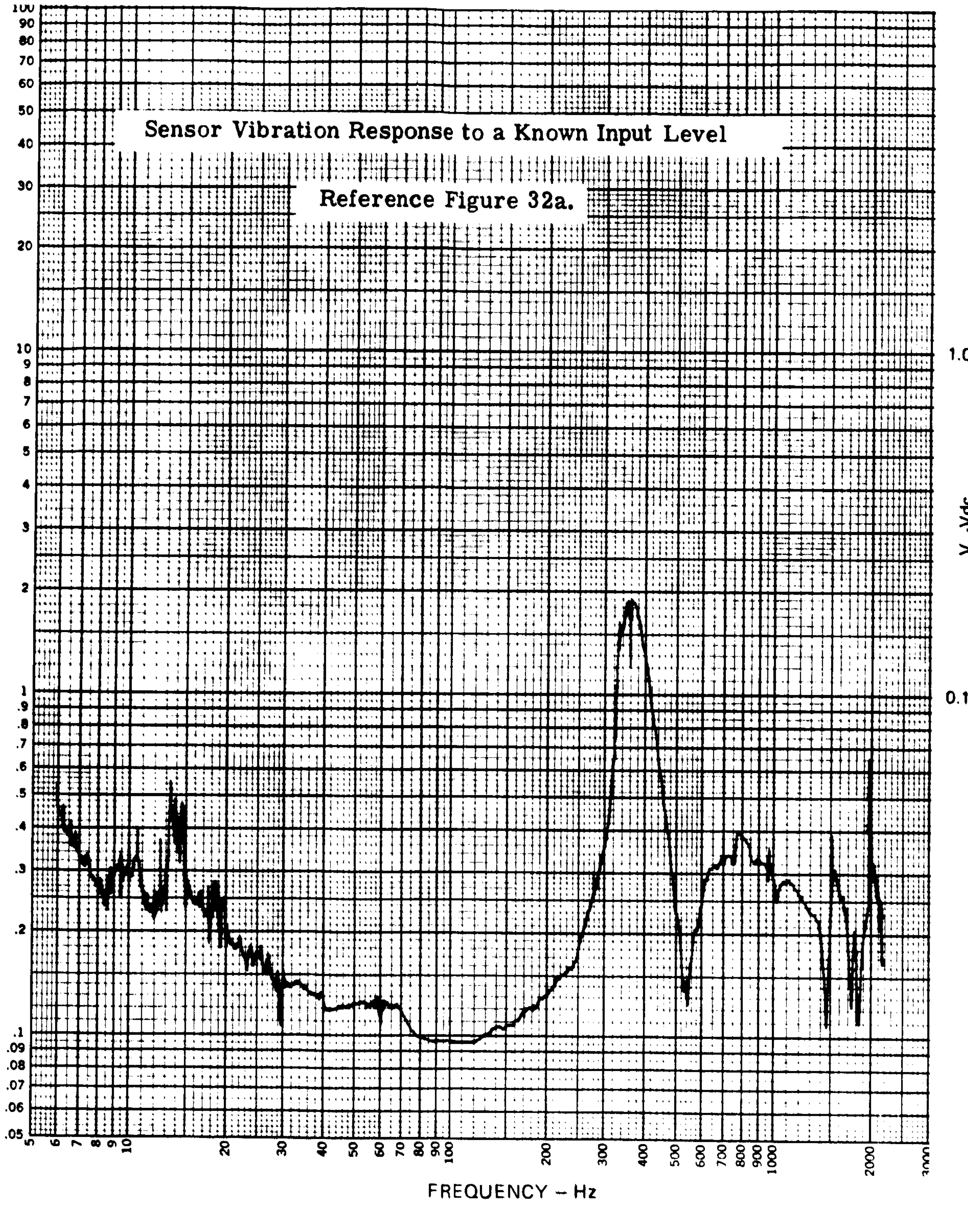

Figure 32b. Unit 2 Axial Plane (Cancelled) - Environmental Test Set 1

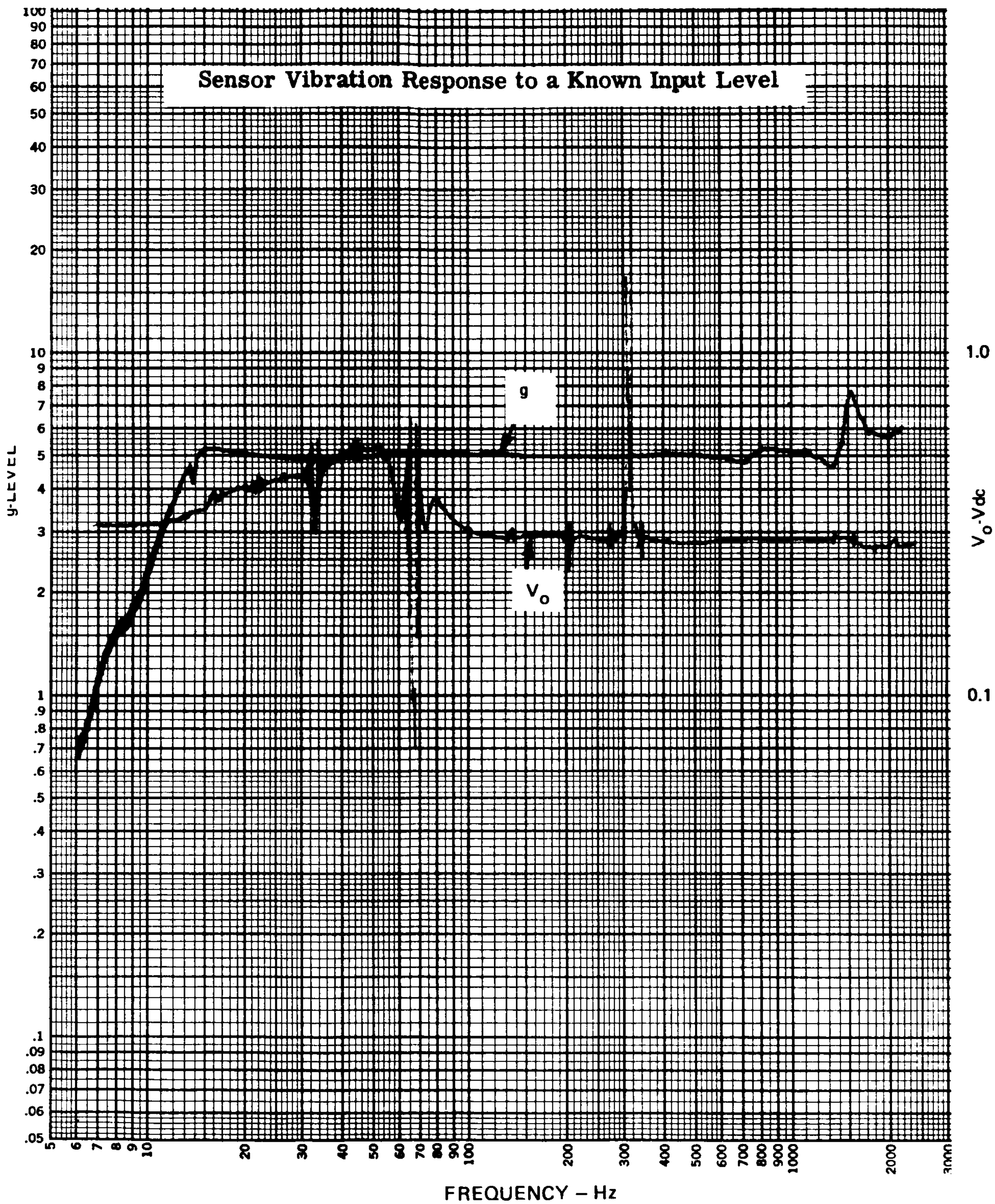

Figure 33a. Unit 3 Readout Plane (Uncancelled) - Environmental Test Set 1

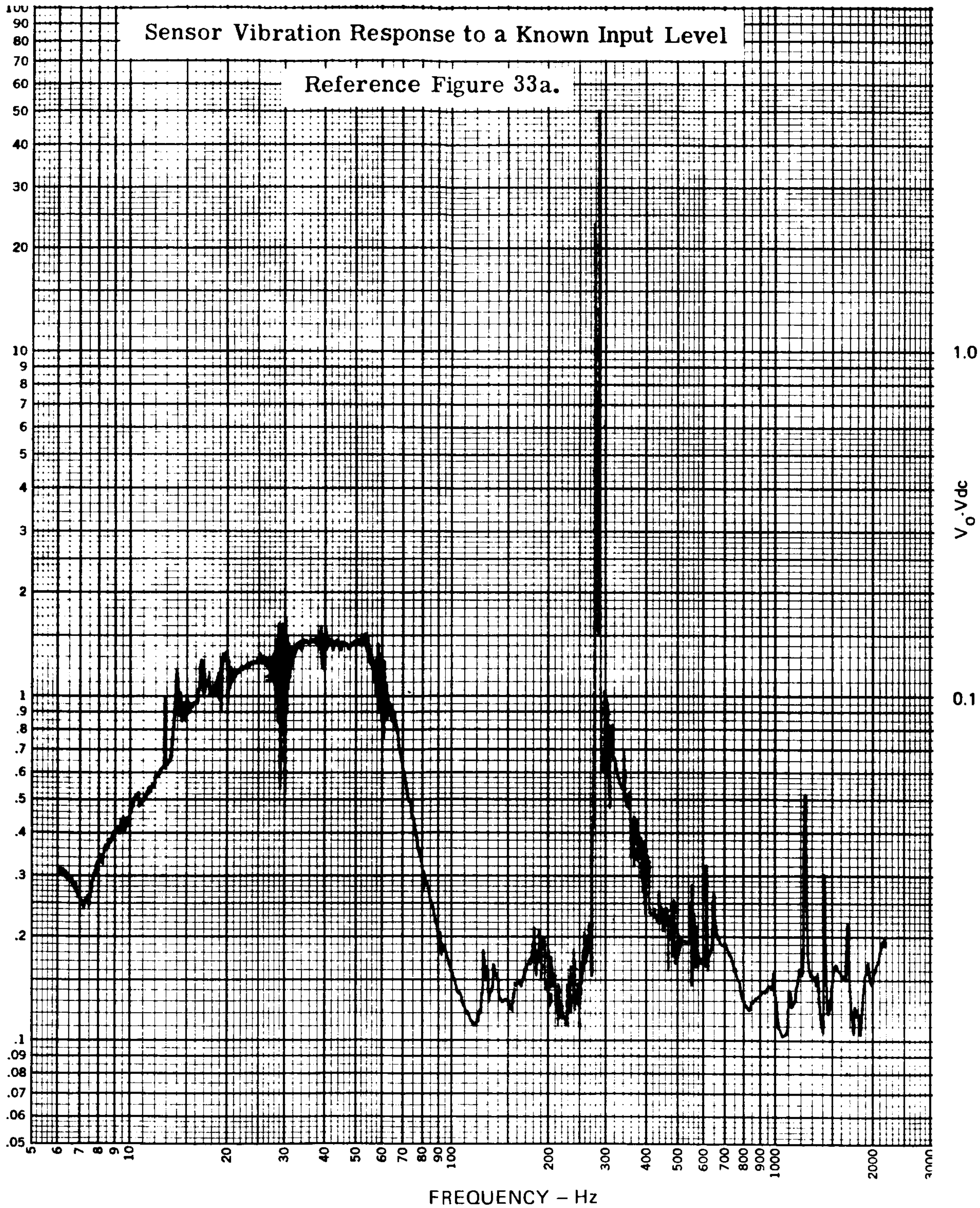

Figure 33b. Unit 3 Readout Plane (Cancelled) - Environmental Test Set 1

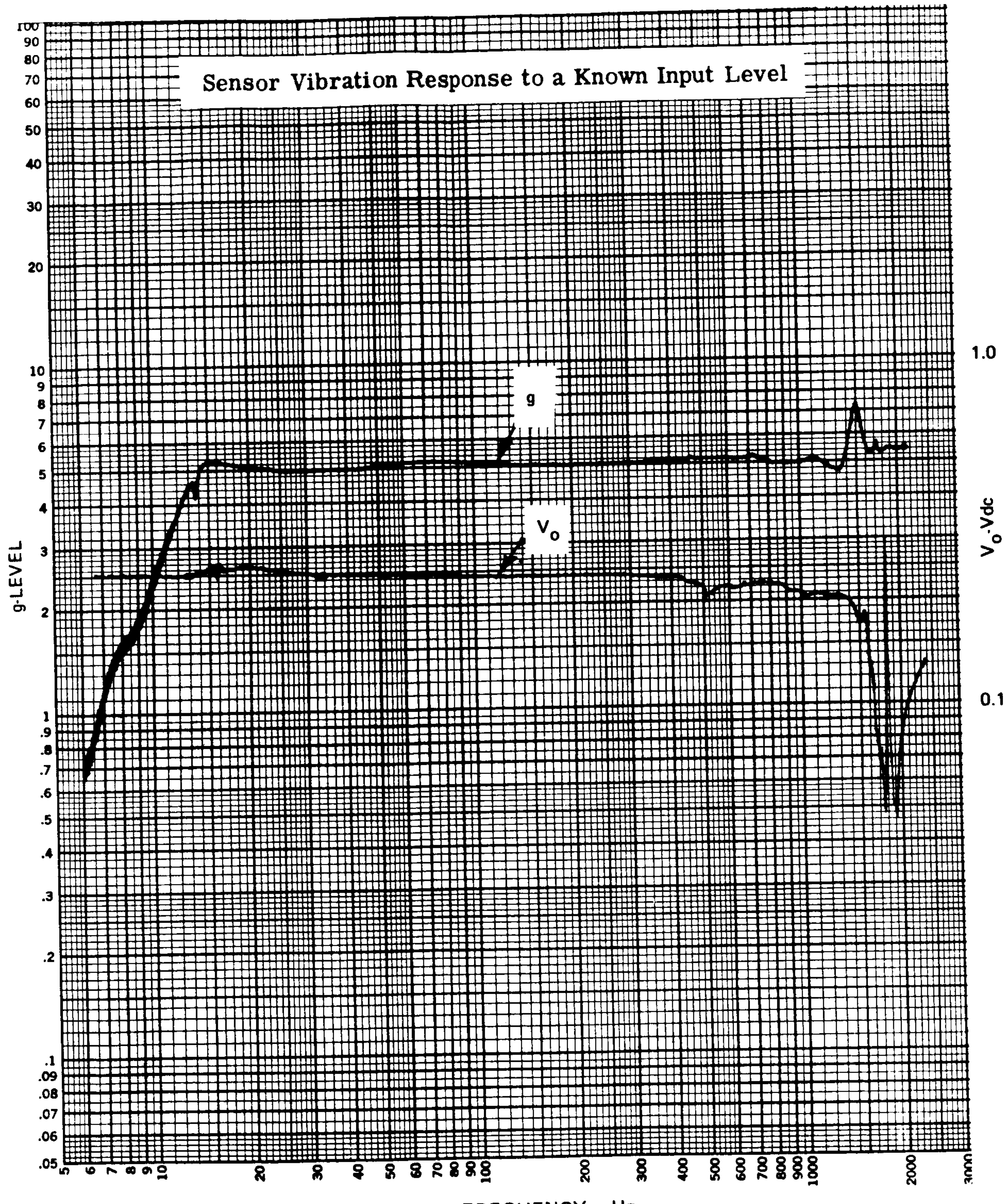

Figure 34a. Unit 3 Drive Plane (Uncancelled) - Environmental Test Set 1

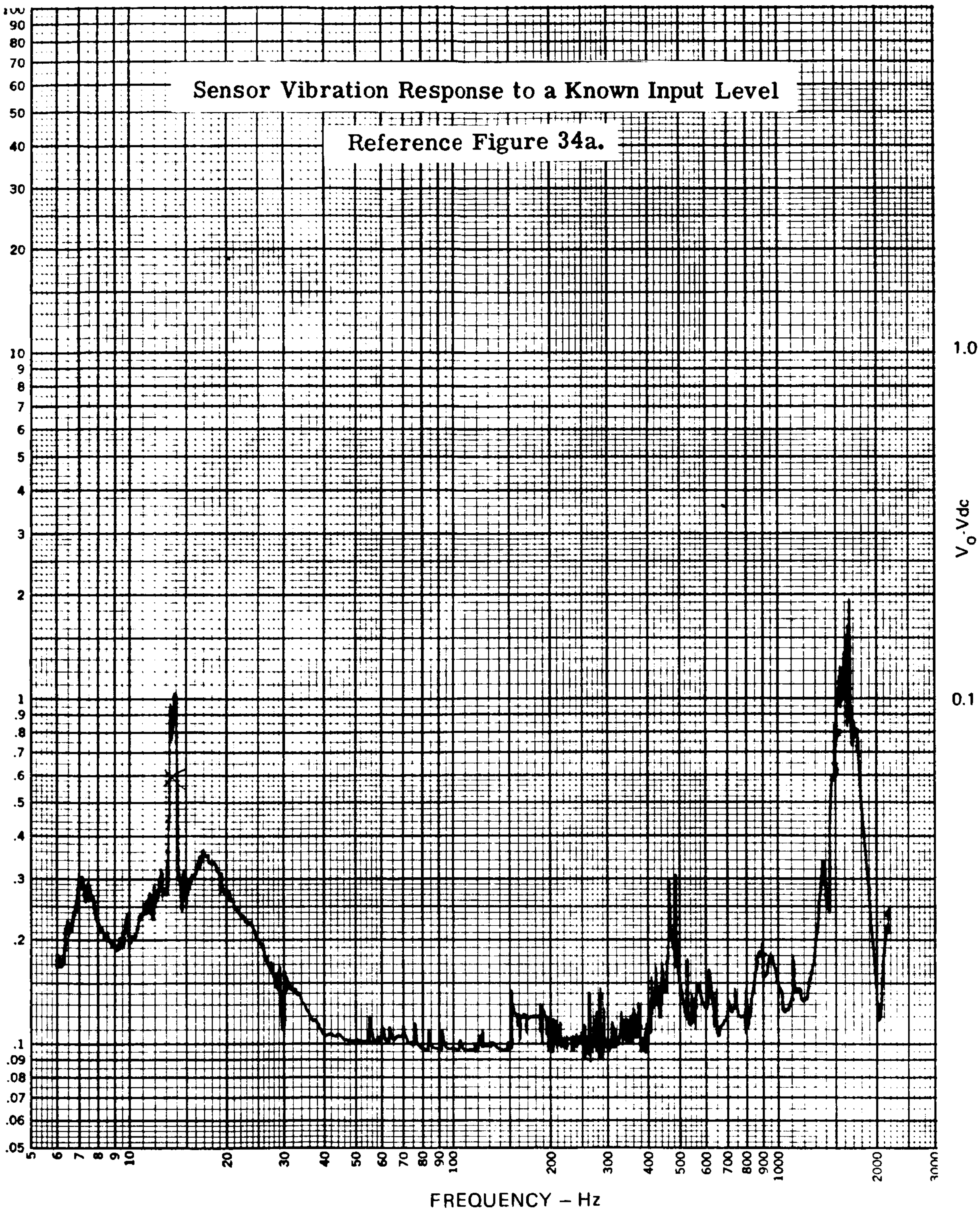

Figure 34b. Unit 3 Drive Plane (Cancelled) - Environmental Test Set 1

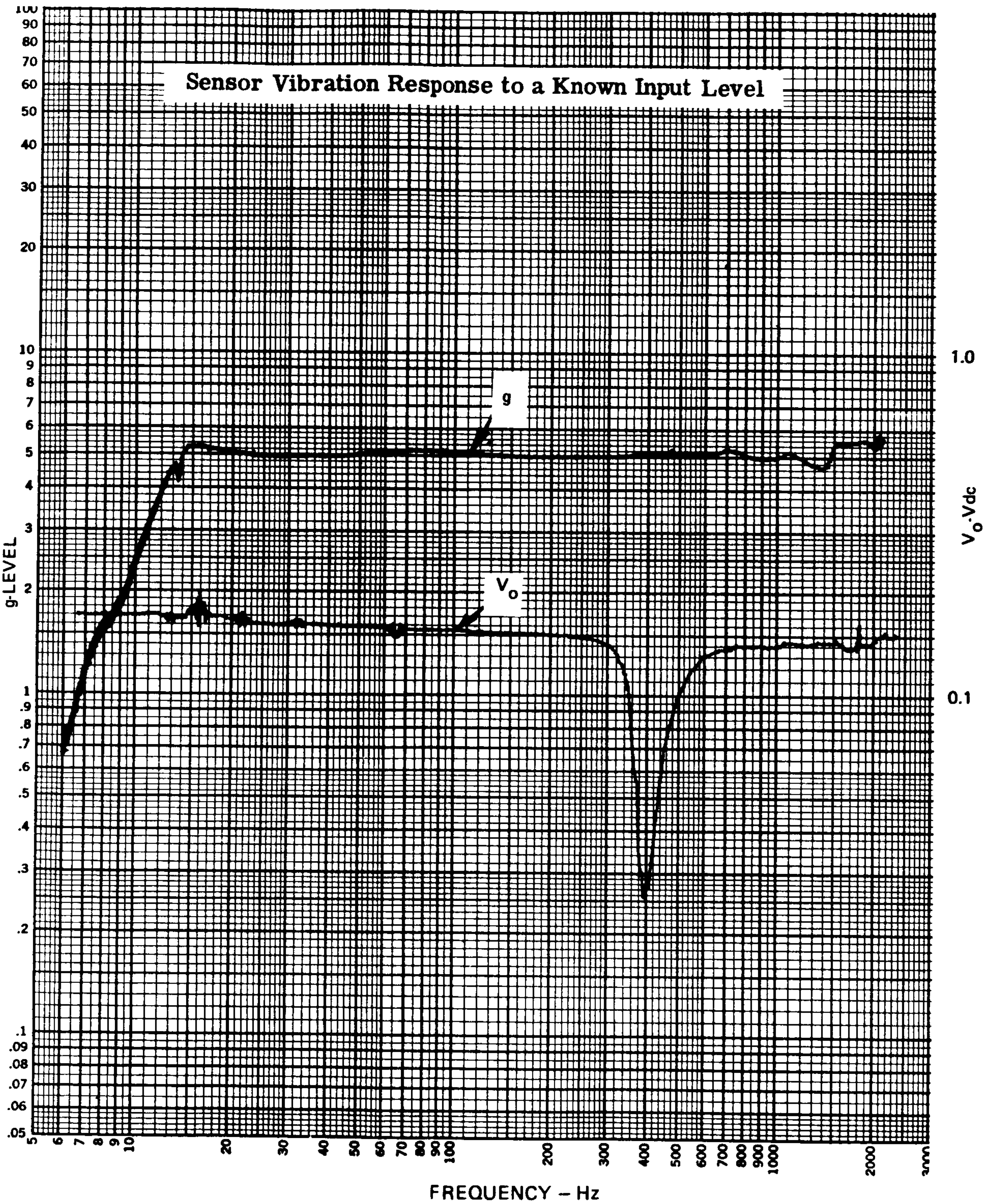

Figure 35a. Unit 3 Axial Plane (Uncancelled) - Environmental Test Set 1

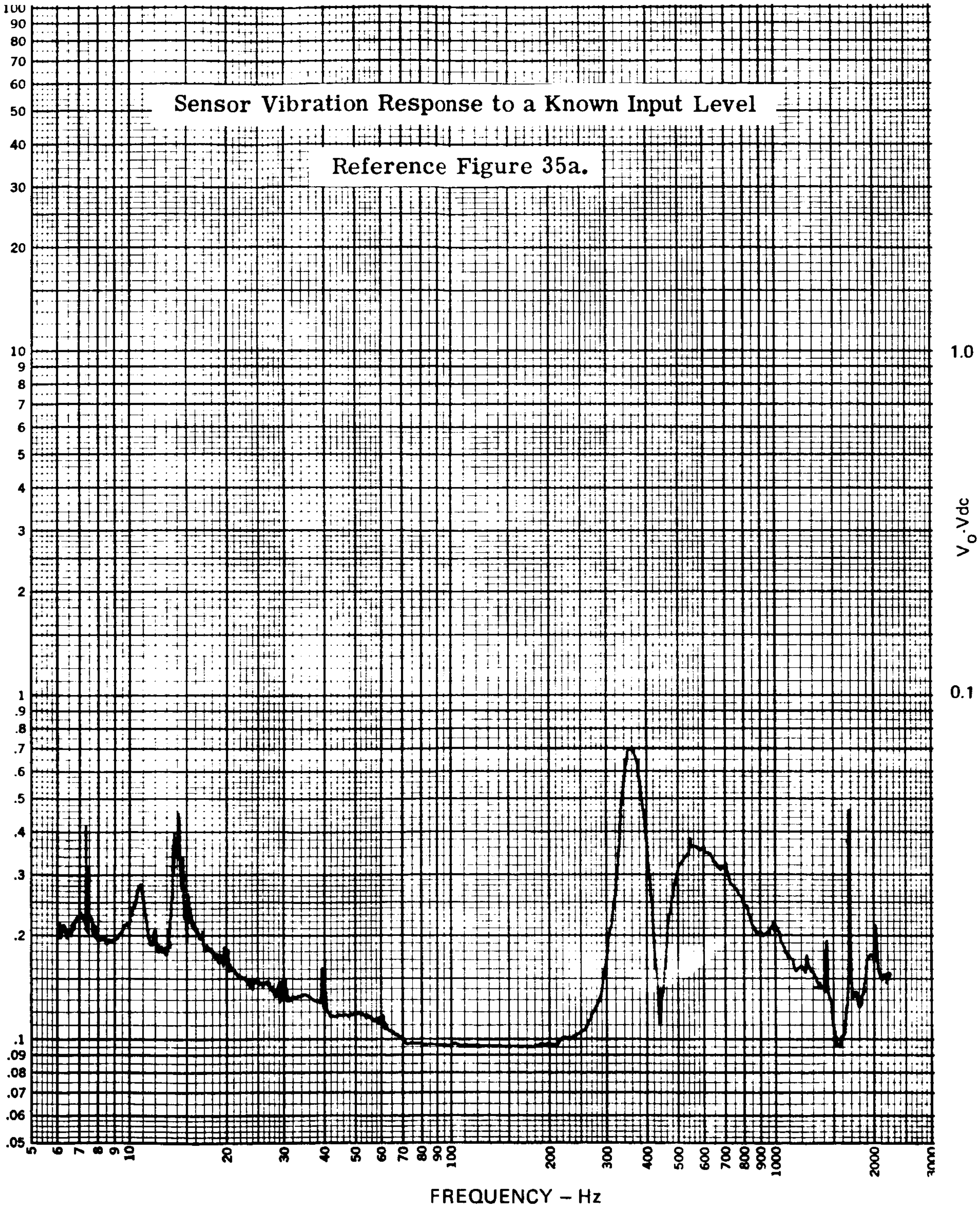

Figure 35b. Unit 3 Axial Plane (Cancelled) - Environmental Test Set 1

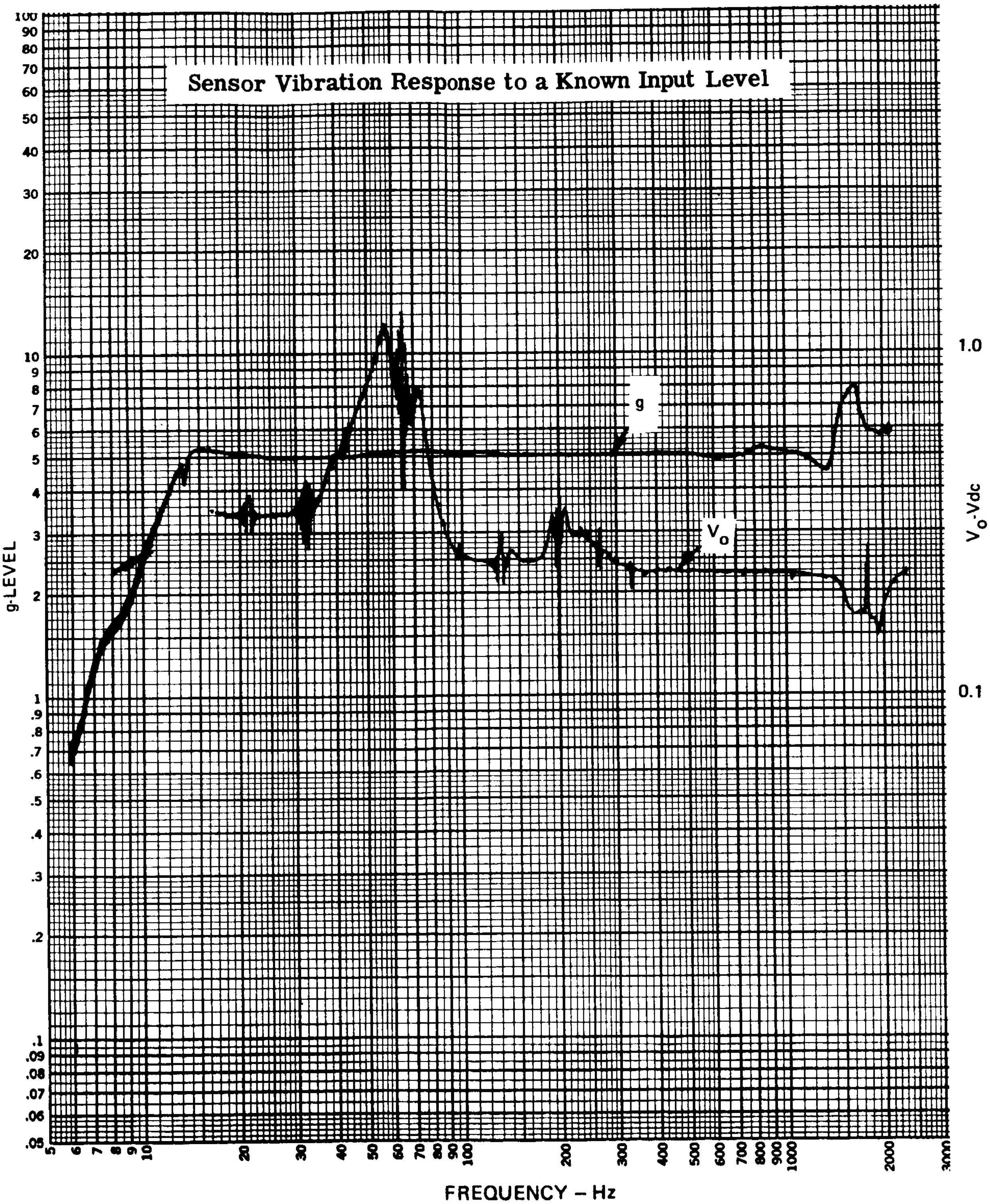

Figure 36a. Unit 4 Readout Plane (Uncancelled) - Environmental Test Set 1

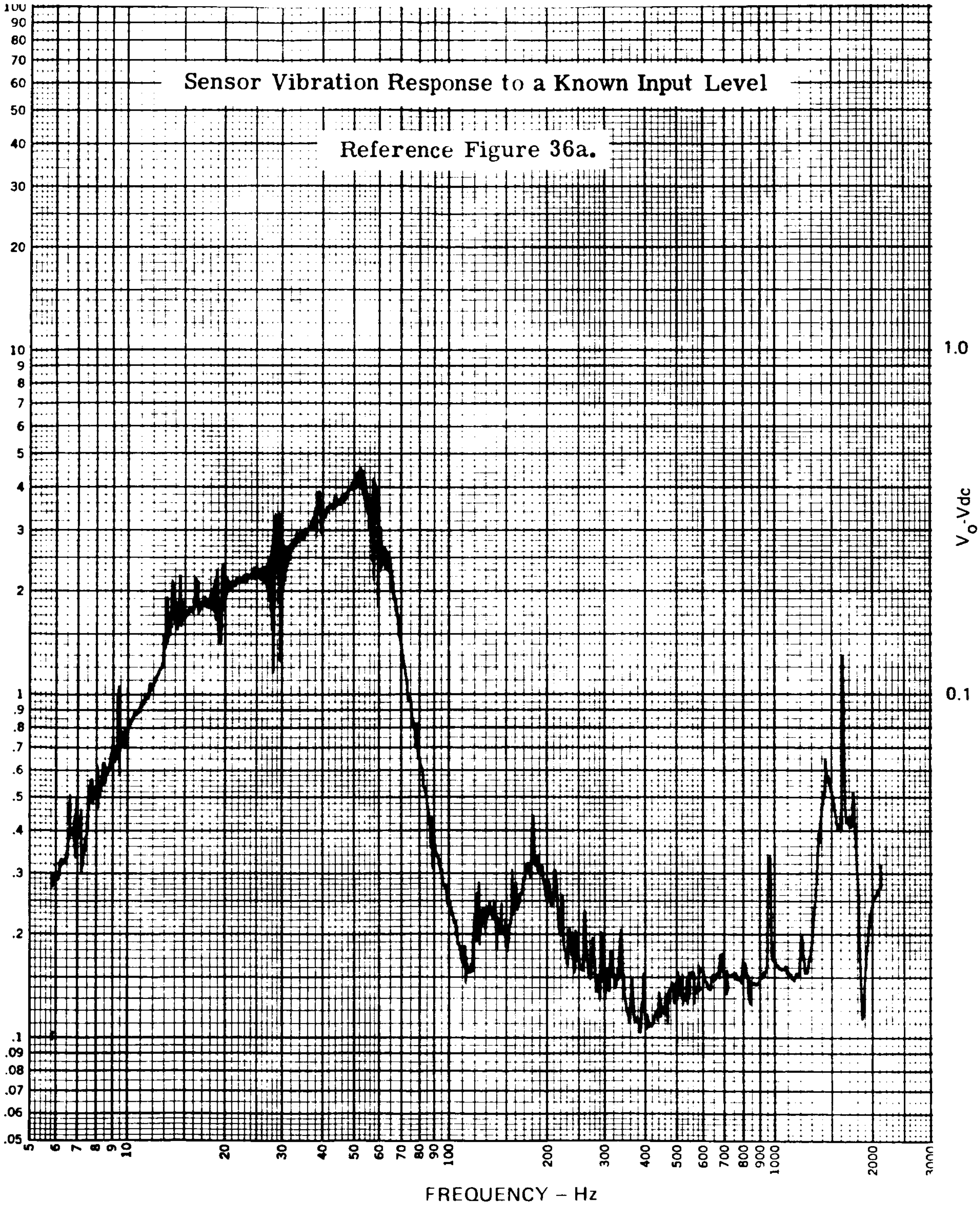

Figure 36b. Unit 4 Readout Plane (Cancelled) - Environmental Test Set 1

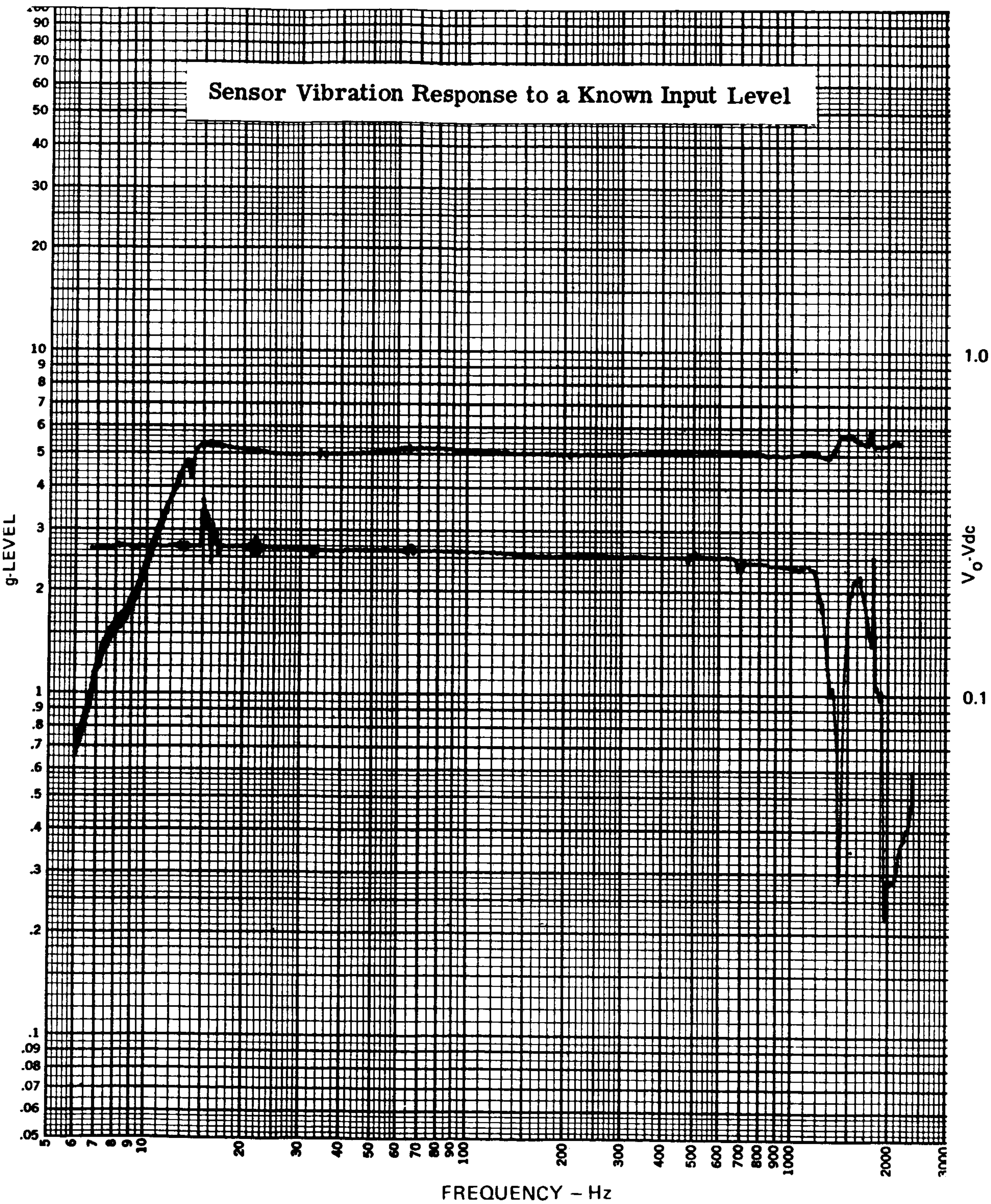

Figure 37a. Unit 4 Drive Plane (Uncancelled) - Environmental Test Set 1

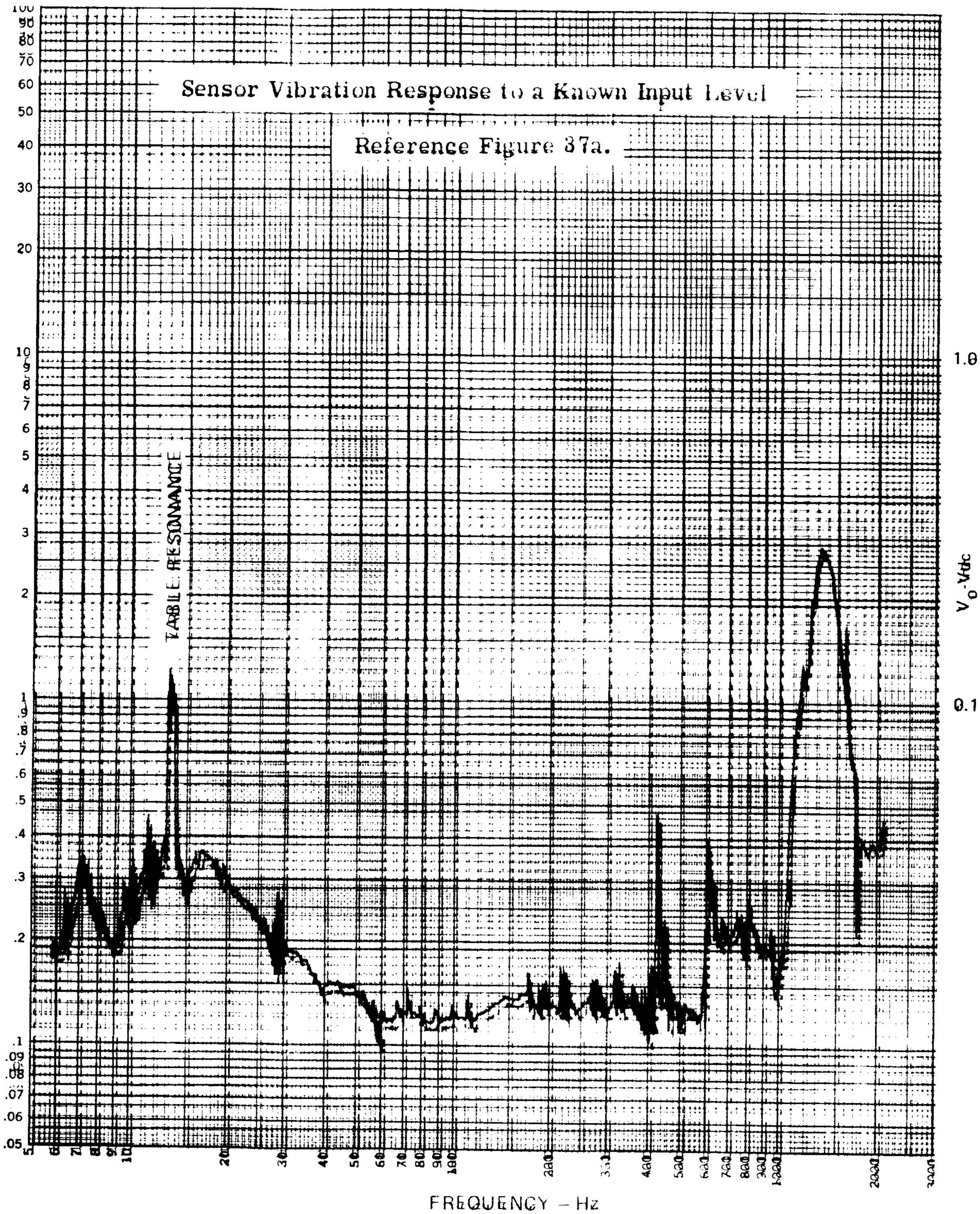

Figure 37b. Unit 4 Drive Plane (Cancelled) - Environmental Test Set 1

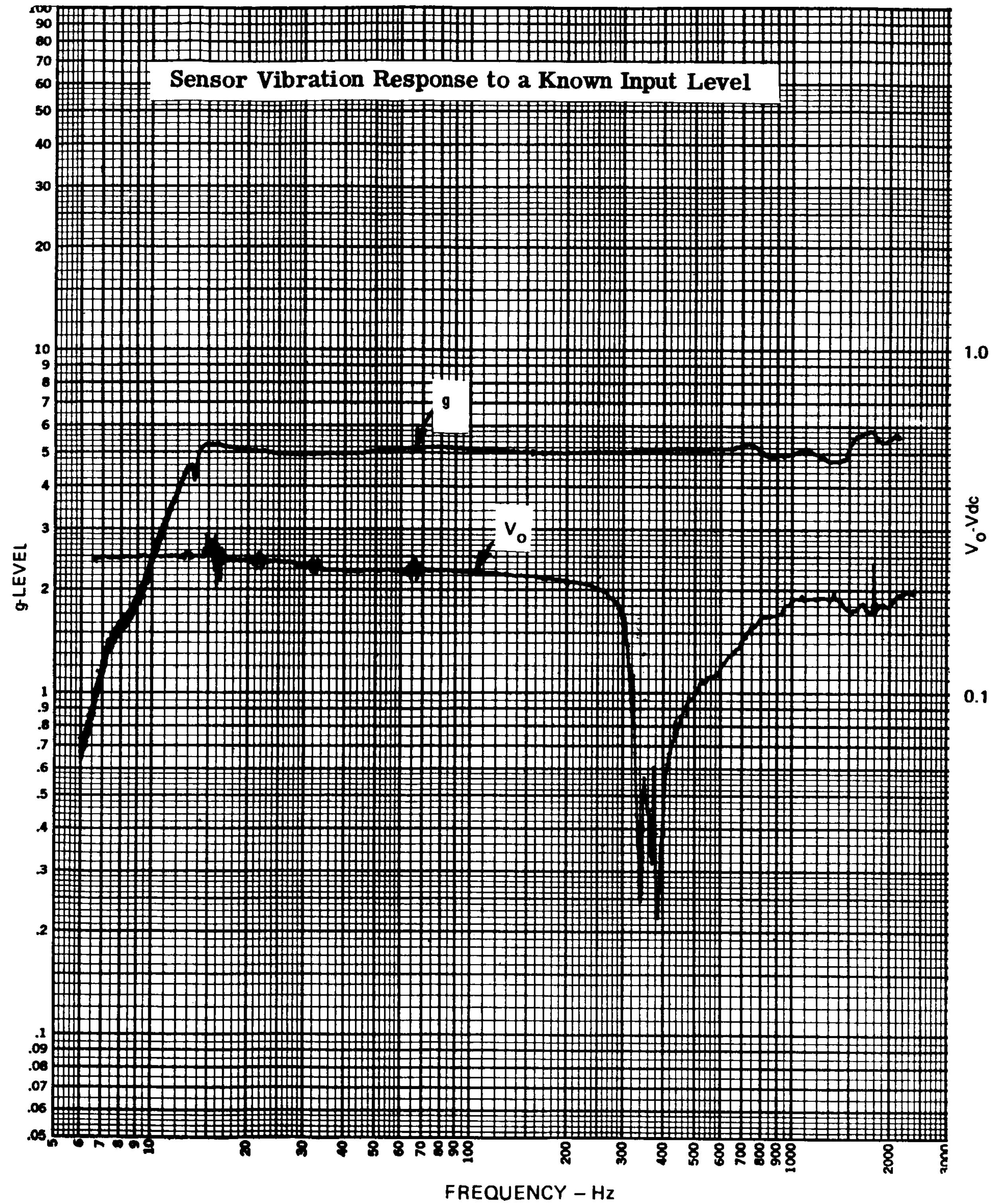

Figure 38a. Unit 4 Axial Plane (Uncancelled) - Environmental Test Set 1

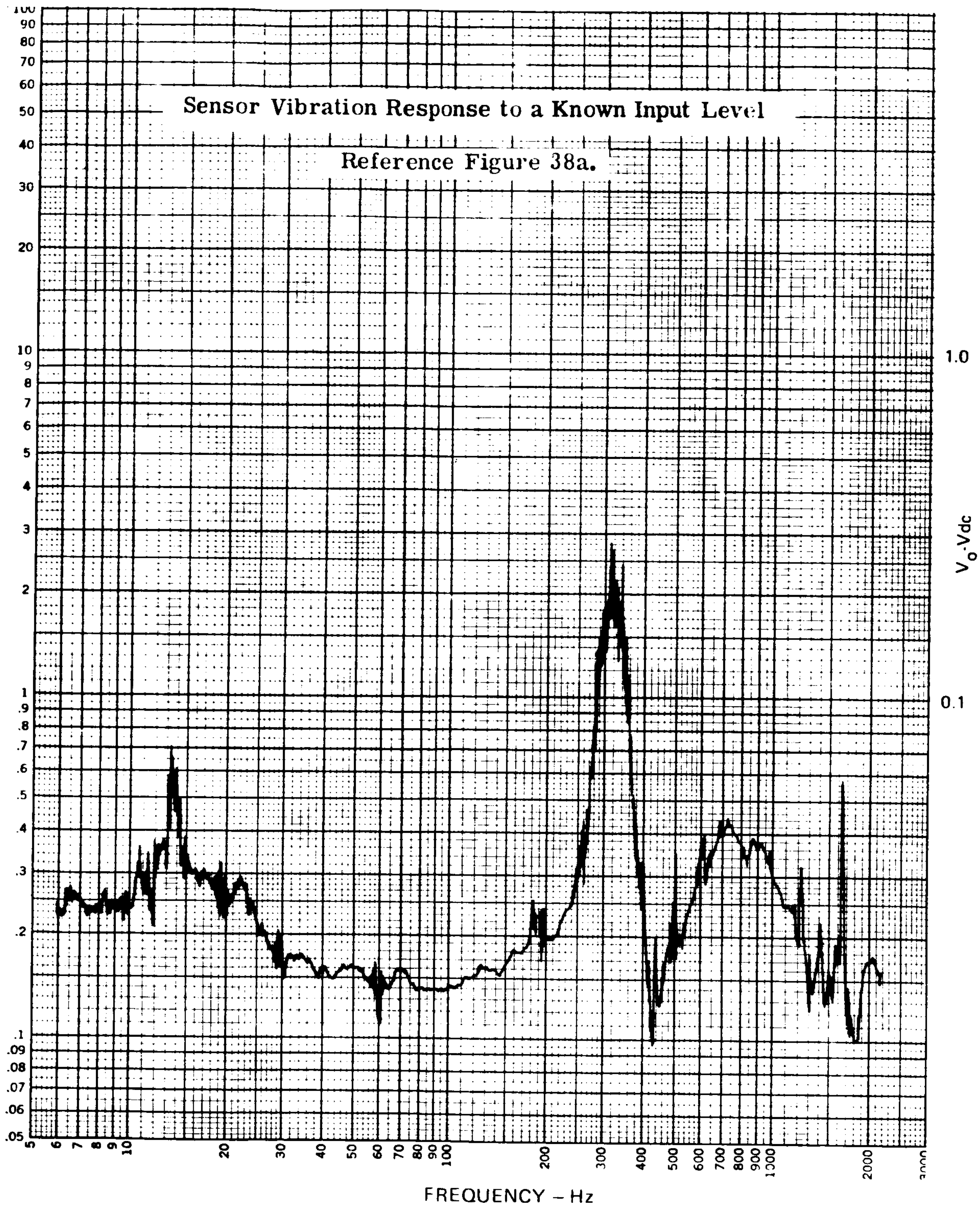

Figure 38b. Unit 4 Axial Plane (Cancelled) - Environmental Test Set 1

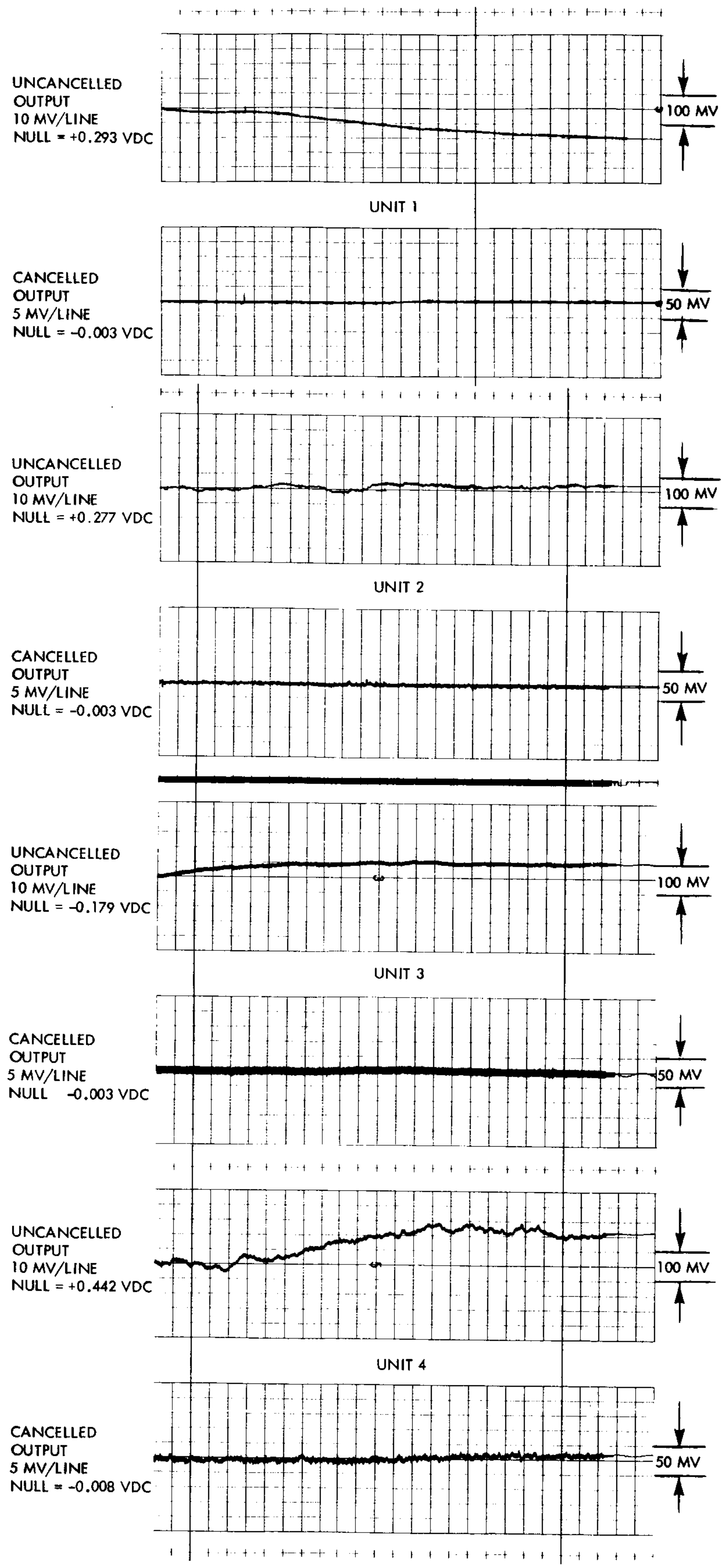

Figure 39. Two Hour Null Stability after Heat Cycle 2

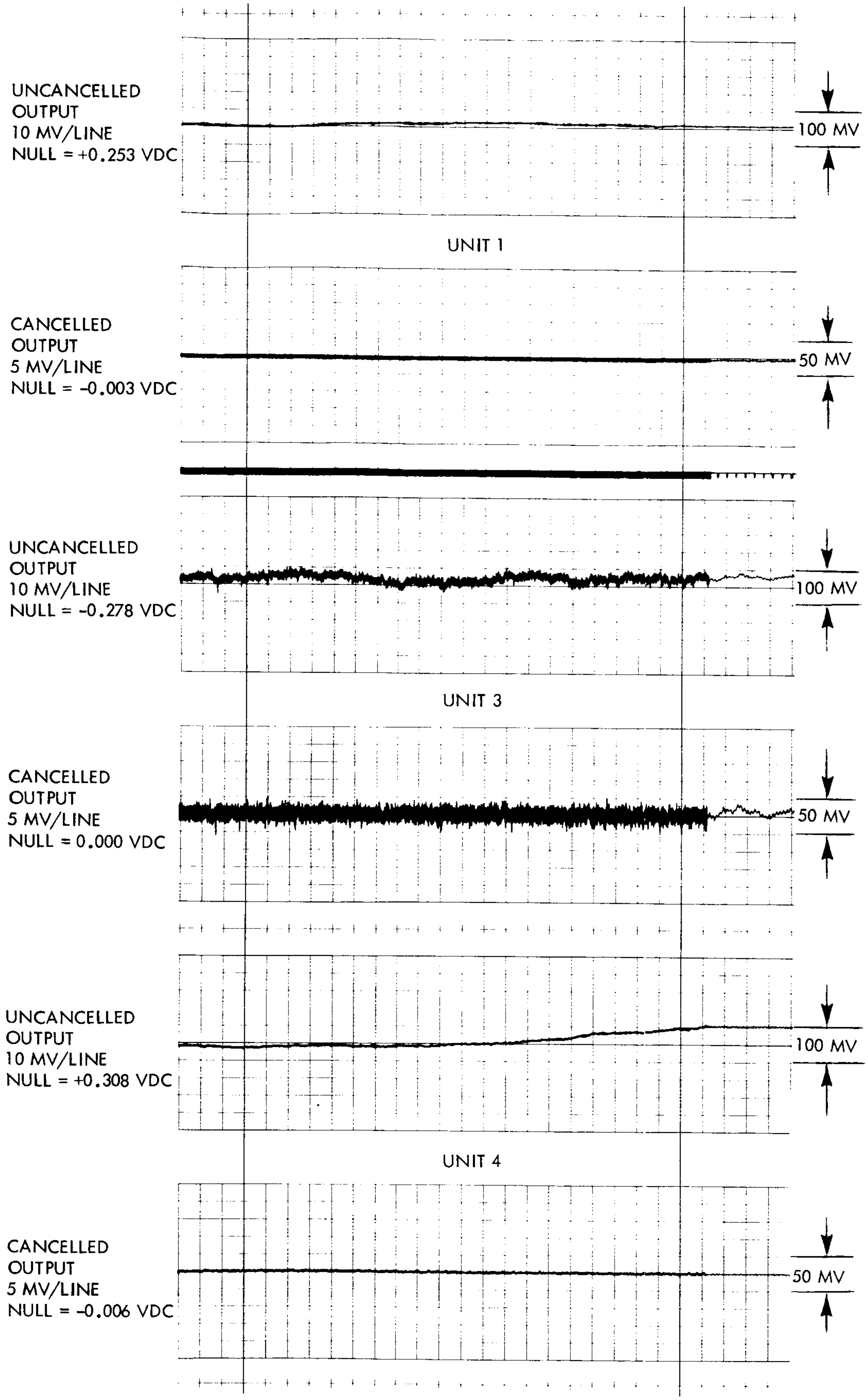

Figure 40. Two Hour Null Stability after Heat Cycle 6

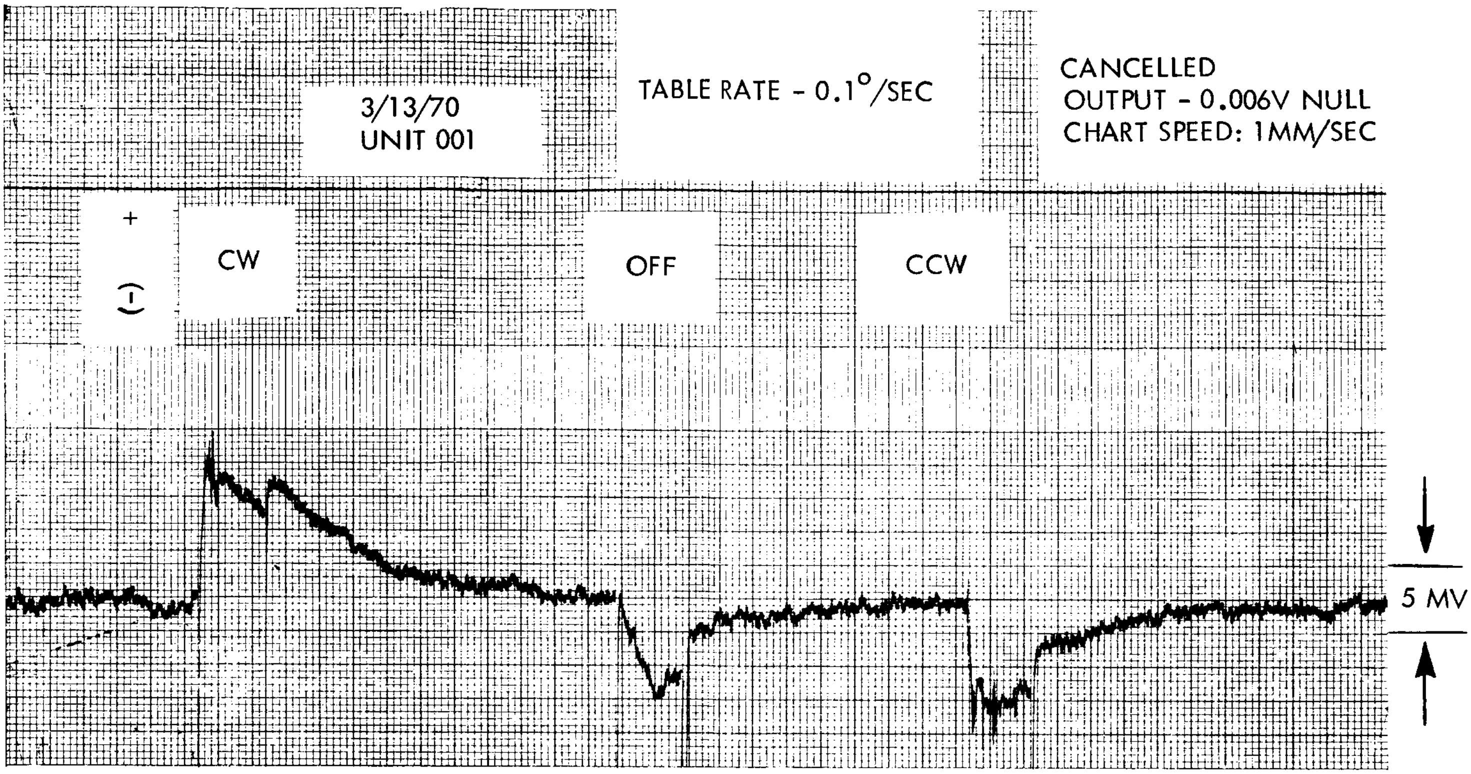

FUNCTIONAL TEST SET 3

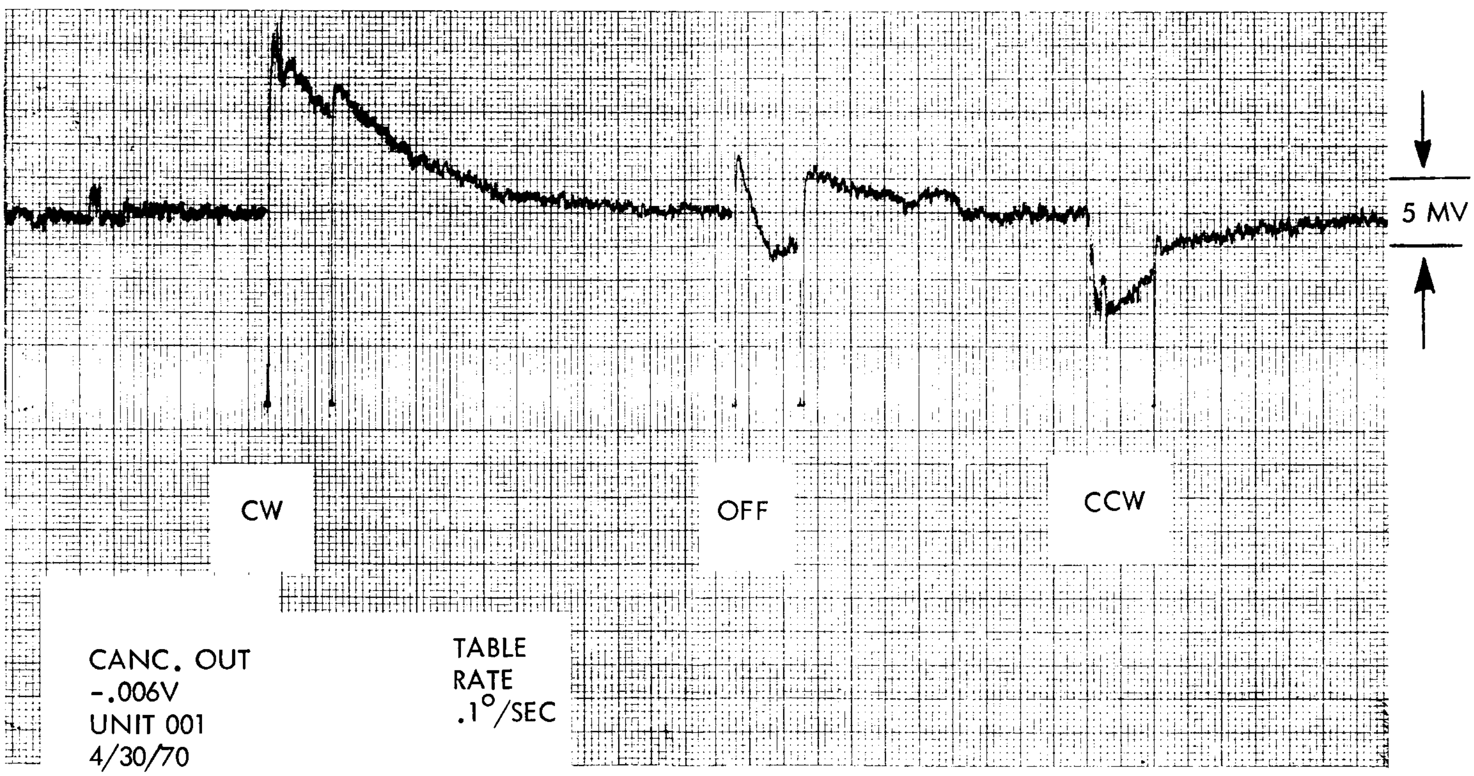

FUNCTIONAL TEST SET 4

Figure 41. Threshold Test - Unit No. 1

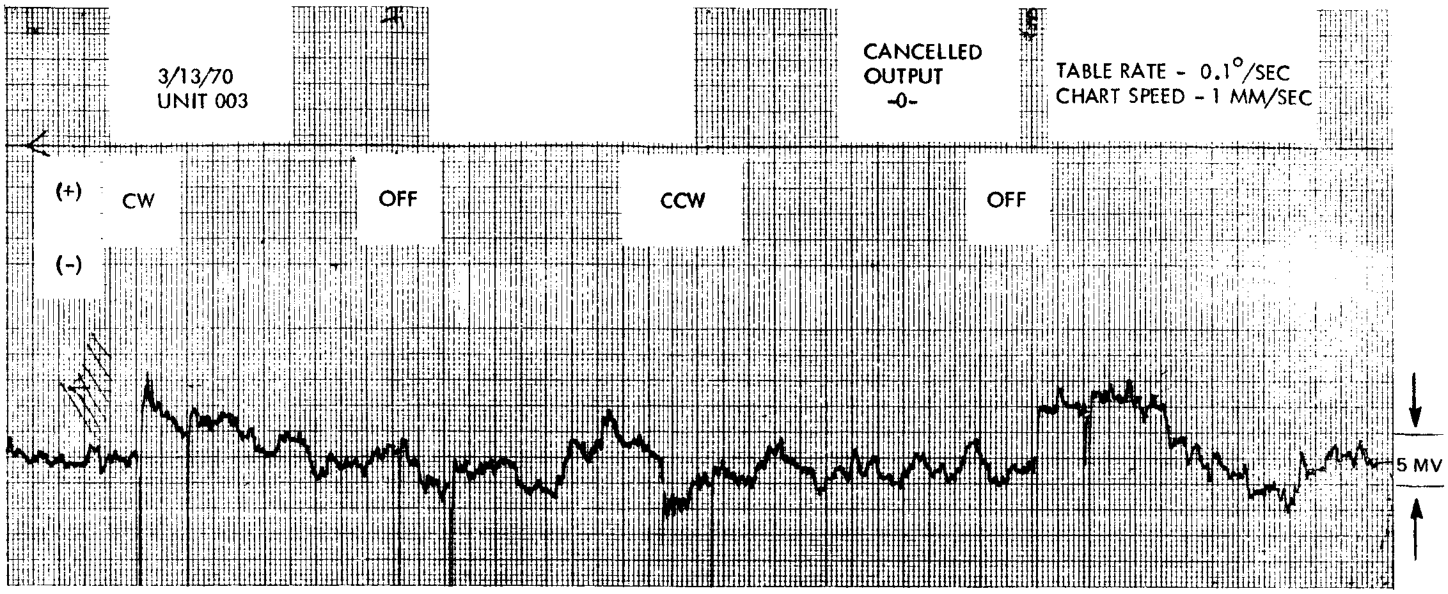

FUNCTIONAL TEST SET 3

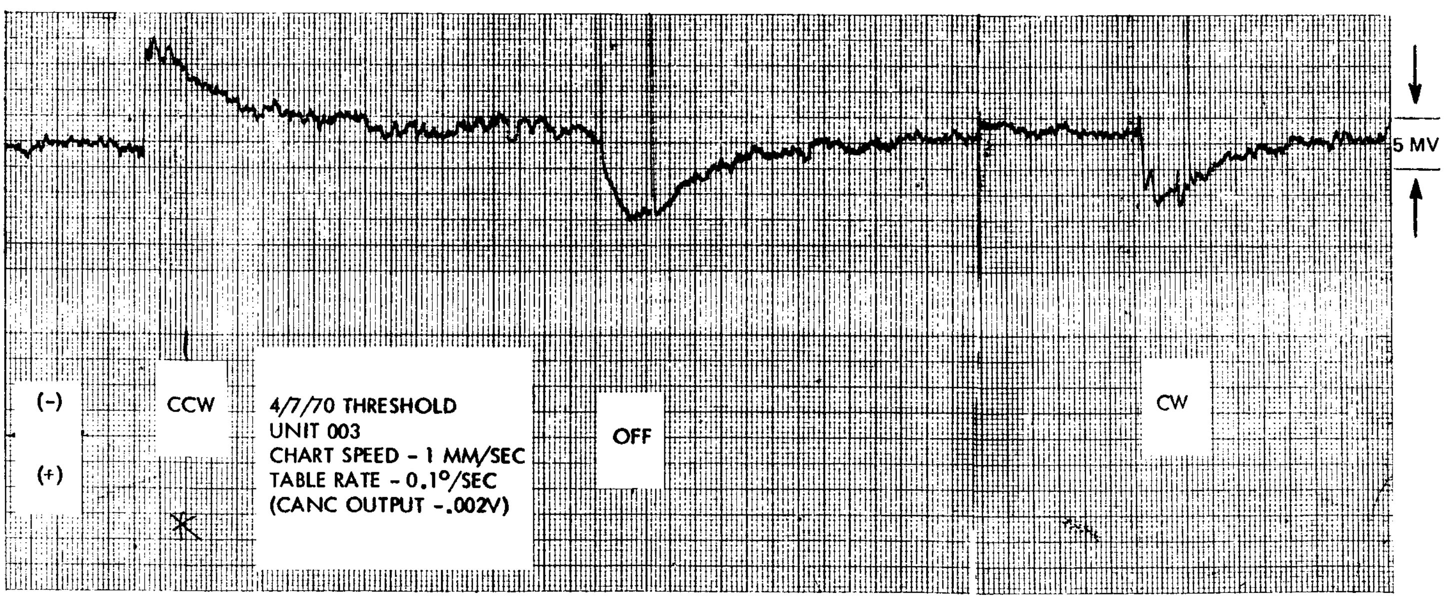

FUNCTIONAL TEST SET 4

Figure 42. Threshold Test - Unit No. 3

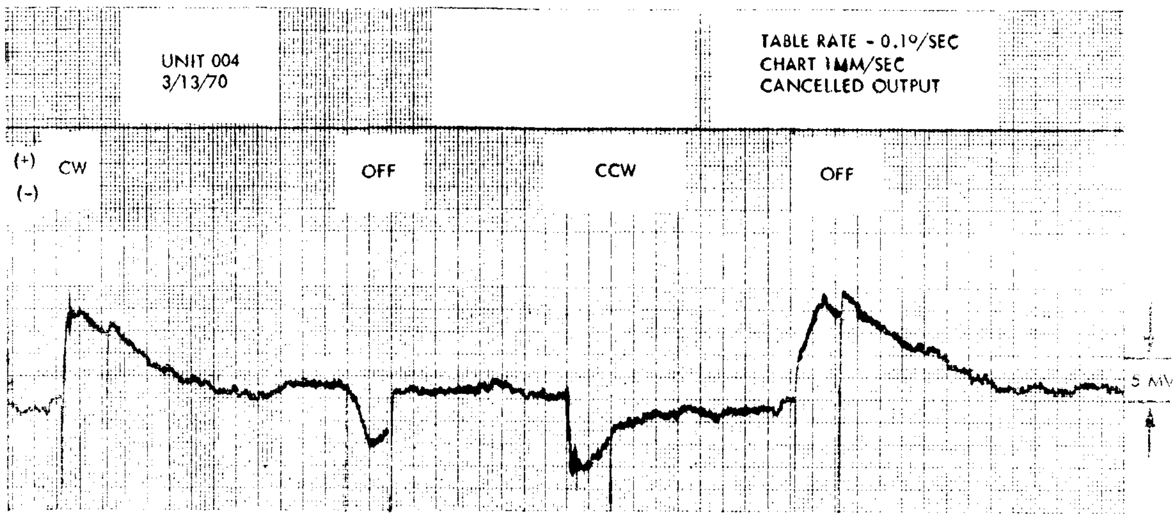

FUNCTIONAL TEST SET 3

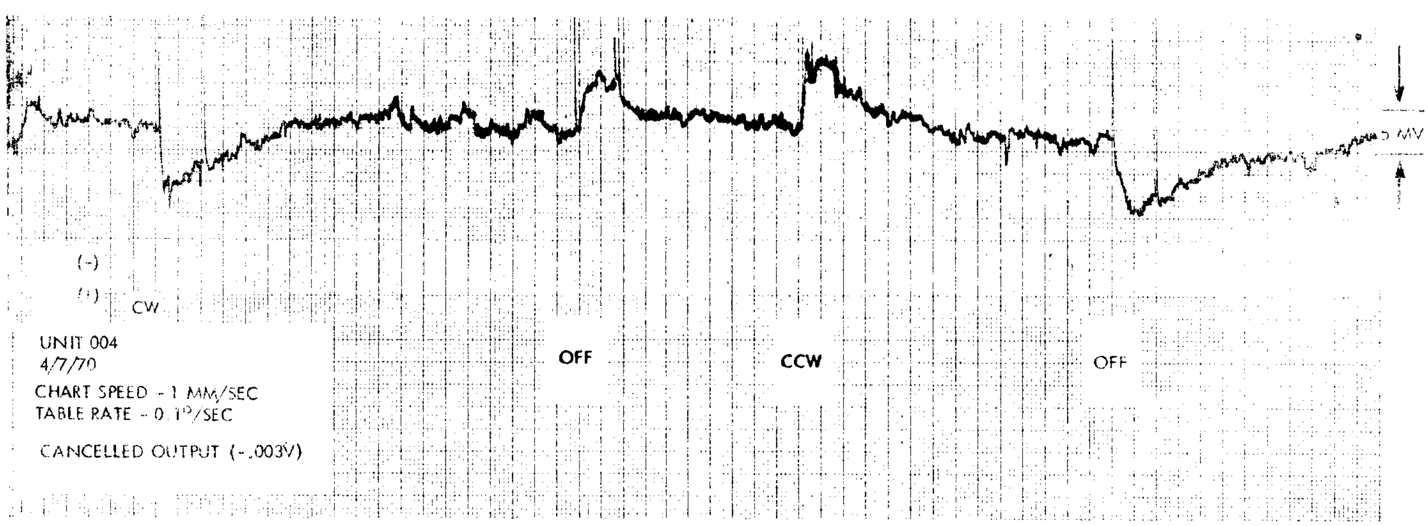

FUNCTIONAL TEST SET 4

Figure 43. Threshold Test - Unit No. 4

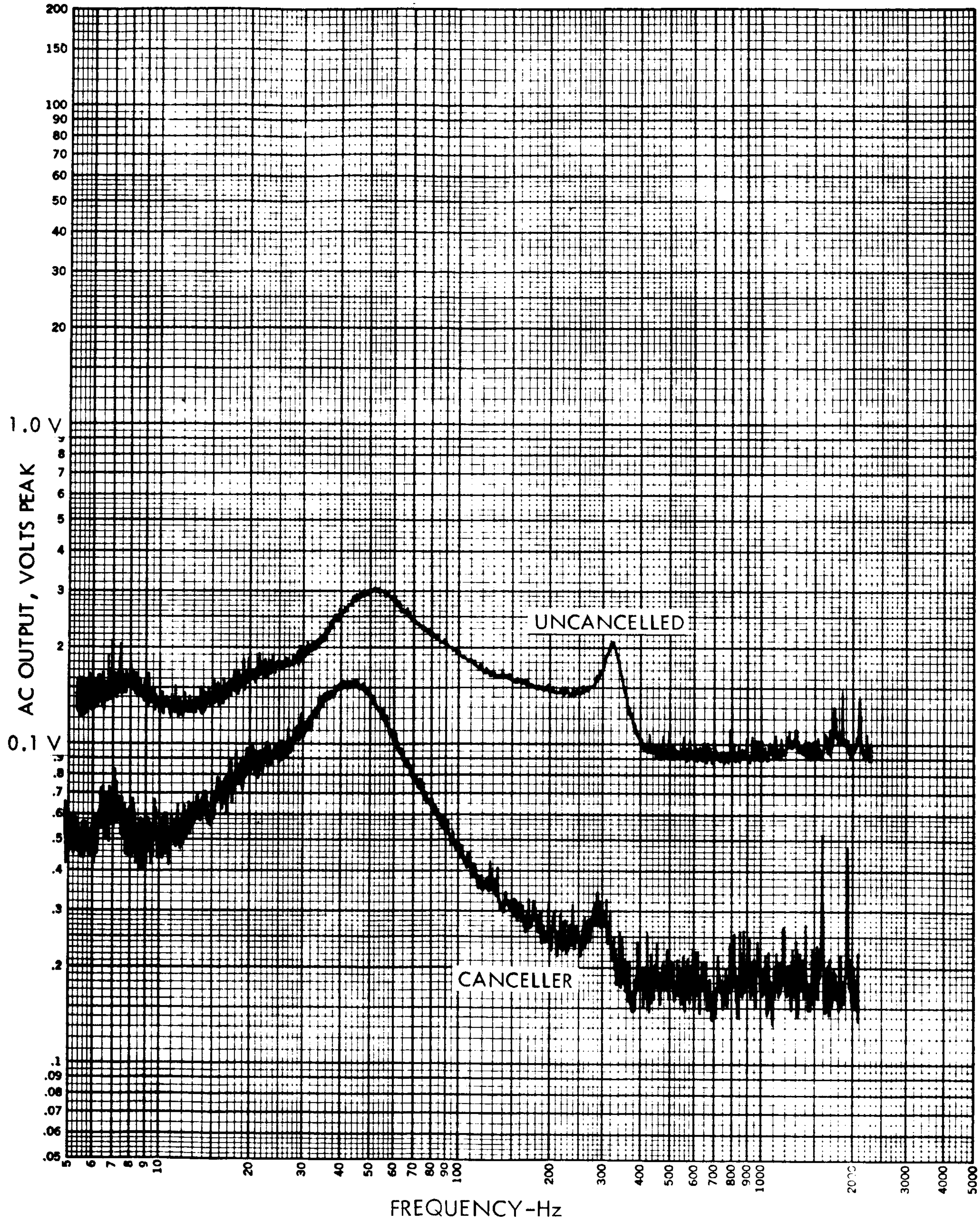

Figure 44. Unit 1, Readout Plane, 1g Input 5 - 2000 Hz - Environmental Test Set 2

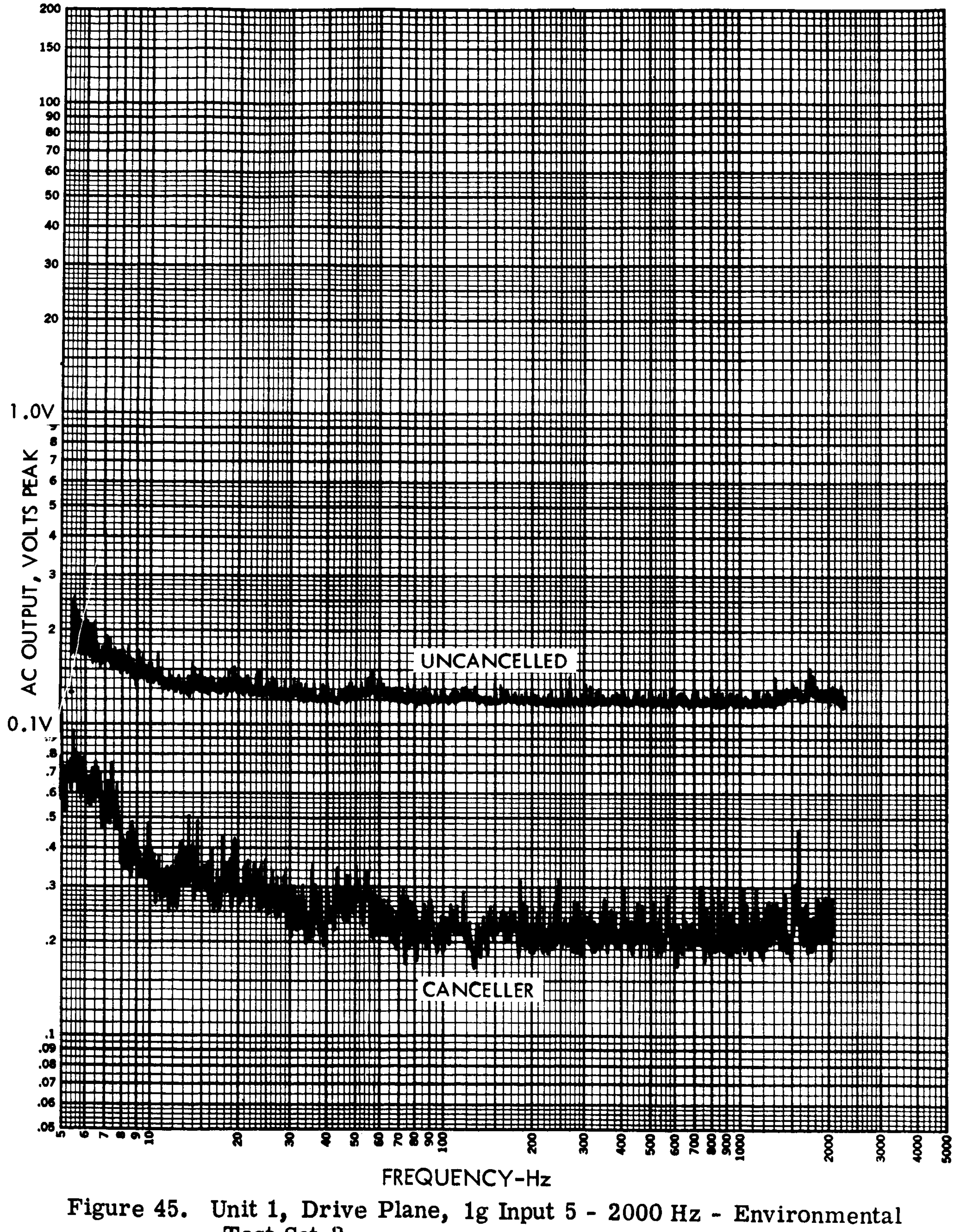

Figure 45. Unit 1, Drive Plane, 1g Input 5 - 2000 Hz - Environmental Test Set 2

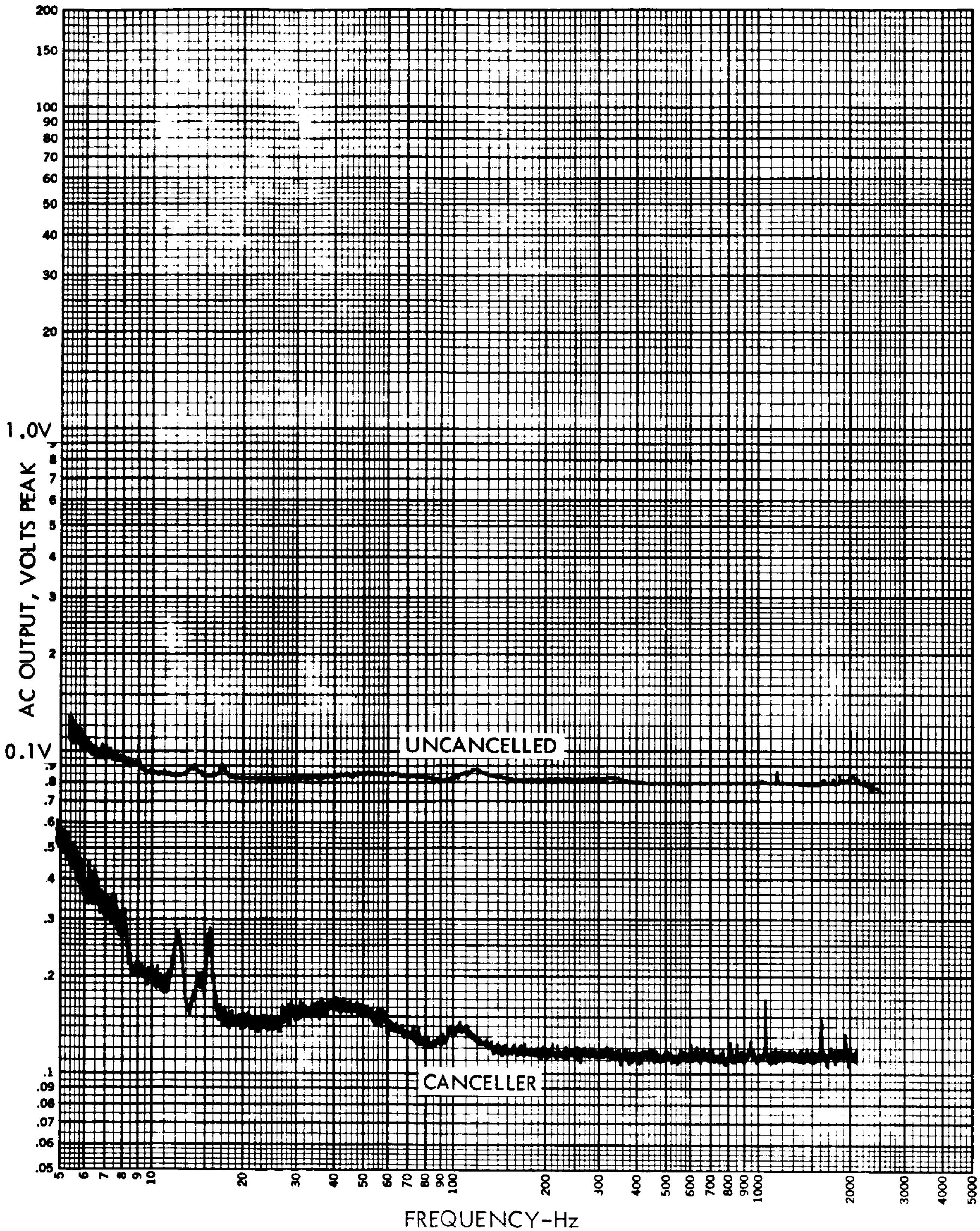

Figure 46. Unit 1, Axial Plane, 1g Input 5 - 2000 Hz - Environmental Test Set 2

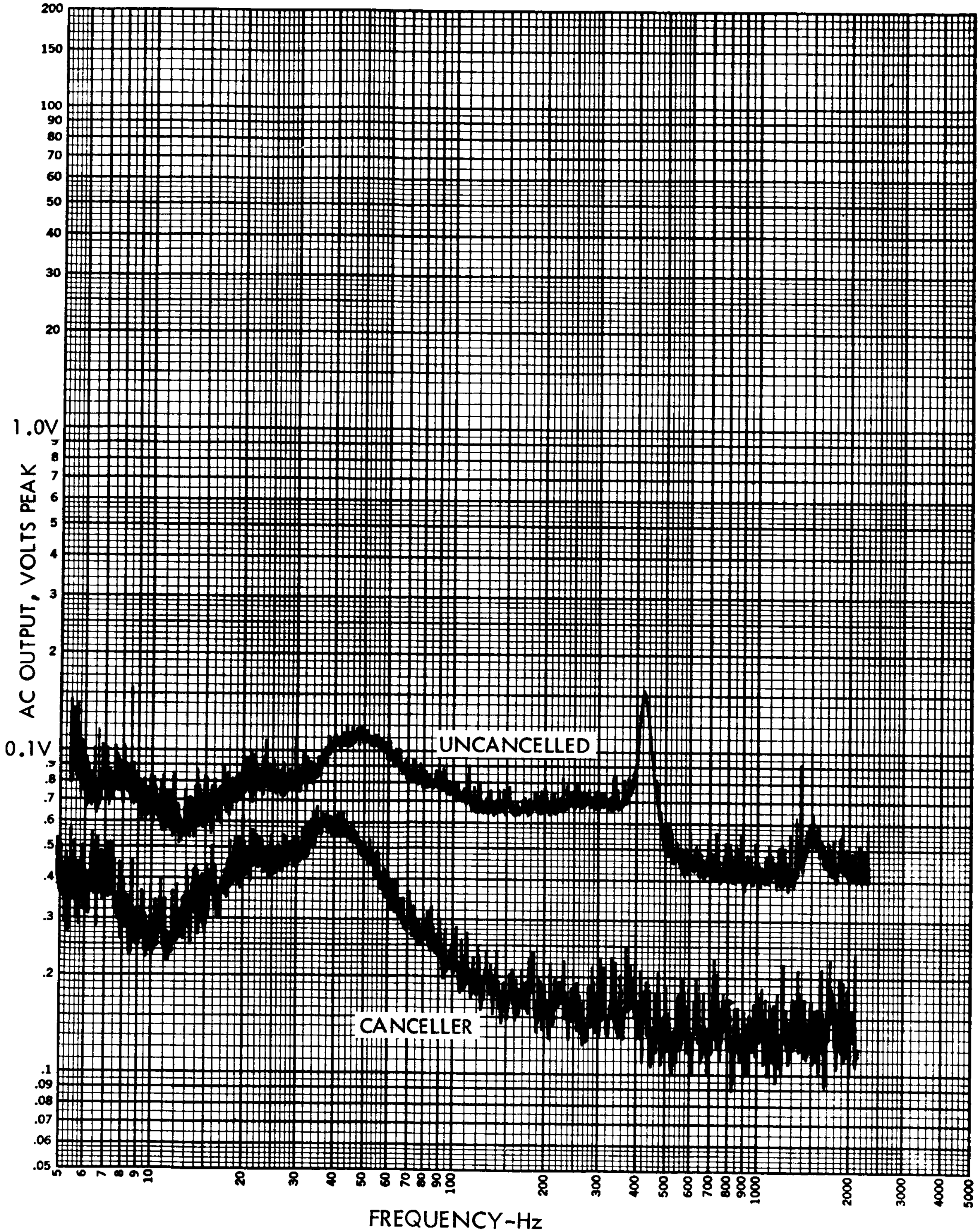

Figure 47. Unit 3, Readout Plane, 1g Input 5 - 2000 Hz - Environmental Test Set 2

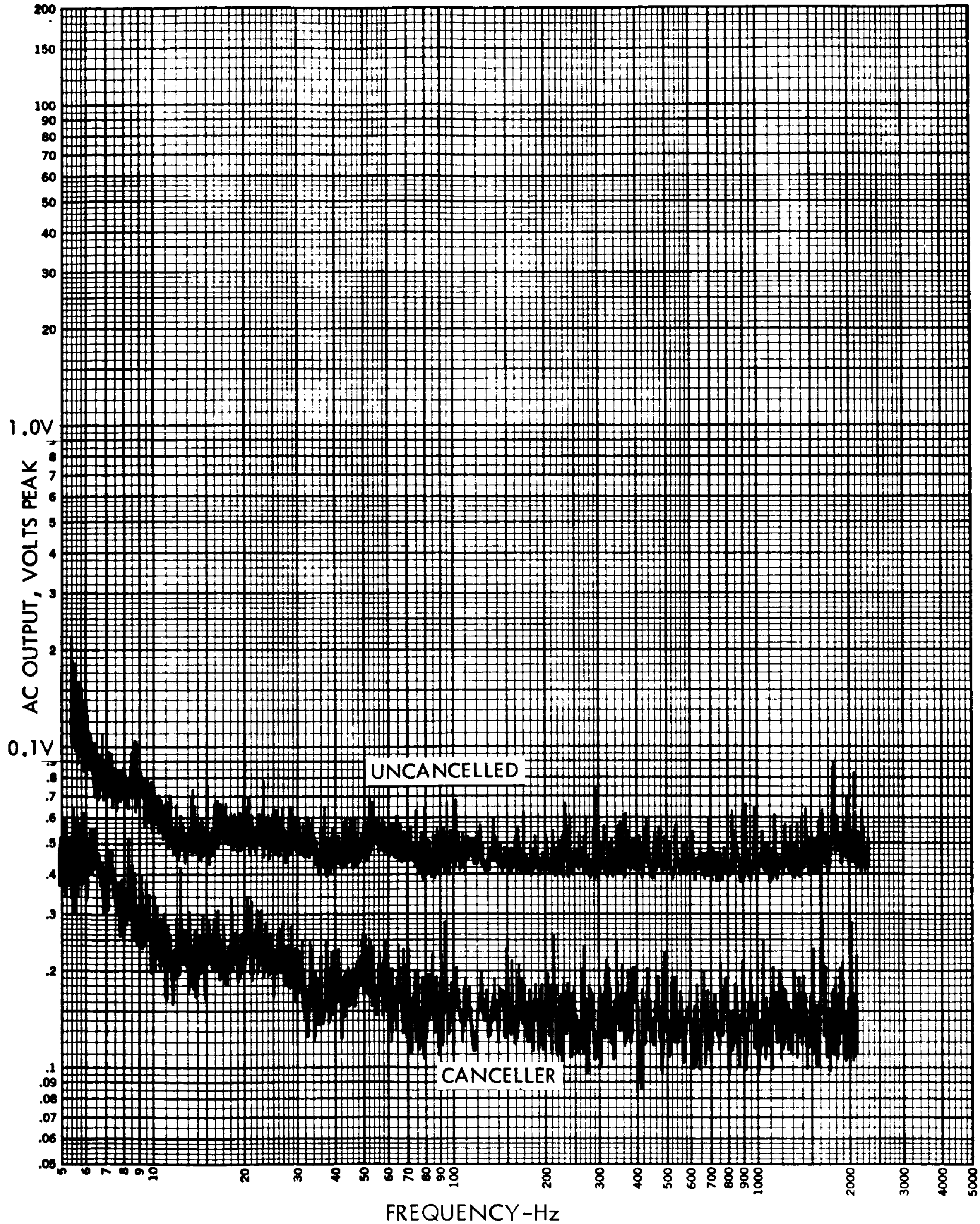

Figure 48. Unit 3, Drive Plane, 1g Input 5 - 2000 Hz - Environmental Test Set 2

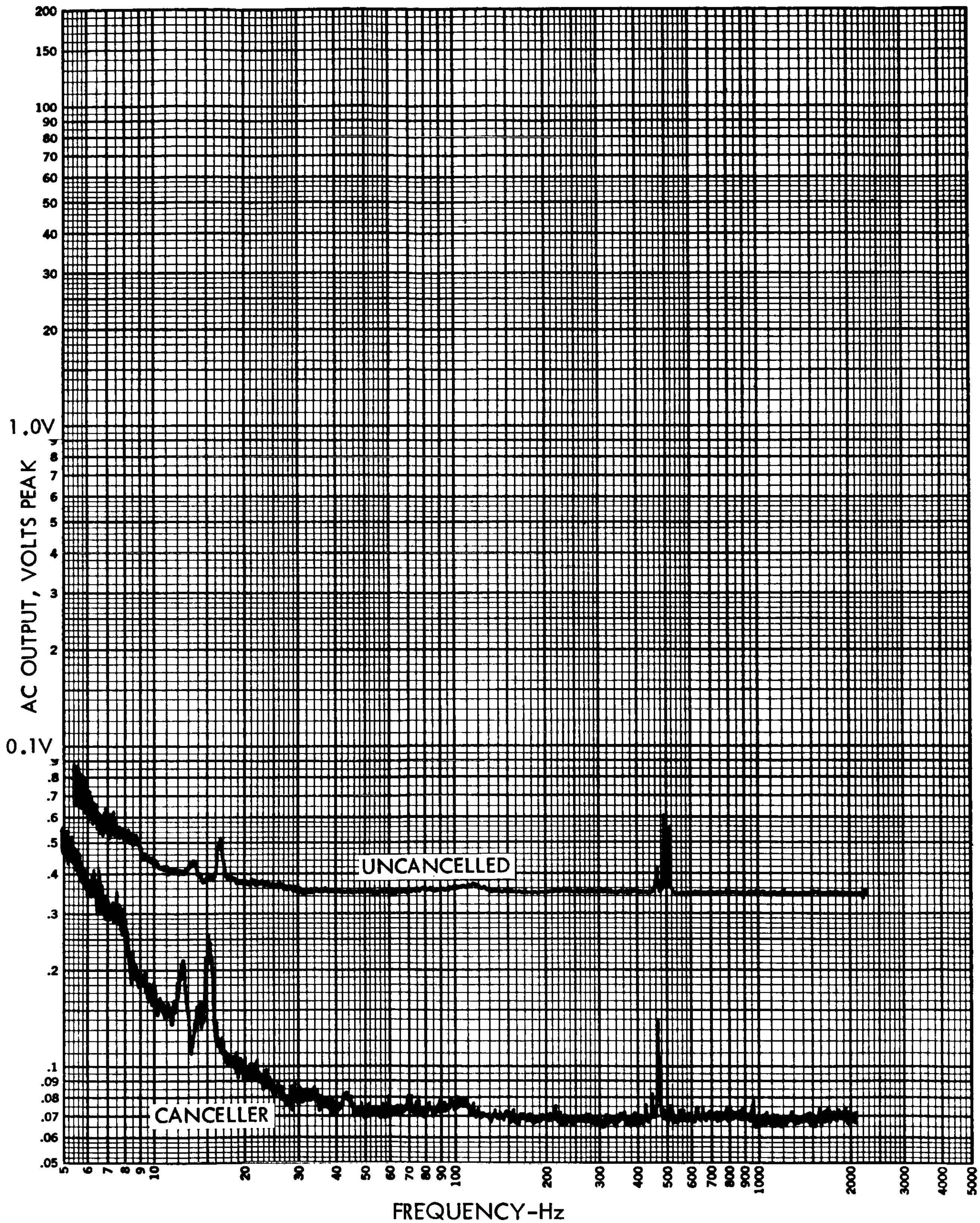

Figure 49. Unit 3, Axial Plane, 1g Input 5 - 2000 Hz - Environmental Test Set 2

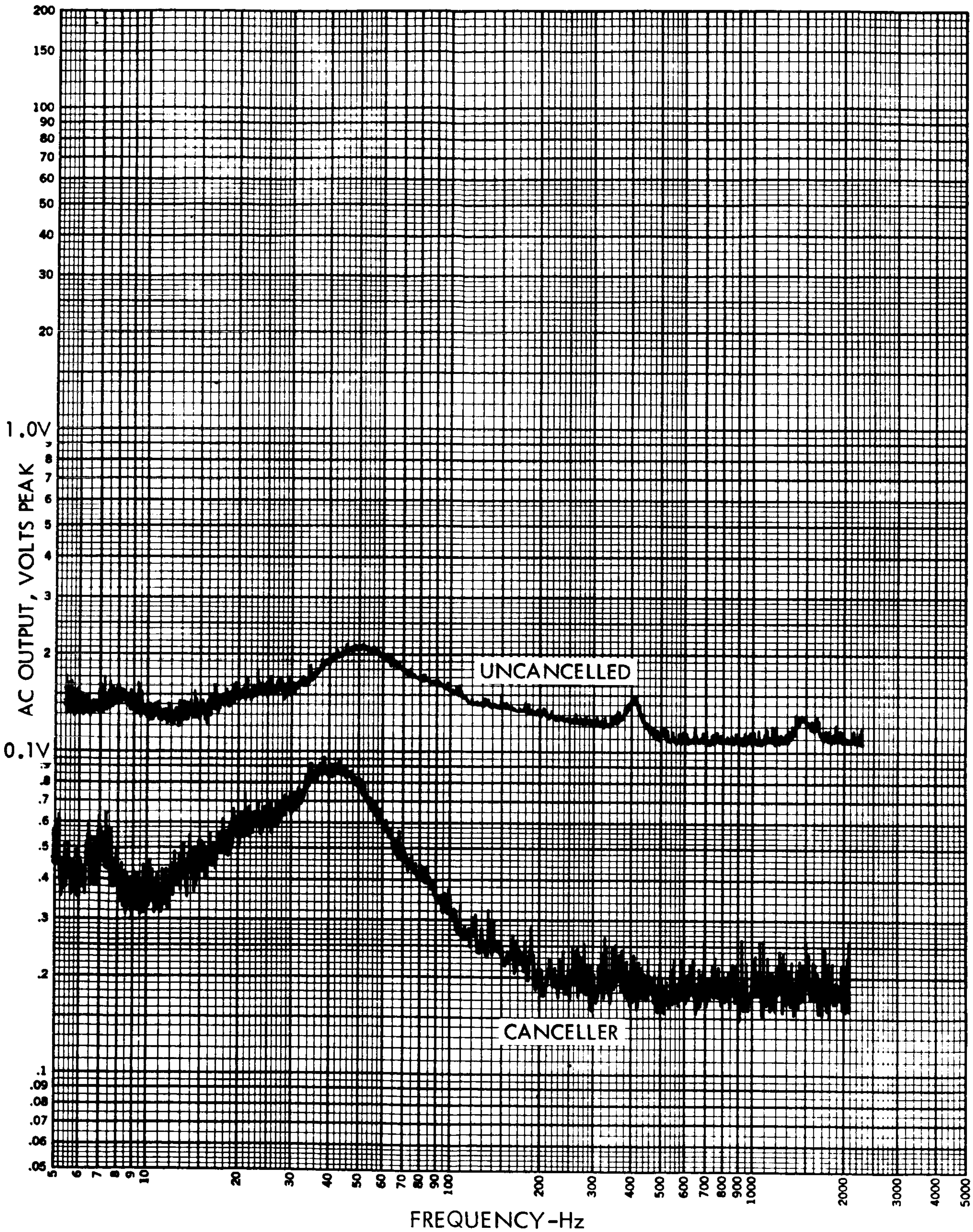

Figure 50. Unit 4, Readout Plane, 1g Input 5 - 2000 Hz - Environmental Test Set 2

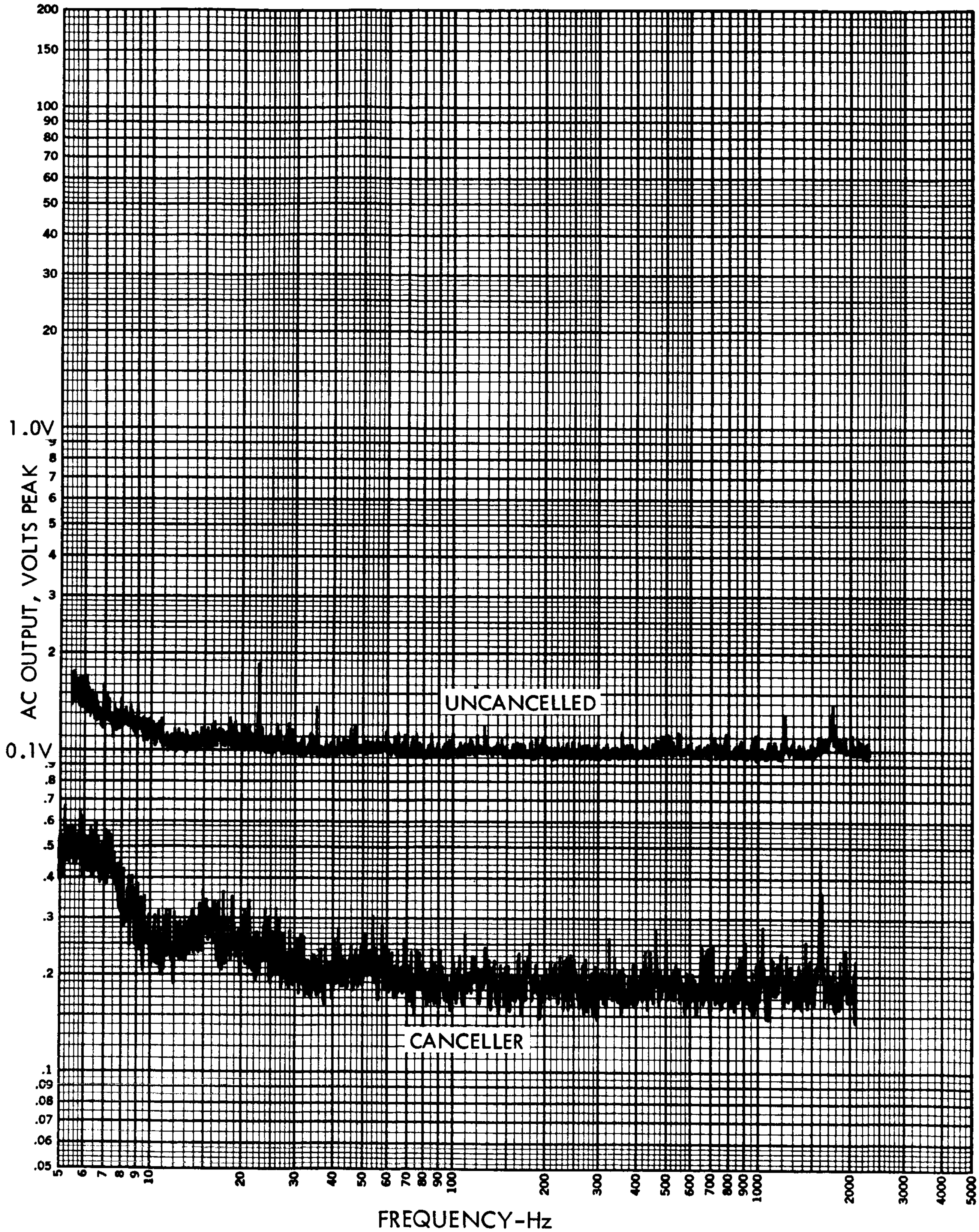

Figure 51. Unit 4, Drive Plane, 1g Input 5 - 2000 Hz - Environmental Test Set 2

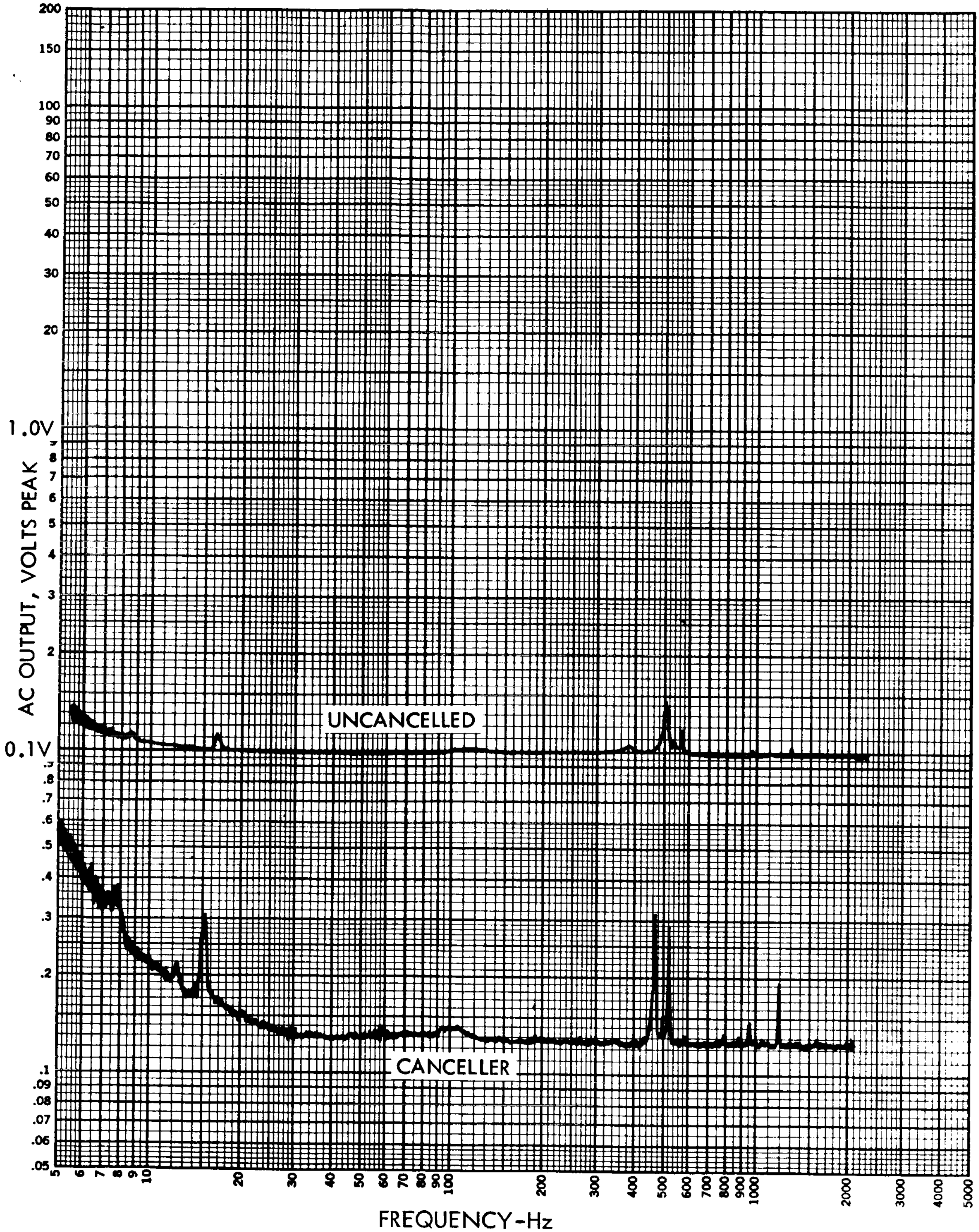

Figure 52. Unit 4, Axial Plane, 1g Input Level 5 - 2000 Hz - Environmental Test Set 2

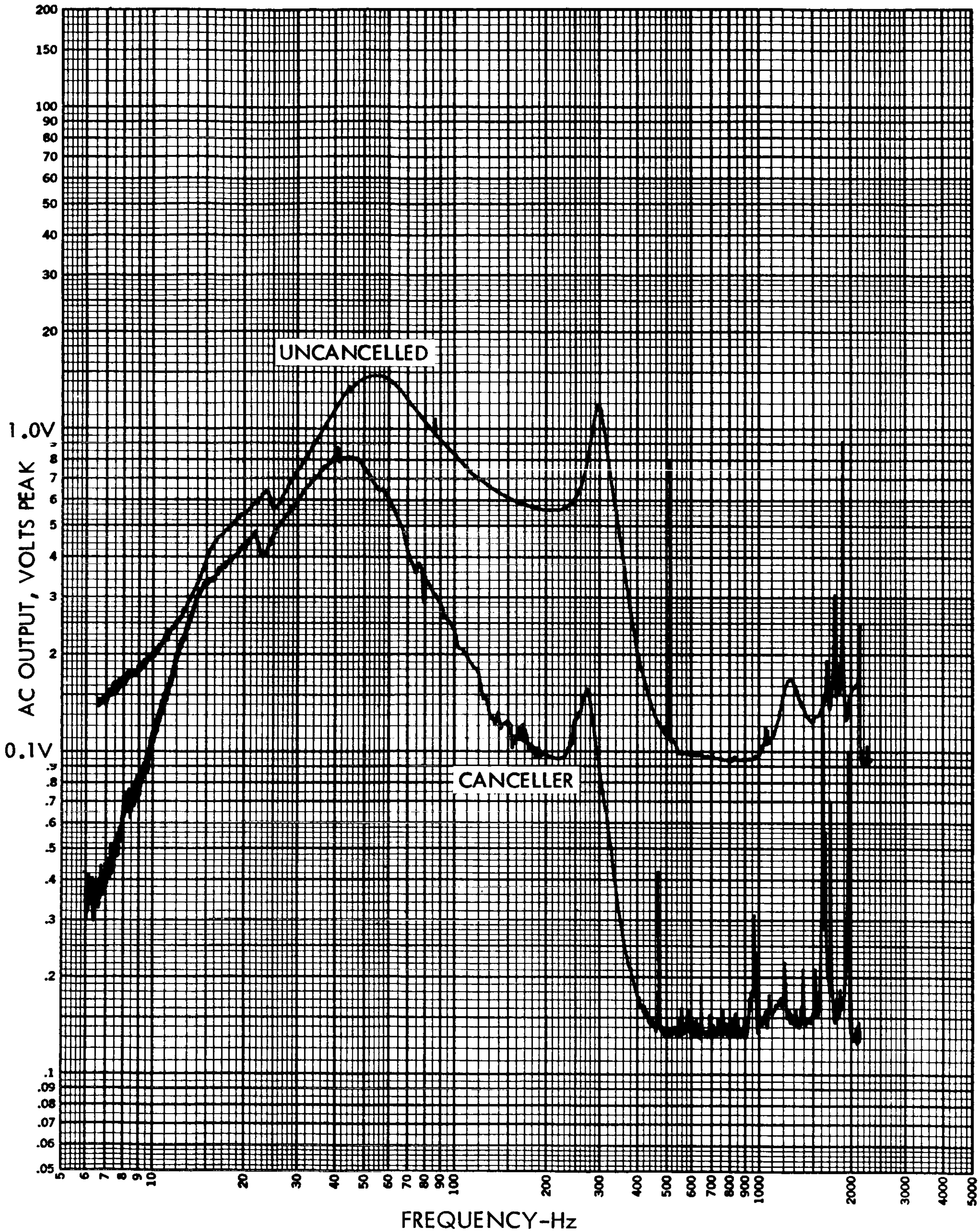

Figure 53. Unit 1, Readout Plane, (Input: 6 to 14 Hz .5" DA, 14 to 2000 Hz ±5g) - Environmental Test Set No. 2

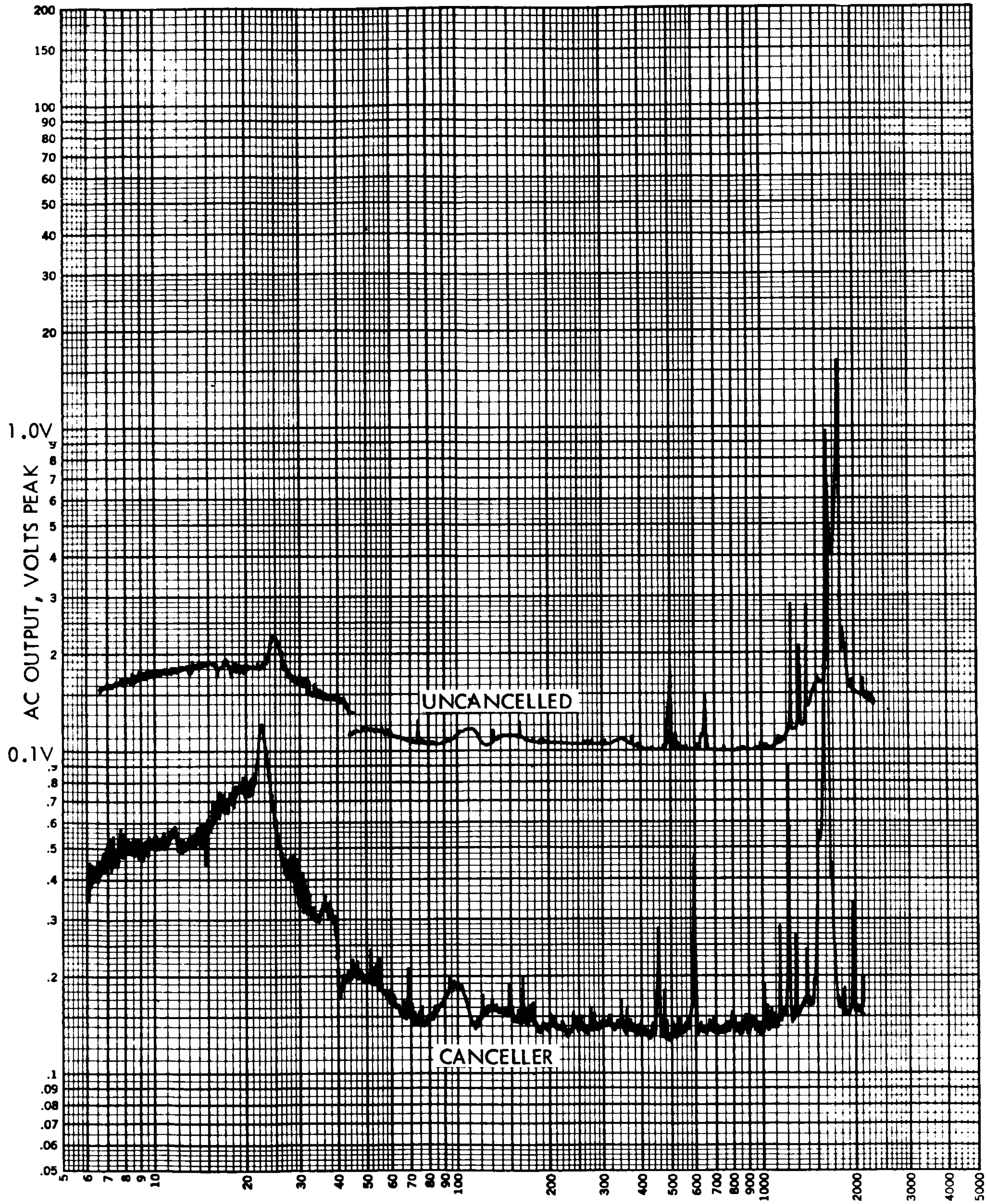

Figure 54. Unit 1, Drive Plane, (Input: 6 to 14 Hz .5" DA, 14 to 2000 Hz ±5g) - Environmental Test Set No. 2

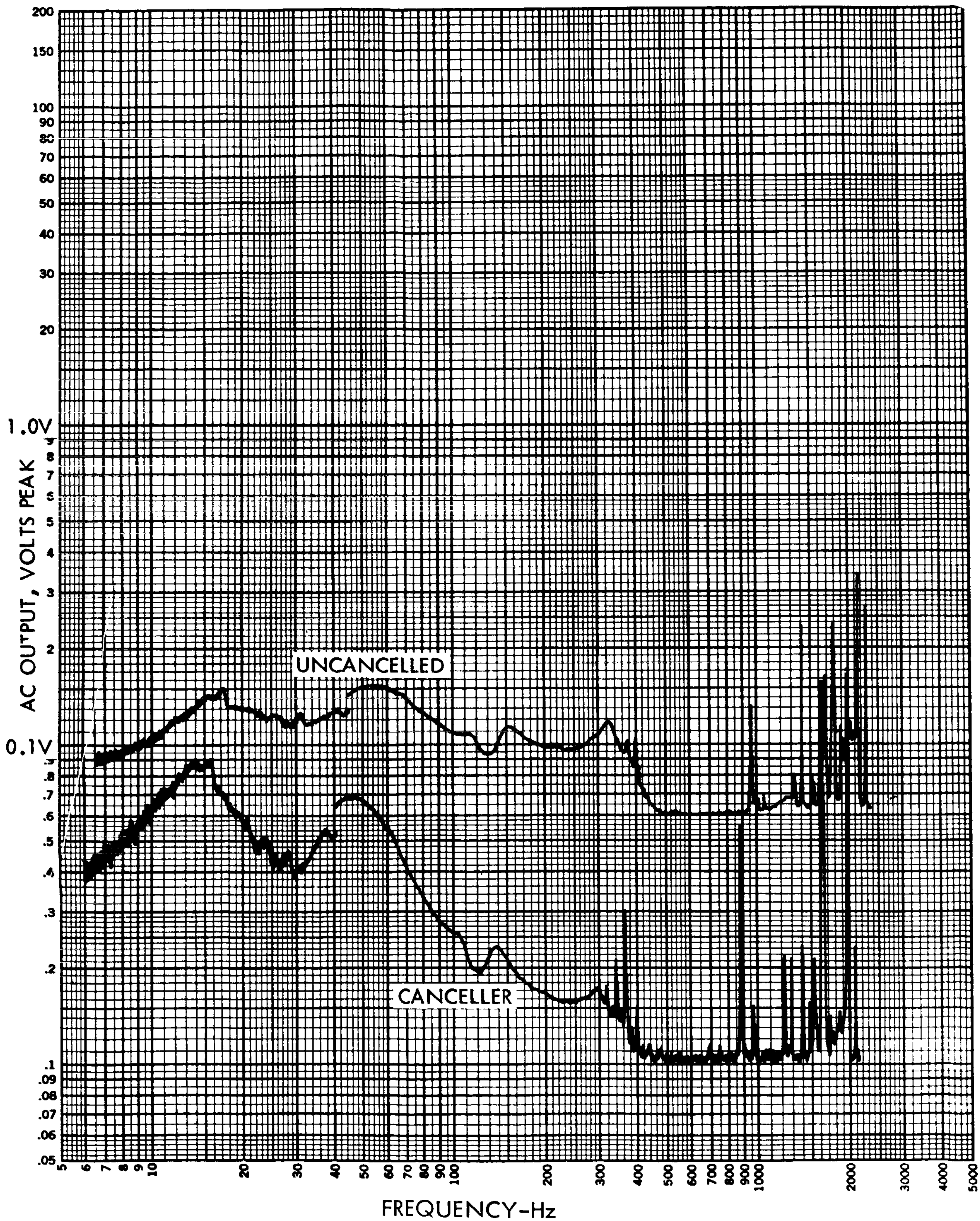

Figure 55. Unit 1, Axial Plane, (Input: 6 to 14 Hz .5" DA, 14 to 2000 Hz ±5g) - Environmental Test Set No. 2

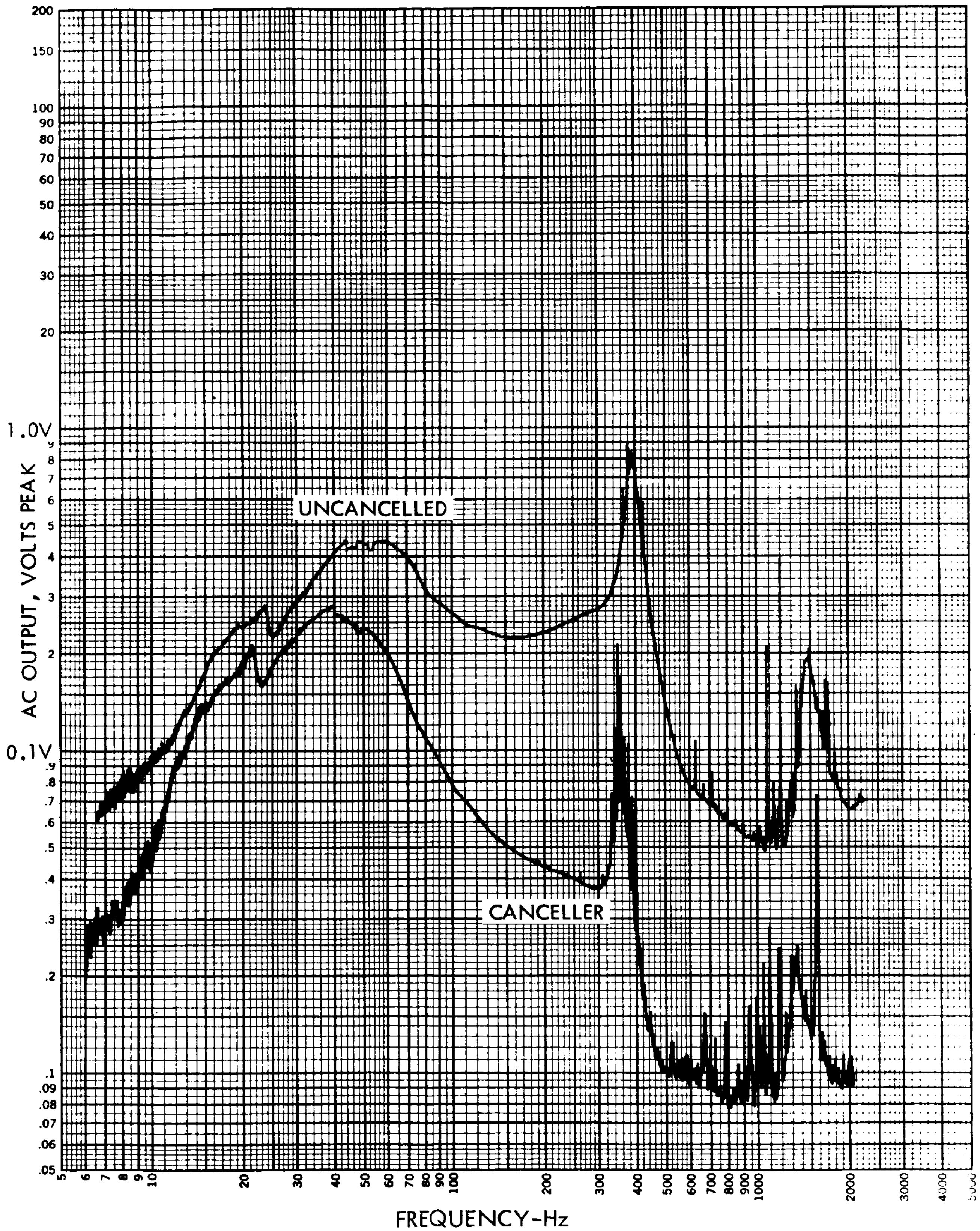

Figure 56. Unit 3, Readout Plane, (Input: 6 to 14 Hz .5" DA, 14 to 2000 Hz ±5g) - Environmental Test Set No. 2

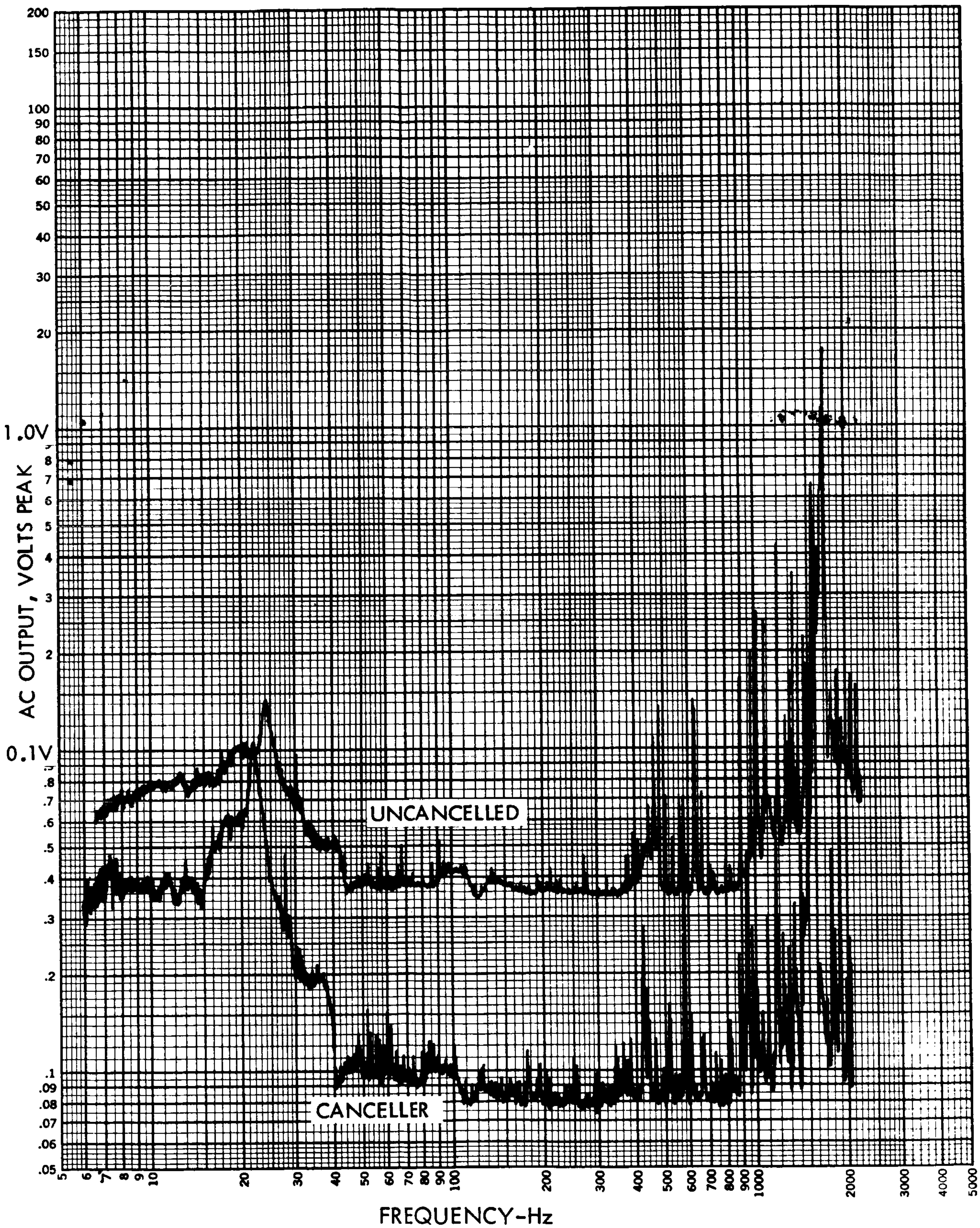

Figure 57. Unit 3, Drive Plane, (Input: 6 to 14 Hz .5" DA, 14 to 2000 Hz ±5g) - Environmental Test Set No. 2

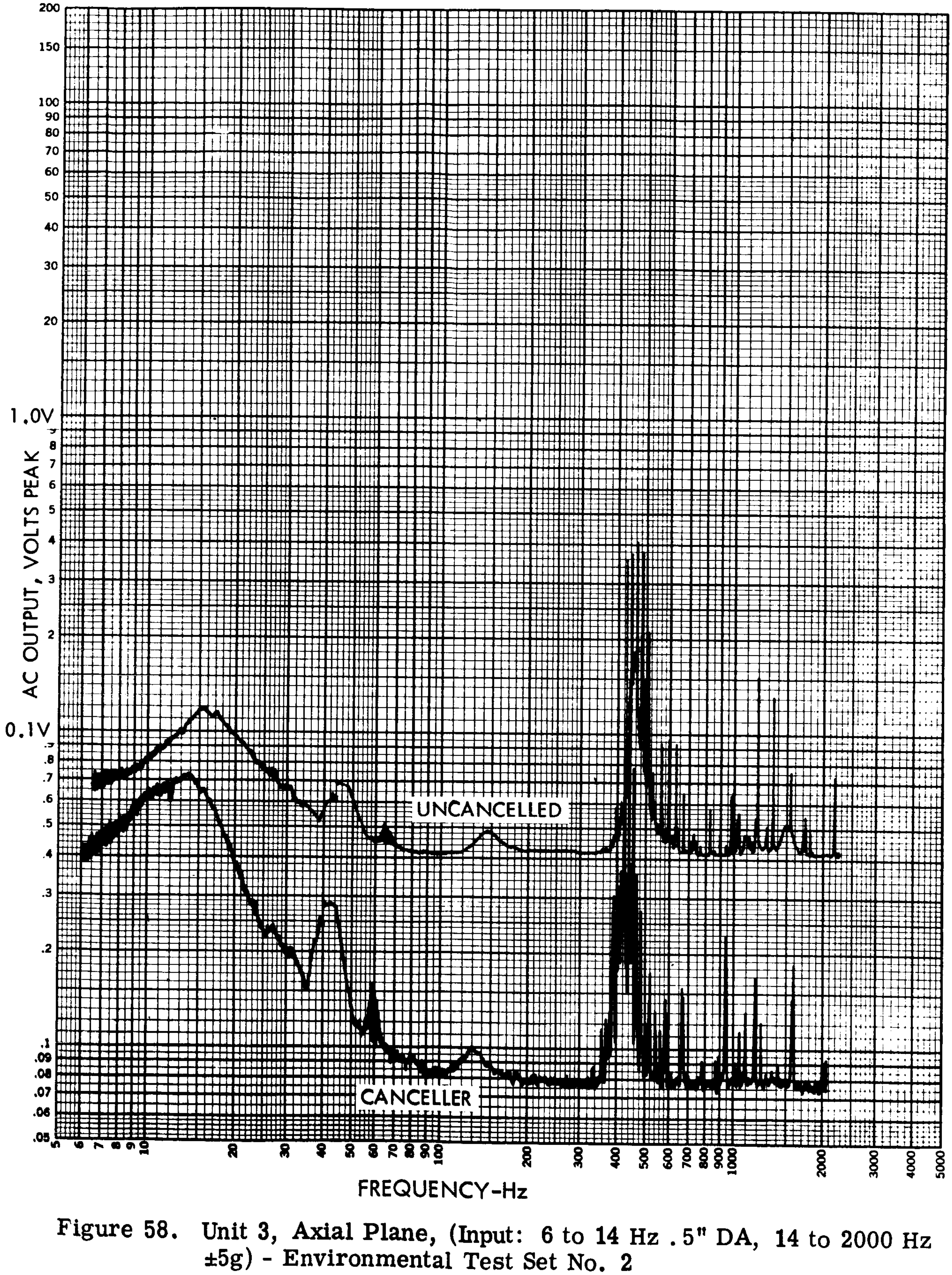

Figure 58. Unit 3, Axial Plane, (Input: 6 to 14 Hz .5" DA, 14 to 2000 Hz ±5g) - Environmental Test Set No. 2

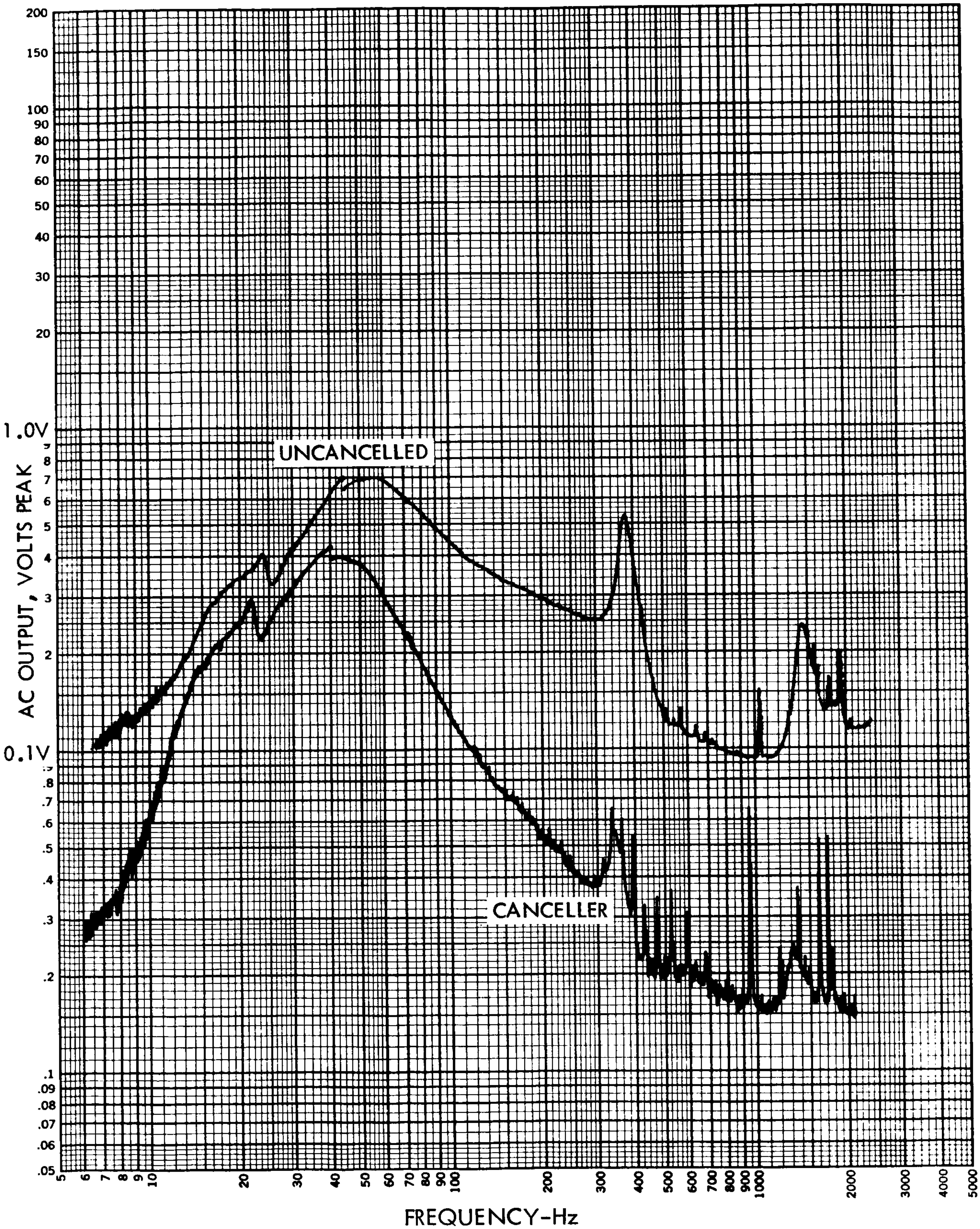

Figure 59. Unit 4, Readout Plane, (Input: 6 to 14 Hz .5" DA, 14 to 2000 Hz ±5g) - Environmental Test Set No. 2

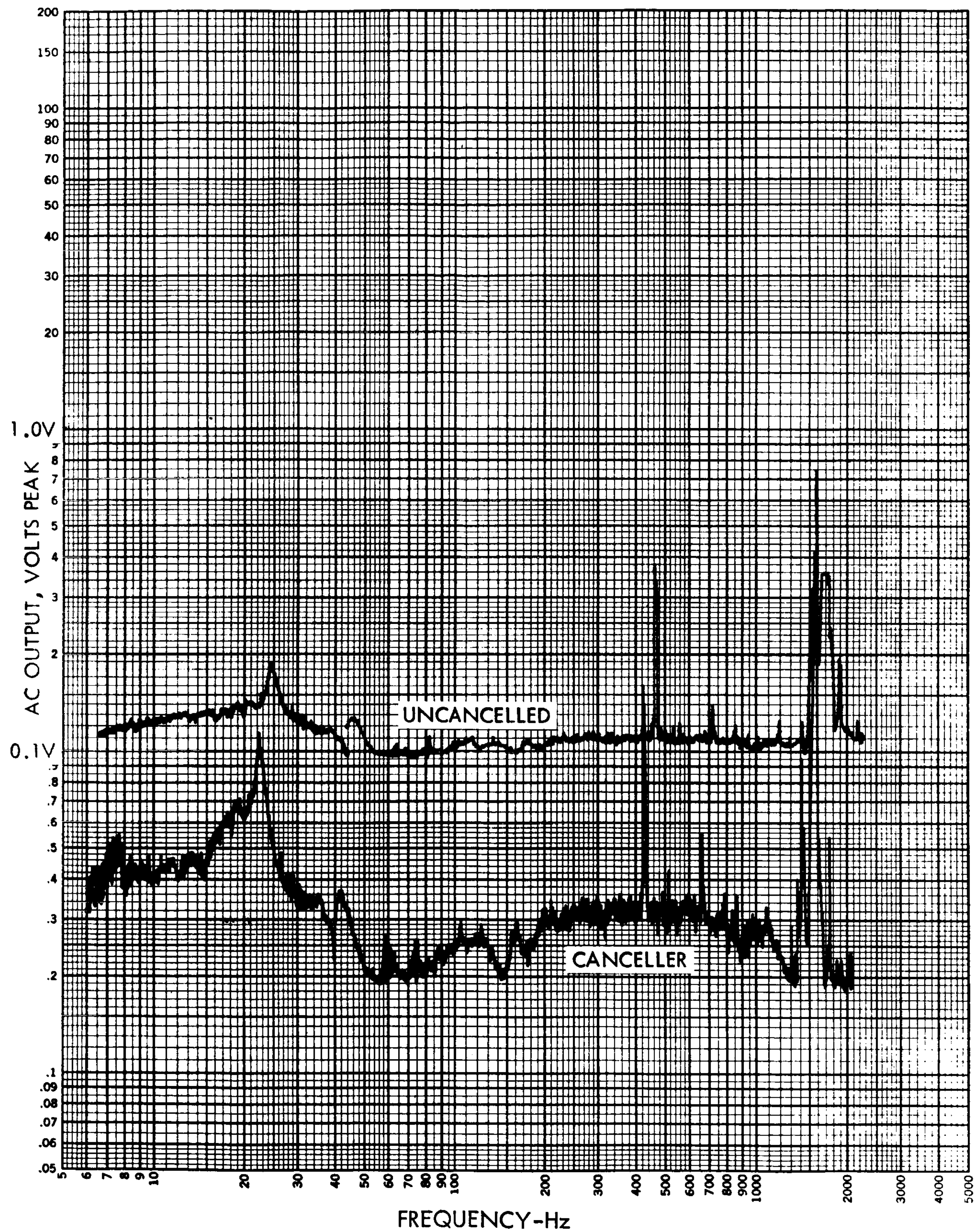

Figure 60. Unit 4, Drive Plane, (Input: 6 to 14 Hz .5" DA, 14 to 2000 Hz ±5g) - Environmental Test Set No. 2

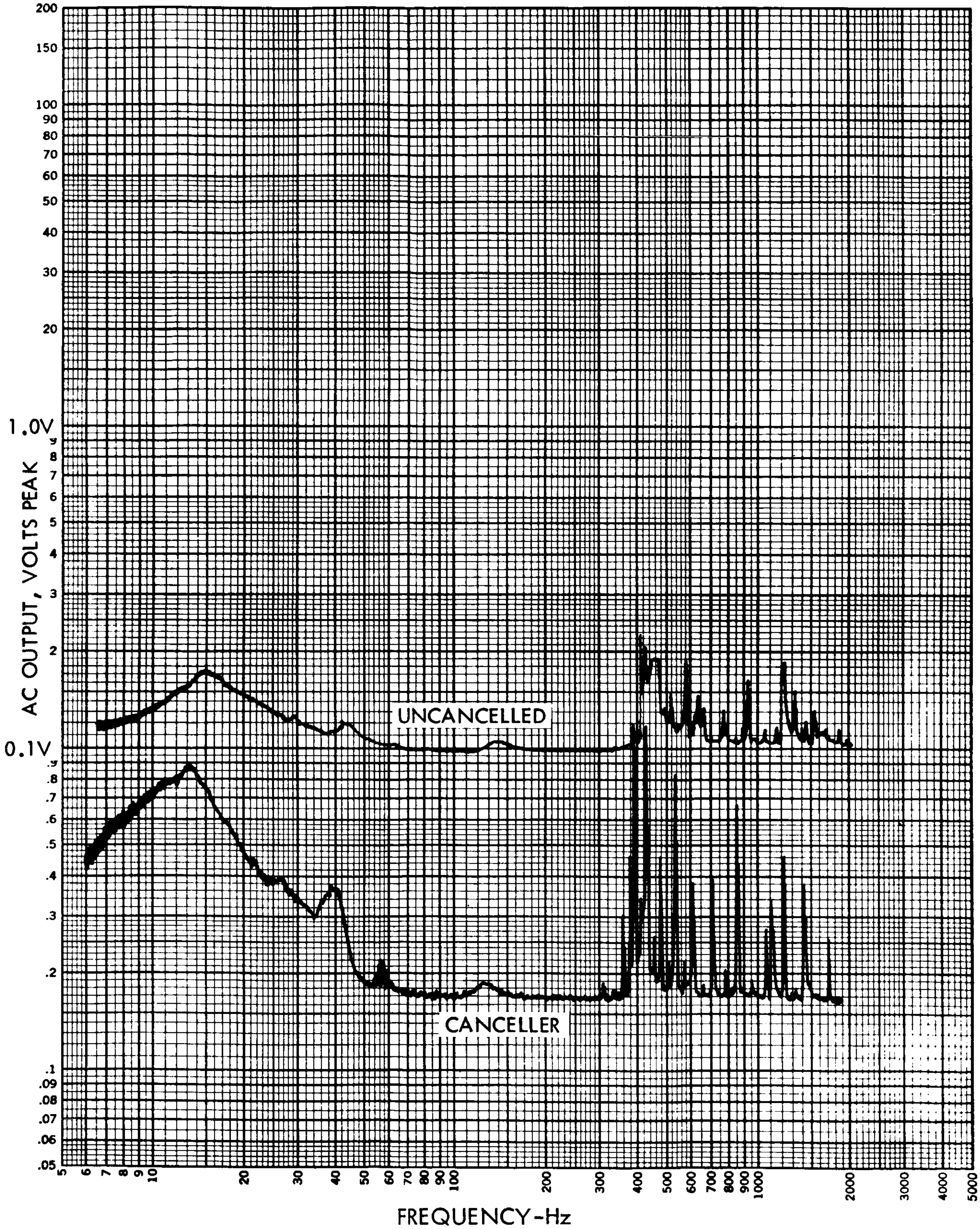

Figure 61. Unit 4, Axial Plane, (Input: 6 to 14 Hz .5" DA, 14 to 2000 Hz ±5g) - Environmental Test Set No. 2

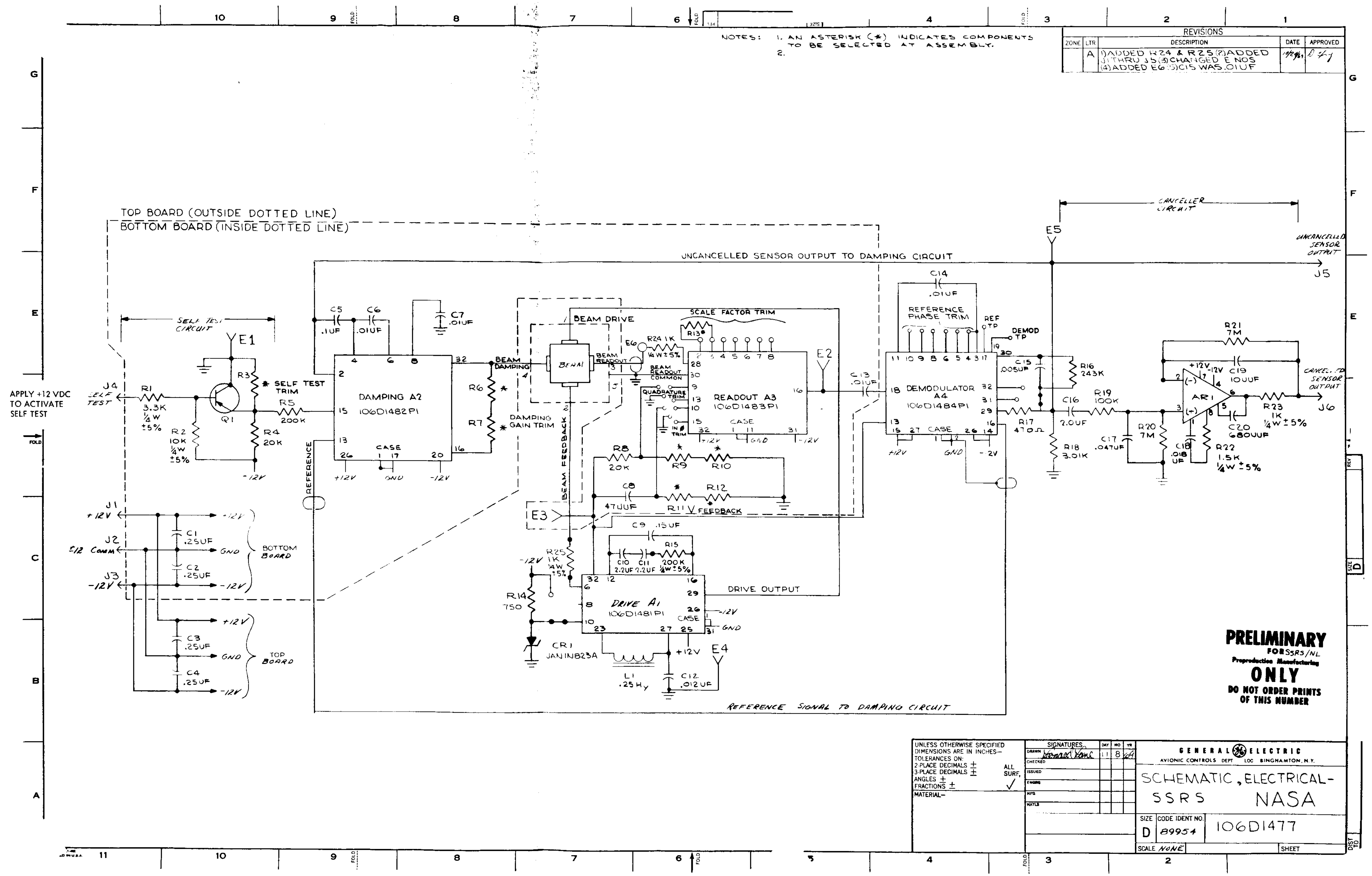

Figure 62. SSRS Electrical Schematic

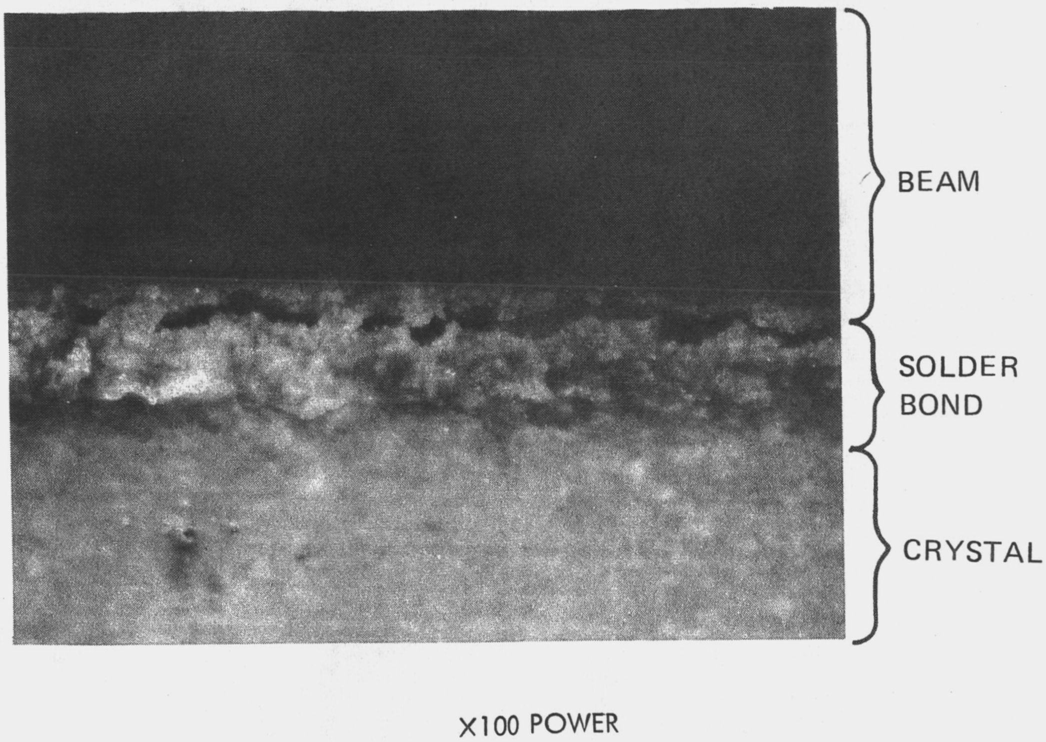

Figure 63. Photograph of Crack in Solder Bond Under One of the Crystals on Beam R2

TABLE 1. BEAM TEST DATA

BEAM # R2
DATE 11-3-69

		+23°C	+70°C
Connect BEAM TEST ELECTRONICS, Hamill-4/4/69. Measure VIN, VFB, VRO with Digital AC VTVM's.			
Sw = DRIVE; Freq. to peak VFB, VIN to cause VFB = 5.00 vac			
READ VIN	(VAC)	0.630	0.813
CALC Dr. Gain = $\frac{182.5}{VIN}$	(μA/V)	290	225
READ f-DR	(Hz)	4625.9	4633.3
ADJ Freq. (High) for VFB = 3.54v; READ F	(Hz)	4627.0	4634.5
ADJ Freq. (Low) for VFB = 3.54v; READ F	(Hz)	4625.4	4632.4
SUBTRACT BW(DR)	(Hz)	1.6	2.1
Sw = DAMPING; Freq. to peak VRO, VIN to cause VRO = 5.00 vac			
READ VIN	(VAC)	0.116	0.119
CALC RO Gain = $\frac{25.0}{VIN}$	(μA/V)	216	210
COPY from above f-DR	(Hz)	4625.9	4633.3
READ f-RO	(Hz)	4548.5	4555.1
SUBTRACT = Separation F	(Hz)	77.4	78.2
ADJ Freq. (High) for VRO = 3.54v; READ F	(Hz)	4549.4	4556.0
ADJ Freq. (Low) for VRO = 3.54v; READ F	(Hz)	4547.8	4554.2
SUBTRACT BW(RO)	(Hz)	1.6	1.8
Connect BEAM RO TEST CIRCUITS, Hamill-4/40/69. Measure VSF with ordinary AC VTVM; Measure VO with Digital DC VTVM.			
DIAL "QUADR" for AC Null of VSF. Read dial. (leave dial as set) I-RO (QUADR)	(μA RMS)	+ .65 A	+ 1.27 μA
DIAL "IN-ϕ" for DC Null of VO. Read dial. (leave dial as set) I-RO (IN-ϕ)	(NA RMS)	+ 70.4 NA	+ 28.9 NA
SCALE FACTOR: RATE TABLE 50.0 deg/sec, CW. VO	(V DC)	- 5.34 v	- 5.33 v
(Beam Scale Factor in nanoamps rms/deg/sec is same as VO above) (Rate Table Off)			
RATE COEFF. SW to Damping input 0.100 VAC, Read VO. VO	(V DC)	+ 4.25 v	+ 4.51 v
CALC RATE COEFF = $\frac{VO}{2}$	(μA RMS/VRMS)	2.125	2.255
(Rate Coeff. Sw. Off)			

TABLE 2. BEAM TEST DATA

BEAM #R3
DATE 10-30-69

	+23°C	+70°C
Connect BEAM TEST ELECTRONICS, Hamill-4/4/69. Measure VIN, VFB, VRO with Digital AC VTVM's.		
Sw = DRIVE; Freq. to peak VFB, VIN to cause VFB = 5.00 vac		
READ VIN (VAC)	0.698	0.711
CALC Dr. Gain = $\frac{182.5}{VIN}$ (μA/V)	262	257
READ f-DR (Hz)	4641.2	4651.5
ADJ Freq. (High) for VFB = 3.54v; READ F (Hz)	4642.3	4652.6
ADJ Freq. (Low) for VFB = 3.54v; READ F (Hz)	4640.7	4650.8
SUBTRACT BW(DR) (Hz)	1.6	1.8
Sw = DAMPING; Freq. to peak VRO, VIN to cause VRO = 5.00 vac		
READ VIN (VAC)	.176	.126
CALC RO Gain = $\frac{25.0}{VIN}$ (μA/V)	142	198
COPY from above		
F-DR (Hz)	4641.2	4651.5
READ F-RO (Hz)	4557.5	4565.9
SUBTRACT = Separation F (Hz)	83.7	85.6
ADJ Freq. (High) for VRO = 3.54v; READ F (Hz)	4558.8	4567.0
ADJ Freq. (Low) for VRO = 3.54v; READ F (Hz)	4556.4	4565.2
SUBTRACT BW(RO) (Hz)	2.4	1.8
Connect BEAM RO TEST CIRCUITS, Hamill-4/30/69. Measure VSF with ordinary AC VTVM; Measure VO with Digital DC VTVM.		
DIAL "QUADR" for AC Null of VSF. Read dial. (leave dial as set) I-RO(QUADR) (μA RMS)	- .09 μA	+ .1 μA
DIAL "IN-ϕ" for DC Null of VO. Read dial. (leave dial as set) I-RO (IN-ϕ) (NA RMS)	+ 33.9 NA	+ 34.8 NA
SCALE FACTOR: RATE TABLE 50.0 deg/sec, CW. VO (V DC)	- 4.93 v	- 4.81 v
(Beam Scale Factor in nanoamps rms/deg/sec is same as VO above)		
(Rate Table Off)		
RATE COEFF. SW to Damping input 0.100 VAC, Read VO. VO (V DC)	+ 3.96 v	+ 4.04 v
CALC RATE COEFF = $\frac{VO}{2}$ (μA RMS/VRMS)	1.98	2.02
(Rate Coeff. Sw. Off)		

TABLE 3. BEAM TEST DATA

BEAM #R4
DATE 11-3-69

		+23°C	+70°C
Connect BEAM TEST ELECTRONICS, Hamill-4/4/69. Measure VIN, VFB, VRO with Digital AC VTVM's.			
Sw = DRIVE; Freq. to peak VFB, VIN to cause VFB = 5.00 vac			
READ VIN	(VAC)	0.711	0.946
CALC Dr. Gain = $\frac{182.5}{VIN}$	(μA/V)	257	193
READ f-DR	(Hz)	4639.4	4646.2
ADJ Freq. (High) for VFB = 3.54v; READ F	(Hz)	4640.6	4647.8
ADJ Freq. (Low) for VFB = 3.54v; READ F	(Hz)	4638.9	4645.4
SUBTRACT BW(DR)	(Hz)	1.7	2.4
Sw = DAMPING; Freq. to peak VRO, VIN to cause VRO = 5.00 vac			
READ VIN	(VAC)	.118	.130
CALC RO Gain = $\frac{25.0}{VIN}$	(μA/V)	212	192
COPY from above f-DR	(Hz)	4639.4	4646.2
READ f-RO	(Hz)	4565.7	4571.2
SUBTRACT = Separation F	(Hz)	73.7	75.0
ADJ Freq. (High) for VRO = 3.54v; READ F	(Hz)	4566.7	4572.3
ADJ Freq. (Low) for VRO = 3.54v; READ F	(Hz)	4564.8	4570.1
SUBTRACT BW(RO)		1.9	2.2
Connect BEAM RO TEST CIRCUITS, Hamill-4/30/69. Measure VSF with ordinary AC VTVM; Measure VO with Digital DC VTVM. DIAL "QUADR" for AC Null of VSF. Read dial.			
(leave dial as set) I-RO (QUADR)	(μA RMS)	+ 1.4 μA	+ 1.05 μA
DIAL "IN-ϕ" for DC Null of VO. Read dial. (leave dial as set) I-RO (IN-ϕ)	(NA RMS)	+ 43.3 NA	+ 93.3 NA
SCALE FACTOR: RATE TABLE 50.0 deg/sec, CW. VO	(V DC)	+ 5.91 v	+ 5.88 v
(Beam Scale Factor in nanoamps rms/deg/sec is same as VO above) (Rate Table Off)			
RATE COEFF. SW to Damping input 0.100 VAC, Read VO VO	(V DC)	+ 4.97 v	+ 5.196
CALC RATE COEFF = $\frac{VO}{2}$	(μA RMS/VRMS)	2.485	2.598
(Rate Coeff. Sw. Off)			

TABLE 4. BEAM TEST DATA

BEAM #R1
DATE 10-30-69

		+23°C	+70°C
Connect BEAM TEST ELECTRONICS, Hamill-4/4/69. Measure VIN, VFB, VRO with Digital AC VTVM's.			
Sw = DRIVE; Freq. to peak VFB, VIN to cause VFB = 5.00 vac			
READ VIN	(VAC)	0.975	1.46
CALC Dr. Gain = $\frac{182.5}{VIN}$	(μA/V)	187.2	125 μA/V
READ f-DR	(Hz)	4627.9	4634.6
ADJ Freq. (High) for VFB = 3.54v; READ F	(Hz)	4629.2	4636.4
ADJ Freq. (Low) for VFB = 3.54v; READ F	(Hz)	4627.2	4633.5
SUBTRACT BW(DR)	(Hz)	2.0	2.9
Sw = DAMPING; Freq. to peak VRO, VIN to cause VRO = 5.00 vac			
READ VIN	(VAC)	0.138	0.124
CALC RO Gain = $\frac{25.0}{VIN}$	(μA/V)	181	202
COPY from above f-DR	(Hz)	4627.9	4634.6
READ f-RO	(Hz)	4551.4	4559.2
SUBTRACT = Separation F	(Hz)	76.5	75.4
ADJ Freq. (High) for VRO = 3.54v; READ F	(Hz)	4552.2	4560.0
ADJ Freq. (Low) for VRO = 3.54v; READ F	(Hz)	4550.6	4558.5
SUBTRACT BW(RO)	(Hz)	1.6	1.5
Connect BEAM RO TEST CIRCUITS, Hamill-4/30/69. Measure VSF with ordinary AC VTVM; Measure VO with Digital DC VTVM.			
DIAL "QUADR" for AC Null of VSF. Read dial. (leave dial as set) I-RO (QUADR)	(μA RMS)	+ 2.88 μA	+ 2.84 μA
DIAL "IN-ϕ" for DC Null of VO. Read dial. (leave dial as set) I-RO (IN-ϕ)	(NA RMS)	+ 19.4 NA	- 51.3 NA
SCALE FACTOR: RATE TABLE 50.0 deg/sec, CW. VO	(V DC)	+ 5.10NA	+ 5.23 v
(Beam Scale Factor in nanoamps rms/deg/sec is same as VO above) (Rate Table Off)			
RATE COEFF. SW to Damping input 0.100 VAC, Read VO. VO	(V DC)	+ 3.704 v	+ 3.89 v
CALC RATE COEFF = $\frac{VO}{2}$	(μA RMS/VRMS)	1.852	1.945
(Rate Coeff. Sw. Off)			

TABLE 5. BEAM DATA

BEAM #R5

DRIVE PLANE			
(a) Gain		=	$238 \mu A/Volt$
(b) Resonant Frequency:	f_{DR}	=	4632.9 Hz
READOUT PLANE			
(a) Quadrature Current out of Readout Crystal:	I_Q	=	$4.05 \mu A$ rms
(b) In-phase Current out of Readout Crystal:	$I_{IN-\phi}$	=	77.6 nanoamps rms
(c) Resonant Frequency:	f_{RO}	=	4552.1 Hz
Separation Frequency:	f_S	=	$f_{DR}-f_{RO}$ = 80.8 Hz

TABLE 6. LINEARITY AND SCALE FACTOR DATA - UNIT 1 FUNCTIONAL TEST SET 1

RATES (DEG/SEC) FROM	TO	SC.FACTOR MV/DEG/SEC	NULL DEG/SEC	OFFSET MV	RMS ERROR DEG/SEC
5.	50.	103.196	-4.158	-429.1	4.118
-5.	-50.	103.392	-4.320	-446.7	4.279
5.	-50.	103.553	-4.252	-440.3	4.211

RATE DEG/SEC	VOLTS MV	ACT.ERROR DEG/SEC	FL.SC.ERROR PER-CENT
0.	-425.	-0.148	-0.29
5.	87.	-0.092	-0.18
10.	600.	-0.046	-0.09
15.	1120.	-0.066	-0.13
20.	1637.	-0.060	-0.12
30.	2667.	-0.007	-0.01
40.	3697.	0.046	0.09
50.	4731.	0.061	0.12
0.	-441.	0.006	0.01
-5.	-965.	0.066	0.13
-10.	-1484.	0.078	0.15
-15.	-1994.	0.003	0.00
-20.	-2514.	0.024	0.04
-30.	-3546.	-0.009	-0.01
-40.	-4583.	0.004	0.00
-50.	-5618.	-0.000	-0.00
0.	-450.	0.093	0.18

NOTE: The computer program used a least squares curve fitting method to compute the best straight line through the points and then computed linearity based on deviation from this straight line and the full scale input of 50^{o}/sec.

TABLE 7. LINEARITY AND SCALE FACTOR DATA - UNIT 1 FUNCTIONAL TEST SET 2

RATES (DEG/SEC) FROM	TO	SC.FACTOR MV/DEG/SEC	NULL DEG/SEC	OFFSET MV	RMS ERROR DEG/SEC
5.	50.	102.447	1.603	164.2	1.587
-5.	-50.	102.182	1.607	164.2	1.591
5.	-50.	102.315	1.636	167.4	1.620

RATE DEG/SEC	VOLTS MV	ACT.ERROR DEG/SEC	FL.SC.ERROR PER-CENT
0.	166.	0.014	0.02
5.	675.	0.039	0.07
10.	1188.	0.025	0.05
15.	1703.	-0.007	-0.01
20.	2215.	-0.011	-0.02
30.	3237.	-0.000	-0.00
40.	4261.	-0.008	-0.01
50.	5287.	-0.036	-0.07
0.	166.	0.008	0.01
-5.	-345.	0.013	0.02
-10.	-857.	0.012	0.02
-15.	-1371.	0.036	0.07
-20.	-1879.	0.001	0.00
-30.	-2901.	-0.009	-0.01
-40.	-3924.	-0.011	-0.02
-50.	-4944.	-0.042	-0.08
0.	171.	-0.034	-0.06

NOTE: The computer program used a least squares curve fitting method to compute the best straight line through the points and then computed linearity based on deviation from this straight line and the full scale input of 50^{o}/sec.

TABLE 8. LINEARITY AND SCALE FACTOR DATA - UNIT 2 FUNCTIONAL TEST SET 1

RATES (DEG/SEC) FROM	TO	SC.FACTOR MV/DEG/SEC	NULL DEG/SEC	OFFSET MV	RMS ERROR DEG/SEC
5.	50.	103.333	-1.256	-129.8	1.244
-5.	-50.	102.835	-1.190	-122.3	1.179
5.	-50.	102.974	-1.166	-120.0	1.155

RATE DEG/SEC	VOLTS MV	ACT.ERROR DEG/SEC	FL.SC.ERROR PER-CENT
0.	-131.	0.106	0.21
5.	387.	0.075	0.15
10.	903.	0.064	0.12
15.	1421.	0.034	0.06
20.	1937.	0.023	0.04
30.	2968.	0.003	0.00
40.	4004.	-0.049	-0.09
50.	5037.	-0.081	-0.16
0.	-129.	0.086	0.17
-5.	-643.	0.078	0.15
-10.	-1154.	0.040	0.08
-15.	-1659.	-0.046	-0.09
-20.	-2173.	-0.054	-0.10
-30.	-3204.	-0.051	-0.10
-40.	-4234.	-0.048	-0.09
-50.	-5270.	0.011	0.02
0.	-100.	-0.194	-0.38

NOTE: The computer program used a least squares curve fitting method to compute the best straight line through the points and then computed linearity based on deviation from this straight line and the full scale input of 50°/sec.

TABLE 9. LINEARITY AND SCALE FACTOR DATA - UNIT 2 FUNCTIONAL TEST SET 2

RATES (DEG/SEC) FROM	TO	SC.FACTOR MV/DEG/SEC	NULL DEG/SEC	OFFSET MV	RMS ERROR DEG/SEC
5.	50.	101.570	0.226	23.0	0.224
-5.	-50.	101.414	0.203	20.6	0.201
5.	-50.	101.527	0.233	23.7	0.232

RATE DEG/SEC	VOLTS MV	ACT.ERROR DEG/SEC	FL.SC.ERROR PER-CENT
0.	20.	0.036	0.07
5.	530.	0.013	0.02
10.	1040.	-0.009	-0.01
15.	1546.	0.006	0.01
20.	2055.	-0.007	-0.01
30.	3068.	0.015	0.03
40.	4089.	-0.041	-0.08
50.	5100.	0.000	0.00
0.	23.	0.007	0.01
-5.	-487.	0.030	0.06
-10.	-993.	0.014	0.02
-15.	-1500.	0.007	0.01
-20.	-2007.	0.001	0.00
-30.	-3023.	0.008	0.01
-40.	-4037.	-0.003	-0.00
-50.	-5049.	-0.035	-0.07
0.	26.	-0.022	-0.04

NOTE: The computer program used a least squares curve fitting method to compute the best straight line through the points and then computed linearity based on deviation from this straight line and the full scale input of 50^{o}/sec.

TABLE 10. LINEARITY AND SCALE FACTOR DATA - UNIT 3 FUNCTIONAL TEST SET 1

RATES (DEG/SEC) FROM	TO	SC.FACTOR MV/DEG/SEC	NULL DEG/SEC	OFFSET MV	RMS ERROR DEG/SEC
5.	50.	113.283	-2.224	-251.9	2.204
-5.	-50.	112.548	-2.183	-245.7	2.164
5.	-50.	112.824	-2.126	-239.9	2.108

RATE DEG/SEC	VOLTS MV	ACT.ERROR DEG/SEC	FL.SC.ERROR PER-CENT
0.	-252.	0.106	0.21
5.	313.	0.090	0.18
10.	879.	0.077	0.15
15.	1446.	0.056	0.11
20.	2014.	0.022	0.04
30.	3152.	-0.063	-0.12
40.	4280.	-0.061	-0.12
50.	5409.	-0.068	-0.13
0.	-250.	0.088	0.17
-5.	-802.	-0.014	-0.02
-10.	-1378.	0.091	0.18
-15.	-1937.	0.041	0.08
-20.	-2495.	-0.012	-0.02
-30.	-3620.	-0.041	-0.08
-40.	-4746.	-0.061	-0.12
-50.	-5875.	-0.055	-0.11
0.	-230.	-0.088	-0.17

NOTE: The computer program used a **least squares** curve fitting method to compute the best straight line through the points and then computed linearity based on deviation from this straight line and the full scale input of 50^{o}/sec.

TABLE 11. LINEARITY AND SCALE FACTOR DATA - UNIT 3 FUNCTIONAL TEST SET 2

RATES (DEG/SEC) FROM	TO	SC.FACTOR MV/DEG/SEC	NULL DEG/SEC	OFFSET MV	RMS ERROR DEG/SEC
5.	50.	95.076	-3.927	-373.3	3.866
-5.	-50.	95.214	-4.014	-382.2	3.972
5.	-50.	95.276	-3.982	-379.4	3.941

RATE DEG/SEC	VOLTS MV	ACT.ERROR DEG/SEC	FL.SC.ERROR PER-CENT
0.	-374.	-0.052	-0.10
5.	103.	-0.066	-0.13
10.	580.	-0.075	-0.15
15.	1035.	0.153	0.30
20.	1541.	-0.156	-0.31
30.	2480.	-0.019	-0.03
40.	3432.	-0.004	-0.00
50.	4377.	0.077	0.15
0.	-378.	-0.015	-0.03
-5.	-855.	-0.001	-0.00
-10.	-1334.	0.018	0.03
-15.	-1808.	-0.001	-0.00
-20.	-2287.	0.020	0.04
-30.	-3250.	0.128	0.25
-40.	-4187.	-0.037	-0.07
-50.	-5140.	-0.034	-0.06
0.	-387.	0.026	0.05

NOTE: The computer program used a least squares curve fitting method to compute the best straight line through the points and then computed linearity based on deviation from this straight line and the full scale input of 50°/sec.

TABLE 12. LINEARITY AND SCALE FACTOR DATA - UNIT 4 FUNCTIONAL TEST SET 1

RATES (DEG/SEC) FROM	TO	SC.FACTOR MV/DEG/SEC	NULL DEG/SEC	OFFSET MV	RMS ERROR DEG/SEC
5.	50.	103.381	1.220	126.1	1.208
-5.	-50.	103.485	1.212	125.4	1.201
5.	-50.	103.443	1.204	124.5	1.192

RATE DEG/SEC	VOLTS MV	ACT.ERROR DEG/SEC	FL.SC.ERROR PER-CENT
0.	124.	0.005	0.01
5.	643.	-0.011	-0.02
10.	1159.	-0.001	-0.00
15.	1676.	0.002	0.00
20.	2195.	-0.014	-0.02
30.	3230.	-0.020	-0.04
40.	4260.	0.022	0.04
50.	5295.	0.017	0.03
0.	125.	-0.004	-0.00
-5.	-389.	-0.035	-0.07
-10.	-912.	0.020	0.04
-15.	-1428.	0.009	0.01
-20.	-1942.	-0.022	-0.04
-30.	-2982.	0.031	0.06
-40.	-4013.	-0.001	-0.00
-50.	-5048.	0.003	0.00
0.	125.	-0.004	-0.00

NOTE: The computer program used a least squares curve fitting method to compute the best straight line through the points and then computed linearity based on deviation from this straight line and the full scale input of 50°/sec.

TABLE 13. LINEARITY AND SCALE FACTOR DATA - UNIT 4 FUNCTIONAL TEST SET 2

RATES (DEG/SEC) FROM	TO	SC.FACTOR MV/DEG/SEC	NULL DEG/SEC	OFFSET MV	RMS ERROR DEG/SEC
5.	50.	99.670	1.947	194.1	1.928
-5.	-50.	99.571	1.962	195.4	1.942
5.	-50.	99.602	1.967	195.9	1.947

RATE DEG/SEC	VOLTS MV	ACT.ERROR DEG/SEC	FL.SC.ERROR PER-CENT
0.	189.	0.062	0.12
5.	689.	0.050	0.10
10.	1194.	-0.020	-0.04
15.	1691.	-0.009	-0.01
20.	2187.	0.010	0.02
30.	3184.	0.000	0.00
40.	4180.	0.000	0.00
50.	5178.	-0.019	-0.03
0.	195.	0.009	0.01
-5.	-303.	0.015	0.03
-10.	-800.	-0.000	-0.00
-15.	-1296.	-0.012	-0.02
-20.	-1797.	0.009	0.01
-30.	-2791.	-0.011	-0.02
-40.	-3787.	-0.011	-0.02
-50.	-4784.	-0.001	-0.00
0.	198.	-0.025	-0.05

NOTE: The computer program used a least squares curve fitting method to compute the best straight line through the points and then computed linearity based on deviation from this straight line and the full scale input of 50°/sec.

TABLE 14. CROSS AXIS SENSITIVITY

Functional Test Set No.	Unit No.	Table Pickoff Voltage	Input Rate About Axis 1 RMS Canceller Output	Input Rate About Axis 2 RMS Canceller Output	Input Rate About Axis 3 RMS Canceller Output
1	1	2.500 ±.025 vrms	3.570	.012	.014
2	1	2.500 ±.025 vrms	3.450	.0203	.013
3	1	2.500 ±.025 vrms	3.49	.034	.016
4	1	2.500 ±.025 vrms	3.507	.018	.029
1	2	2.500 ±.025 vrms	3.493	.0064	.0345
2	2	2.500 ±.025 vrms	3.387	.013	.032
1	3	2.500 ±.025 vrms	3.472	.0063	.0092
2	3	2.500 ±.025 vrms	3.215	.0050	.012
3	3	2.500 ±.025 vrms	3.369	.036	.035
4	3	2.500 ±.025 vrms	3.22	.019	.015
1	4	2.500 ±.025 vrms	3.51	.0063	.0063
2	4	2.500 ±.025 vrms	3.374	.023	.0065
3	4	2.500 ±.025 vrms	3.403	.0072	.0274
4	4	2.500 ±.025 vrms	3.361	.025	.016

NOTES: 1(a) Axis 1 is sensitive axis of unit.
(b) Axis 2 DRIVE direction of beam (vertical to package)
(c) Axis 3 is in beam readout direction (in direction of connector)

2 INPUT RATE = 37°/SEC PEAK

TABLE 15. UNIT 1 TEMPERATURE DATA

Temperature C°	Maximum Uncancelled Output from Initial Null (Absolute Value) vdc	Settled Uncancelled Output from Initial Null (Absolute Value) vdc	Maximum Change In Cancelled Output During Temperature Change vdc	
+20	-.250*	-.250	+.025	Before Environmental Test Set 1
+45	-.350	-.250	-.100	
+70	-.100	-.250	-.050	
+45	-.500	-.300	0	
+20	-.600	-.400	0	
45	-.450	-.050	+.025	
70	-.200	-.100	0	
45	-.250	-.100	0	
20	-.300	----	----	
20	+.200*	-.060	0	After Environmental Test Set 1
45	+.160	+.060	0	
70	+.240	+.240	0	
45	+.400	+.100	0	
20	+.200	+.100	0	
45	+.200	+.060	0	
+20	+.253*	----	----	Before Environmental Test Set 2
+70	-.197	-.197	-.004	
+45	-.347	-.122	-.007	
+20	-.172	+.128	0	
+45	-.072	-.072	-.003	
+70	-.172	-.147	-.007	
+45	-.322	-.156	-.007	
+20	-.196	+.284	-.003	
+45	-.096	-.076	-.005	
+70	-.106	+.105	0	
+20	+.251*	----	----	After Environmental Test Set 2
+45	-.046	-.046	0	
+70	-.148	-.138	+.003	
+45	-.288	-.148	0	
+20	-.178	-.008	+.003	
+45	-.138	-.073	+.003	
+70	-.133	-.113	+.005	
+45	-.268	-.110	+.007	
+20	-.148	-.003	+.005	
+45	-.133	-.063	+.007	
+70	-.118	-.115	+.002	

*Initial Null

TABLE 16. UNIT 2 TEMPERATURE DATA

Temperature °C	Maximum Uncancelled Output From Initial Null (Absolute Value) vdc	Settled Uncancelled Output From Initial Null (Absolute Value) vdc	Maximum Change In Cancelled Output During Temperature Change vdc	
20	0*	0	-.005	Before Environmental Test Set 1
45	+ .300	.300	0	
70	+1.15	1.1	-.005	
45	+ .400	+ .400	0	
20	- .050	0	0	
45	+ .350	+ .350	+.005	
70	+ .600	+ .600	+.005	
45	+ .250	+ .350	-.020	
20	- .050	0	-.020	
+20	- .150 *	- .150	0	After Environmental Test Set 1
+45	- .450	- .500	0	
+70	- .800	- .800	0	
+45	- .350	- .350	0	
+20	- .150	- .350	0	

* Initial Null

Note: Unit No. 2 failed before functional test sets after heat sterilization

TABLE 17. UNIT 3 TEMPERATURE DATA

Temperature °C	Maximum Uncancelled Output from Initial Null (Absolute Value) vdc	Settled Uncancelled Output from Initial Null (Absolute Value) vdc	Maximum Change In Cancelled Output During Temperature Change vdc	
20	-.150 *	-.150	0	Before Environmental Test Set 1
45	-.050	-.075	0	
70	+.025	-.375	+.01	
45	-.350	-.250	0	
20	-.400	-.300	-.005	
45	-.250	-.200	+.005	
70	-.150	-.300		
45	-.360	-.280	-.005	
20	-.450	-.280	-.005	
20	-.400*	-.360	0	After Environmental Test Set 1
45	-.320	-.300	0	
70	-.440	-.440	0	
45	-.600	-.550	0	
20	-.600	-.400	0	
45	-.380	-.360	0	
70	-.320	-.380	0	
45	-.520	-.420	0	
20	-.500	-.380	0	
+20	-.460*	----	----	Before Environmental Test Set 2
+70	-.285	-.285	0	
+45	-.285	-.360	0	
+20	-.360	-.435	0	
+45	-.310	-.335	0	
+70	-.310	-.310	0	
+45	-.310	-.344	0	
+20	-.304	-.324	0	
+45	-.264	-.324	0	
+70	-.294	-.324	0	
+20	-.593*	----	----	After Environmental Test Set 2
+45	-.433	-.473	0	
+70	-.290	-.290	+.013	
+45	-.060	-.350	+.005	
+20	-.200	-.340	0	
+45	-.395	-.330	0	
+70	-.375	-.280	-.003	
+45	-.355	-.340	0	
+20	-.195	-.220	0	
+45	-.270	-.290	+.003	
+70	-.220	-.279	+.003	

*Initial Null

TABLE 18. UNIT 4 TEMPERATURE DATA

Temperature °C	Maximum Uncancelled Output from Initial Null (Absolute Value) vdc	Settled Uncancelled Output from Initial Null (Absolute Value) vdc	Maximum Change In Cancelled Output During Temperature Change vdc	
20	+.200*	+.150	0	Before Environmental Test Set 1
45	+.250	+.250	0	
70	+.600	+.550	+.005	
45	+.100	+.250	0	
20	+.100	+.200	0	
45	+.200	+.200	0	
70	+.500	+.500	0	
45	+.200	+.250	0	
20	+.100	+.200	0	
20	+.300*	+.300	0	After Environmental Test Set 1
45	+.525	+.525	0	
70	+.600	+.500	0	
45	+.200	+.300	0	
20	+.050	+.150	0	
45	+.350	+.200	0	
70	+.400	+.400	0	
45	+.150	+.250	0	
20	+.274*	----	----	Before Environmental Test Set 2
70	+.574	+.574	-.007	
45	+.099	+.149	-.010	
20	-.001	+.109	-.007	
45	+.074	+.174	-.007	
70	+.649	+.649	-.007	
45	+.229	+.249	-.010	
20	+.089	+.129	-.010	
45	+.064	+.229	-.010	
70	+.049	+.186	-.010	
20	+.545	----	----	After Environmental Test Set 2
45	+.355	+.495	+.005	
70	+.700	+.665	0	
45	+.305	+.370	-.005	
20	+.325	+.255	+.003	
45	+.440	+.385	Recorder Pen Stopped Working	
70	**	**		
45	**	+.615		
20	+.223	+.343		
45	+.563	+.563		
70	+.793	+.783		

*Initial Null
**Trace Went off Scale In + Direction.

TABLE 19. NULL STABILITY - UNCANCELLED OUTPUT
(Data is the standard deviation from the computed mean)

		Long Term	Short Term
Unit No. 1			
(a)	Before Environmental Test Set No. 1	$.34^{o}$/sec	0.33^{o}/sec
(b)	After Environmental Test Set No. 1	.24	0.22
After ETO and Heat Sterilization:			
(a)	Before Environmental Test Set No. 2	$.085^{o}$/sec	.085
(b)	After Environmental Test Set No. 2	$.05^{o}$/sec	$.051^{o}$/sec
Unit No. 2			
(a)	Before Environmental Test Set No. 1	.20	0.13
(b)	After Environmental Test Set No. 1	—	—
After ETO and Heat Sterilization:			
(a)	Before Environmental Test Set No. 2	No Data	No Data
(b)	After Environmental Test Set No. 2		
Unit No. 3			
(a)	Before Environmental Test Set No. 1	.13	0.13
(b)	After Environmental Test Set No. 1	.093	0.092
After ETO and Heat Sterilization:			
(a)	Before Environmental Test Set No. 2	$.28^{o}$/sec	$.29^{o}$/sec
(b)	After Environmental Test Set No. 2	$.24^{o}$/sec	$.023^{o}$/sec
Unit No. 4			
(a)	Before Environmental Test Set No. 1	.22	0.21
(b)	After Environmental Test Set No. 1	.16	0.15
After ETO and Heat Sterilization:			
(a)	Before Environmental Test Set No. 2	$.29^{o}$/sec	0.32^{o}/sec
(b)	After Environmental Test Set No. 2	0.30^{o}/sec	$.292^{o}$/sec

TABLE 20. SUPPLY VOLTAGE SENSITIVITY

	Maximum Change of Uncancelled Output From the Output With ± 12 vdc Applied	
Unit 1	53 MV	Before environmental test set 1
	37 MV	After environmental test set 1
Unit 2	24 MV	Before environmental test set 1
	32 MV	After environmental test set 1
Unit 3	52 MV	Before environmental test set 1
	27 MV	After environmental test set 1
Unit 4	36 MV	Before environmental test set 1
	34 MV	After environmental test set 1

Change of cancelled outputs was less than 5.6 MV for all units and all cases of supply voltage.

	Maximum Change of Uncancelled Output From the Output With ±12 vdc Applied	
Unit 1	7 MV	Before Environmental test set 2
	23 MV	After environmental test set 2
Unit 2	—	
	—	
Unit 3	107 MV	Before environmental test set 2
	90 MV	After environmental test set 2
Unit 4	60 MV	Before environmental test set 2
	45 MV	After environmental test set 2

Change of cancelled output was less than 4 MV for all units tested and all cases of supply voltage.

TABLE 21. NULL AND SELF TEST DATA AFTER EACH 5g VIBRATION TEST IN EACH PLANE

(a) = uncancelled null
(b) = uncancelled output with self test activated

Unit No.	Plane of 5g Vibration	Environmental Test Set 1 vdc	Environmental Test Set 2 vdc
1	Drive:	(a) = -0.158	
		(b) = +4.121	
	Readout:	(a) = -0.142	
		(b) = +4.140	
	Axial:	(a) = -0.181	+ .245
		(b) = +4.096	+4.476
2	Drive:	(a) = +0.075	
		(b) = +4.462	
	Readout:	(a) = +0.133	NO
		(b) = +4.524	DATA
	Axial:	(a) = +0.100	
		(b) = +4.496	
3	Drive:	(a) = -0.206	- .440
		(b) = +4.068	+3.412
	Readout:	(a) = -0.199	- .485
		(b) = +4.067	+3.393
	Axial:	(a) = -0.260	- .453
		(b) = +3.946	+3.418
* 4	Drive:	(a) = +0.229	+ .242
		(b) = +5.222	+5.163
	Readout:	(a) = +0.254	+ .456
		(b) = +5.252	+5.375
	Axial:	(a) = +0.199	+ .337
		(b) = +5.185	+5.245

*Data for this unit is that after replacement of second defective damping flat pack

TABLE 22. NULL AND SELF TEST DATA AFTER EACH 2 MINUTE RANDOM VIBRATION TEST IN EACH AXIS

(a) = uncancelled null
(b) = uncancelled output with self test activated.

Unit No.	Plane of 0.5 g^2/Hz (20-2000 Hz Bandwidth) Random Vibration	Environmental Test Set 1 vdc	Environmental Test Set 2 vdc
1	Drive:	(a) = -0.327	- .195
		(b) = +3.859	+3.893
	Readout:	(a) = -0.325	- .073
		(b) = +3.891	+4.062
	Axial:	(a) = -0.303	- .043
		(b) = +3.903	+4.088
2	Drive:	(a) = -0.160	
		(b) = +4.235	
	Readout:	(a) = +0.207	
		(b) = +4.553	
	Axial:	(a) = +0.160	
		(b) = +4.512	
3	Drive:	*(a) = -0.060	- .242
		(b) = +4.046	+3.380
	Readout:	(a) = -0.086	- .321
		(b) = +4.037	+3.341
	Axial:	(a) = -0.150	- .236
		(b) = +3.949	+3.415
4	Drive:	(a) = +0.131	+ .313
		(b) = +5.022	+4.971
	Readout:	(a) = +0.123	+ .171
		(b) = +5.017	+4.936
	Axial:	(a) = +0.126	+ .055
		(b) = +4.981	+4.822

*Note: A broken wire to pin 4 of the beam on unit no. 3 occurred during this test

TABLE 23. NULL AND SELF TEST DATA AFTER SHOCK TEST OF 100 g-1 MILLISECOND, HALF SINE 2 DROPS IN EACH DIRECTION OF THE 3 PRINCIPAL AXES (12 DROPS TOTAL)

(a) = uncancelled null
(b) = uncancelled output with self test activated

Unit No.	Direction of Drops	Environmental Test Set 1 Reading After Shock vdc	Environmental Test Set 2 vdc Reading Before Shock	Reading After Shock
1	Drive:	(a) = -0.348	a. + .181	+ .099
		(b) = +3.765	b. +4.393	+4.251
	Readout:	(a) = -0.419	+0.168	+ .096
		(b) = +3.658	+4.384	+4.242
	Axial:	(a) = -0.389	+0.023	+ .121
		(b) = +3.683	+4.071	+4.233
2	Drive:	(a) = -0.079	NO DATA	NO DATA
		(b) = +4.259		
	Readout:	(a) = -0.101		
		(b) = +4.206		
	Axial:	(a) = -0.200		
		(b) = +4.037		
3	Drive:	(a) = -0.464	- .397	- .265
		(b) = +3.617	+3.207	+3.373
	Readout:	(a) = -0.139	- .256	- .257
		(b) = +3.816	+3.351	+3.382
	Axial:	(a) = -0.141	- .689	- .236
		(b) = +3.828	+2.873	+3.406
4	Drive:	(a) = -0.084	+ .074	+ .381
		(b) = +4.802	+4.785	+5.123
	Readout:	(a) = -0.133	+ .138	+ .382
		(b) = +4.730	+4.991	+5.132
	Axial:	(a) = +0.128	+ .126	+ .351
		(b) = +4.848	+4.782	+5.093

TABLE 24. NULL AND SELF TEST DATA AFTER 45 g STEADY STATE ACCELERATION TEST FOR 1 MINUTE IN EACH DIRECTION ALONG EACH OF THE 3 PRINCIPAL AXES OF THE UNIT

(a) = uncancelled null
(b) = uncancelled output with self test activated

Unit No.	Direction of Acceleration	Environmental Test Set 1 vdc	Environmental Test Set 2 vdc
1	Drive:	(a) = +0.115	+ .208
		(b) = +4.26	+4.32
	Readout:	(a) = +0.118	+ .205
		(b) = +4.26	+4.32
	Axial:	(a) = +0.125	+ .206
		(b) = +4.26	+4.32
2	Drive:	(a) = -0.014	
		(b) = +4.21	
	Readout:	(a) = -0.010	
		(b) = +4.20	
	Axial:	(a) = -0.033	
		(b) = +4.15	
3	Drive:	(a) = -0.453	- .615
		(b) = +3.46	+2.99
	Readout:	(a) = -0.452	- .566
		(b) = +3.46	+3.08
	Axial:	(a) = -0.435	- .595
		(b) = +4.37	+3.04
4	Drive:	(a) = +0.102	+ .562
		(b) = +4.88	+5.27
	Readout:	(a) = +0.110	+ .583
		(b) = +4.89	+5.29
	Axial:	(a) = +0.101	+ .571
		(b) = +4.88	+5.27

TABLE 25. NULL AND SELF TEST DATA BEFORE AND AFTER THE ACOUSTIC NOISE TEST

(a) = uncancelled null
(b) = uncancelled output with self test activated

Unit No.	Pre-Acoustic Test Data vdc	Environmental Test Set 1 (Acoustic) vdc	Pre-Acoustic Test Data vdc	Environmental Test Set 2 (Acoustic) vdc
1	(a) = +0.159	+0.050	(a) + .292	+ .206
	(b) = +4.31	+4.33	(b) +4.38	+4.45
2	(a) = -0.115	-0.258		
	(b) = +4.09	+4.06		
3	(a) = -0.482	-0.578	- .386	- .392
	(b) = +3.45	+3.40	+3.27	+3.28
4	(a) = +0.037	-0.041	+ .454	+ .310
	(b) = +4.84	+4.85	+5.21	+5.08

TABLE 26. LINEARITY AND SCALE FACTOR DATA - UNIT 1 FUNCTIONAL TEST SET 3

RATES (DEG/SEC) FROM	TO	SC.FACTOR MV/DEG/SEC	NULL DEG/SEC	OFFSET MV	RMS ERROR DEG/SEC
5.	50.	102.768	2.347	241.2	2.324
-5.	-50.	104.426	1.644	171.7	1.629
5.	-50.	104.624	1.781	186.3	1.777

RATE DEG/SEC	VOLTS MV	ACT.ERROR DEG/SEC	FL.SC.ERROR PER-CENT
0.	239.	-0.504	-1.00
5.	756.	-0.446	-0.89
10.	1272.	-0.376	-0.75
15.	1781.	-0.241	-0.48
20.	2294.	-0.144	-0.28
30.	3323.	0.019	0.03
40.	4351.	0.194	0.38
50.	5382.	0.339	0.67
0.	181.	0.046	0.09
-5.	-347.	0.098	0.19
-10.	-872.	0.115	0.23
-15.	-1393.	0.095	0.19
-20.	-1923.	0.161	0.32
-30.	-2963.	0.101	0.20
-40.	-4005.	0.061	0.12
-50.	-5047.	0.020	0.04

NOTE: The computer program used a least squares curve fitting method to compute the best straight line through the points and then computed linearity based on deviation from this straight line and the full scale input of 50°/sec.

TABLE 27. LINEARITY AND SCALE FACTOR DATA - UNIT 1 FUNCTIONAL TEST SET 4

RATES (DEG/SEC) FROM	TO	SC.FACTOR MV/DEG/SEC	NULL DEG/SEC	OFFSET MV	RMS ERROR DEG/SEC
5.	50.	102.945	2.113	217.6	2.093
-5.	-50.	103.126	2.037	210.0	2.017
5.	-50.	103.147	2.051	211.6	2.032

RATE DEG/SEC	VOLTS MV	ACT.ERROR DEG/SEC	FL.SC.ERROR PER-CENT
0.	219.	-0.071	-0.14
5.	733.	-0.054	-0.10
10.	1248.	-0.047	-0.09
15.	1761.	-0.020	-0.04
20.	2276.	-0.013	-0.02
30.	3305.	0.010	0.02
40.	4335.	0.024	0.04
50.	5366.	0.029	0.05
0.	210.	0.015	0.03
-5.	-307.	0.028	0.05
-10.	-821.	0.011	0.02
-15.	-1336.	0.004	0.00
-20.	-1852.	0.006	0.01
-30.	-2883.	0.002	0.00
-40.	-3915.	0.007	0.01
-50.	-4947.	0.012	0.02

NOTE: The computer program used a least squares curve fitting method to compute the best straight line through the points and then computed linearity based on deviation from this straight line and the full scale input of 50^{o}/sec.

TABLE 28. LINEARITY AND SCALE FACTOR DATA - UNIT 3 FUNCTIONAL TEST SET 3

RATES (DEG/SEC) FROM	TO	SC.FACTOR MV/DEG/SEC	NULL DEG/SEC	OFFSET MV	RMS ERROR DEG/SEC
5.	50.	101.054	-2.873	-290.3	2.846
-5.	-50.	99.683	-2.198	-219.1	2.177
5.	-50.	99.315	-2.397	-238.0	2.384

RATE DEG/SEC	VOLTS MV	ACT.ERROR DEG/SEC	FL.SC.ERROR PER-CENT
0.	-351.	1.143	2.28
5.	201.	0.578	1.15
10.	722.	0.324	0.64
15.	1236.	0.157	0.31
20.	1743.	0.052	0.10
30.	2731.	0.104	0.20
40.	3751.	-0.165	-0.33
50.	4762.	-0.345	-0.69
0.	-228.	-0.101	-0.20
-5.	-724.	-0.107	-0.21
-10.	-1222.	-0.093	-0.18
-15.	-1714.	-0.139	-0.27
-20.	-2202.	-0.225	-0.45
-30.	-3201.	-0.166	-0.33
-40.	-4204.	-0.067	-0.13
-50.	-5213.	0.091	0.18

NOTE: The computer program used a least squares curve fitting method to compute the best straight line through the points and then computed linearity based on deviation from this straight line and the full scale input of 50^{o}/sec.

TABLE 29. LINEARITY AND SCALE FACTOR DATA - UNIT 3 FUNCTIONAL TEST SET 4

RATES (DEG/SEC) FROM	TO	SC.FACTOR MV/DEG/SEC	NULL DEG/SEC	OFFSET MV	RMS ERROR DEG/SEC
5.	50.	95.378	-6.199	-591.3	6.134
-5.	-50.	95.776	-6.306	-603.9	6.240
5.	-50.	95.764	-6.291	-602.5	6.225

RATE DEG/SEC	VOLTS MV	ACT.ERROR DEG/SEC	FL.SC.ERROR PER-CENT
0.	-582.	-0.214	-0.42
5.	-111.	-0.132	-0.26
10.	363.	-0.081	-0.16
15.	837.	-0.031	-0.06
20.	1313.	-0.002	-0.00
30.	2269.	0.015	0.03
40.	3226.	0.021	0.04
50.	4178.	0.080	0.16
0.	-604.	0.015	0.03
-5.	-1083.	0.017	0.03
-10.	-1562.	0.019	0.03
-15.	-2040.	0.010	0.02
-20.	-2519.	0.012	0.02
-30.	-3478.	0.026	0.05
-40.	-4436.	0.030	0.06
-50.	-5392.	0.013	0.02

NOTE: The computer program used a least squares curve fitting method to compute the best straight line through the points and then computed linearity based on deviation from this straight line and the full scale input of 50^{o}/sec.

TABLE 30. LINEARITY AND SCALE FACTOR DATA - UNIT 4 FUNCTIONAL TEST SET 3

RATES (DEG/SEC) FROM	TO	SC.FACTOR MV/DEG/SEC	NULL DEG/SEC	OFFSET MV	RMS ERROR DEG/SEC
5.	50.	103.456	3.760	389.0	3.724
-5.	-50.	103.463	3.651	377.8	3.616
5.	-50.	103.626	3.699	383.3	3.663

RATE DEG/SEC	VOLTS MV	ACT.ERROR DEG/SEC	FL.SC.ERROR PER-CENT
0.	388.	-0.044	-0.08
5.	907.	-0.053	-0.10
10.	1419.	0.005	0.01
15.	1942.	-0.041	-0.08
20.	2462.	-0.059	-0.11
30.	3494.	-0.017	-0.03
40.	4525.	0.032	0.06
50.	5562.	0.025	0.05
0.	371.	0.119	0.23
-5.	-144.	0.089	0.17
-10.	-655.	0.020	0.04
-15.	-1171.	-0.000	-0.00
-20.	-1691.	0.017	0.03
-30.	-2724.	-0.013	-0.02
-40.	-3764.	0.022	0.04
-50.	-4795.	-0.028	-0.05

NOTE: The computer program used a least squares curve fitting method to compute the best straight line through the points and then computed linearity based on deviation from this straight line and the full scale input of 50^{o}/sec.

TABLE 31. LINEARITY AND SCALE FACTOR DATA - UNIT 4 FUNCTIONAL TEST SET 4

RATES (DEG/SEC) FROM	TO	SC.FACTOR MV/DEG/SEC	NULL DEG/SEC	OFFSET MV	RMS ERROR DEG/SEC
5.	50.	99.801	6.667	665.3	6.600
-5.	-50.	99.995	6.674	667.4	6.608
5.	-50.	99.867	6.649	664.0	6.583

RATE DEG/SEC	VOLTS MV	ACT.ERROR DEG/SEC	FL.SC.ERROR PER-CENT
0.	660.	0.040	0.08
5.	1161.	0.024	0.04
10.	1665.	-0.022	-0.04
15.	2168.	-0.059	-0.11
20.	2660.	0.014	0.02
30.	3657.	0.031	0.06
40.	4656.	0.027	0.05
5C.	5657.	0.004	0.00
0.	666.	-0.019	-0.03
-5.	167.	-0.022	-0.04
-10.	-332.	-0.026	-0.05
-15.	-830.	-0.039	-0.07
-20.	-1332.	-0.012	-0.02
-30.	-2333.	0.010	0.02
-40.	-3341.	0.103	0.20
-50.	-4326.	-0.033	-0.06

NOTE: The computer program used a least squares curve fitting method to compute the best straight line through the points and then computed linearity based on deviation from this straight line and the full scale input of 50^{o}/sec.

TABLE 32. NOMINAL PERFORMANCE TESTS AFTER EACH HEAT STERILIZATION CYCLE

(a) Self Test
(b) Scale Factor

(a) Self Test

Unit No.	Heat Cycle	1	2	3	4	5	6
		Uncancelled Output Volts dc					
1	Uncancelled Null	+.327	+0.282	+0.324	+0.254	+0.278	+0.280
	Uncancelled Null with Self Test Applied	+4.51	+4.418	+4.524	+4.397	+4.391	+4.392
2	Uncancelled Null	+0.195	+0.277	+0.660	+0.174	-0.127	-
	Uncancelled Null with Self Test Applied	+4.55	+4.85	+5.456	+4.305	+3.457	-
3	Uncancelled Null	-0.396	-0.226	+1.543	-0.377	-0.340	-0.241
	Uncancelled Null with Self Test Applied	+3.57	+3.981	+5.130	+3.886	+3.855	+3.93
4	Uncancelled Null	+0.371	+0.570	+0.650	+0.847	+0.637	+0.432
	Uncancelled Null with Self Test Applies	+5.192	+5.780	+5.826	+5.941	+5.696	+5.51

TABLE 32. NOMINAL PERFORMANCE TESTS AFTER EACH HEAT STERILIZATION CYCLE (Cont.)

(b) Scale Factor

Unit No.	Heat Cycle → / Input Rate Deg/Sec	1	2	3	4	5	6
		Uncancelled Output Volts dc					
1	0.00	+0.290	+0.249	+0.262	+0.254	+0.286	+0.270
	CW + 10.00+.01	+1.32	+1.289	+1.298	+1.295	+1.321	+1.310
	" + 50.00∓.05	+5.49	+5.438	+5.466	+5.464	+5.500	+5.479
	0.00	+0.286	+0.246	+0.259	+0.254	+0.286	+0.262
	CCW-10.00+.01	-0.754	-0.790	-0.780	-0.783	-0.751	-0.773
	" -50.00∓.05	-4.923	-4.947	-4.946	-4.954	-4.926	-4.953
2	0.00	+0.189	-1.569	+0.689	+0.179	+0.132	BEAM FAILURE
	+10.00+.01	+1.204	-0.480	+1.812	+1.224	+0.761	
	+50.00∓.05	+5.277	+3.859	+6.304	+5.420	+4.342	
	0.00	+0.188	-1.566	+0.693	+0.173	-0.135	
	-10.00+.01	-0.834	-2.652	-0.428	-0.880	-1.032	
	-50.00∓.05	-4.913	-6.996	-4.923	-5.074	-4.612	
3	0.00	-0.311	-0.182	-0.507	-0.356	-0.370	-0.240
	+10.00+.01	+0.645	+0.807	+0.492	+0.648	+0.628	+0.756
	+50.00∓.05	+4.463	+4.764	+4.481	+4.684	+4.666	+4.750
	0.00	-0.3106	-0.156	-0.508	-0.358	-0.382	-0.225
	-10.00+.01	-1.267	-1.156	-1.504	-1.367	-1.396	-1.220
	-50.00∓.05	-5.086	-5.076	-5.500	-5.408	-5.447	-5.231
4	0.00	+0.425	+0.548	+0.687	+0.869	+0.635	+0.422
	+10.00+.01	+1.462	+1.575	+1.723	+1.915	+1.671	+1.449
	+50.00∓.05	+5.516	+5.680	+5.856	+6.075	+5.824	+5.578
	0.00	+0.436	+0.523	+0.679	+0.878	+0.639	+0.412
	-10.00+.01	-0.588	-0.499	-0.357	-0.162	-0.392	-0.625
	-50.00∓.05	-4.662	-4.600	-4.509	-4.320	-4.547	-4.760

APPENDIX

GENERAL ELECTRIC

AVIONIC CONTROLS DEPARTMENT

TRAVELER: John Russell	PLACE VISITED: NASA/Langley — DATE: 1/22/70
ACCOMPANIED BY:	COPIES OF THIS REPORT TO: J. Eichler, R. Szczech, J. Hamill, R. Hamby, H. Cook, W. Schiller, R. D'Ambrosio, J. Callahan
OBJECT OF VISIT: Performing decontamination tests	DATE OF VISIT: 1/19 & 1/20

People Contacted:

J. Reid - Head, Navigation and Guidance Research Branch

J. Zanks - Head of ETO test facilities

H. Ricker - Mgr. Reliability Section

C. Husson - Micro Electronics Section Head

R. Stermer - Micro Electronics Section

TRIP REPORT

Purpose:

1. To deliver three VYRO units built under contract NAS1-8885 for the purpose of performing Ethylene Oxide (ETO) decontamination tests. Six cycles are required and at 30 hours per cycle the tests will be completed in about 2 weeks. The units will then be returned to GE at Binghamton via a GE representative on approximately February 2, 1970 for further testing to be performed here.

2. To show H. Ricker, C. Husson and R. Stermer one of the failed damping flatpacks.

Units no. 2, no. 3 and no. 4 were delivered on 1/19/70 by the writer. They were given a short electrical test just prior to being placed in the ETO chamber and all were found to operate properly. These three units were started on their first 30 hour ETO cycle at 9:15 AM on 1/19/70. Six cycles are required.

Next, the NASA representatives H. Ricker, C. Husson and, R. Stermer, and the writer inspected the open damping flatpack. Two chip capacitors were removed from the substrate by use of tweezers. These were observed on the bottom side. There appeared to be very little adherence of the gold-tin solder preform to the silver electrode.

As a result of this inspection a call was placed to Mepco in Morristown, N. J. and the following questions and answers were discussed with Mike Snyder of Mepco and Robert Stermer (NASA) and the writer.

a. Do they heat the whole substrate when bonding their chips down?
answer: Yes with a heat column to a temperature of 300° to 320°C.

b. What is the discoloration around the bond?
answer: Alpha 100 flux was used in the bonding operation and this is probably the cause of most of the discoloration.

c. Did they use a solder ball to perform the bonding?
answer: No they used an 80% gold 20% tine solder preform.

d. What was the procedure Mepco used in bonding down the capacitor chip.
answer: The pad on the circuit substrate that the capacitor is to be bonded to is gold with a glass fritt (type C5011 made by Alloys Unlimited). The gold-tin solder preform is put on top of the gold pad and then a small amount of the Alpha 100 flux is placed over the solder preform and gold pad. Then the silvered electrode of the capacitor is placed on top of the solder preform. The flux is then allowed to harden for a short time in air. Then the heat column is brought up to the melting point of the solder to make the bond, but no pressure is applied to the capacitor chip.

In the damping flatpack which was inspected at NASA there were no fillets of solder around the base of the silver electrodes of the capacitor chips indicating possibly not enough heat. However, it was also noted that when the capacitor chips were removed the gold pad under the chip was no longer present on the substrate.

GENERAL ELECTRIC

AVIONIC CONTROLS DEPARTMENT

TRAVELER:	PLACE VISITED:	DATE:
John N. Russell	Mepco, Inc.	2/3/70
ACCOMPANIED BY:	COPIES OF THIS REPORT TO: J Eichler, D Szczech J Hamill, R Hamby, H Cook, W Schiller, R D'Ambrosio, J Callahan, R Litynski, G Macko	
OBJECT OF VISIT: Discussion and failure analysis of	DATE OF VISIT:	

TRIP REPORT

the Mepco thick film flatpack failures on the VYRO program.

People Contacted: Mr. Francis (Bud) - their Chief Metallurgist
Mike Snyder - Electrical Engineer

Discussion: Two damping circuit flatpacks and one drive circuit flatpack were analyzed for failures. GE part nos are 106D1482P1(damping)& 106D1481P1 (drive) respectively. The first damping flatpack to be inspected was the pack that had been previously opened at GE. In this pack it had been previously determined that there was a bad bond to the silver electrode of a rather large (physically) NPO chip capacitor to the gold pad on the alumina substrate.

As a result of calls to Mepco previous to this trip Mr. Francis had inspected some of their first substrates of this circuit and he stated that the problem had been discovered on these substrates also. In general, the capacitor chips in these circuits had poor looking bonds to the gold pads in that the 80% Au, 20% Sn solder preform did not wet to the surface of the capacitor electrodes and the gold pad on the alumina substrate. There were no fillets visible at the junction between the gold pad and the silver electrode of the capacitors. It was stated by Mr. Francis that the problem was that the tin in the solder had dissolved the gold pad on the substrate due to either over heating during bonding or due to too prolonged heating during the bonding operation.

As a result of the investigation it was stated by Mr. Francis that the following items would be considered toward a solution of this problem:

1. Time control of heating during bonding of no more than 1-minute.
2. More precise temperature control
3. 100% visual inspection
4. 100% dynamometer check, with 250 gram limit, of each part.

As a result of this visit Mr. Francis is going to send the writer several samples of chip capacitors bonded to substrates that he feels will satisfy the NASA requirements.

On the second damping flatpack, the cover was removed and the cause of the short circuit between pin 26 and the case was determined to be a small piece or chip of solder that came from the solder sealing of the cover. The quality of the solder seal appears to be excellent, however, in sealing the cover to the flatpack a small solder preform is used and local heating applied to the area to be bonded. When the solder flows along the cover toward the inside of the flatpack it reaches a cooler portion of the cover (about 0.1 inch) and the solder does not adhere well to this portion of the cover. Thus during vibration chips of solder can break off the cover on the inside of the flatpack. This problem might be overcome by applying the local heating to a wider portion of the flatpack cover or by using a case and cover designed with a lip to avoid this problem entirely.

The last flatpack inspected was the drive flatpack. This was connected to our test jig to show the rate limiting in the output of the drive amplifier AR3. The cover was then removed and the circuit probed during operation in the test jig to determine more precisely where the problem was. The compensation capacitor for AR3 was removed by 2 applications of about 250 grams with a dynamometer. Its capacitance was measured to be about 24 pf. This capacitor was replaced with a 33 pf capacitor and the problem found to still exist. Then the input to the amplifier was disconnected and a sine wave applied to it. The output rate limiting was still present. From these investigations it was concluded that the problem was most likely in the LM101 chip. Incidentally, it was determined that all operational amplifier chips in the circuit were made by National Semiconductor through the ID registration marks observed on each by the writer.

It is the writers opinion that Mepco will investigate the possibility of checking the output slew rate capability of the LM101 chips before putting them in the circuit. However, this problem can be easily specified out of existence by one additional test required of Mepco on the completed circuit.

Vendor cooperation on working out these problems has been excellent up to this point.

GENERAL ELECTRIC
RESEARCH AND DEVELOPMENT CENTER
SCHENECTADY, NEW YORK

METALLOGRAPHIC UNIT

ELECTRON MICROPROBE ANALYSIS

File No. 986 MP

Date: May 18, 1970

To: H.T. Gregg

Rm: Johnson City

A lead titanite-lead zirconate crystal was removed from the bar; two pieces were mounted on a sample holder, a fractured edge and a side containing the whiskers.

X-ray spectra were taken from the solid state X-ray detector on the scanning electron microscope at three points across the crystal face (photo A) and four points across the fracture (photo B). The later face gave an uncontaminated spectra of the crystal. See Figure 1.

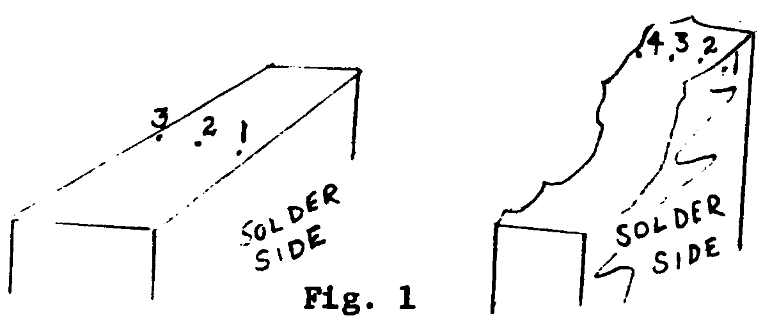

Fig. 1

Indium appeared to be present at least one half way across the crystal face from the solder edge. In comparison, no indium was detected on the fracture face.

Individual whiskers could not be analyzed because they were too thin or they melted under the electron beam.

Scanning electron micrographs of some whiskers are included at the end of this report.

Remarks

Analyst Carol F. Kirk

Approved by Eric Lifshin

METALLURGY AND CERAMICS LABORATORY
K-1, Room 2C24

Neg. No. 5,1 Mag. 850 X

Remarks

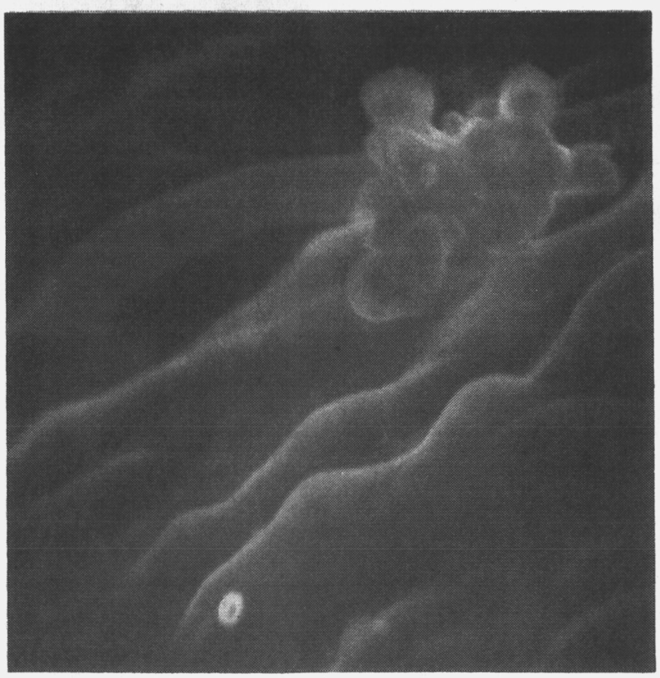

Neg. No. 6,1 Mag. 16,400 X

Remarks a melted whisker

Neg. No. 2,1 Mag. 500 X

Remarks

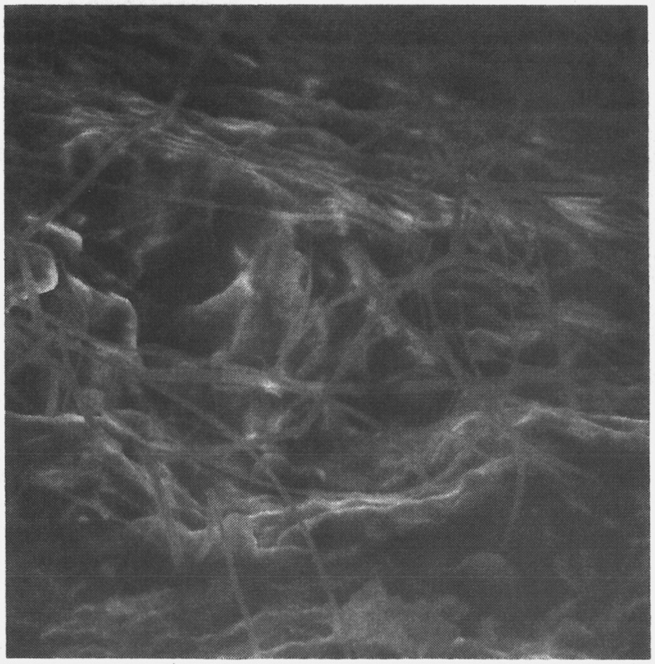

Neg. No. 2,2 Mag. 2000 X

Remarks

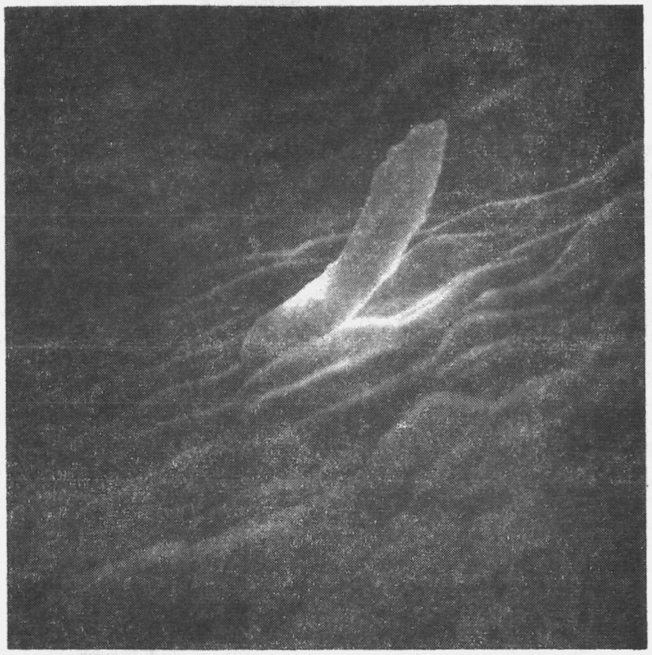

Neg. No. 4,1 Mag. 8200 X

Remarks

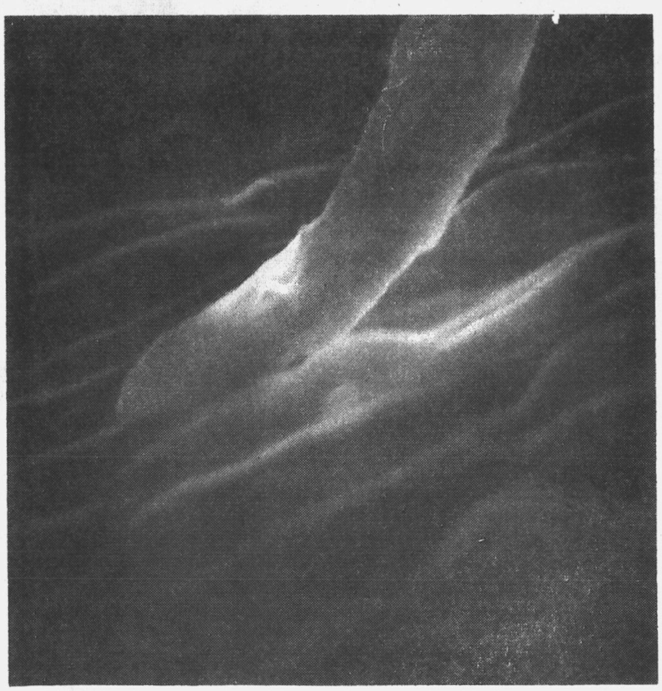

Neg. No. 4,2 Mag. 16,400 X

Remarks

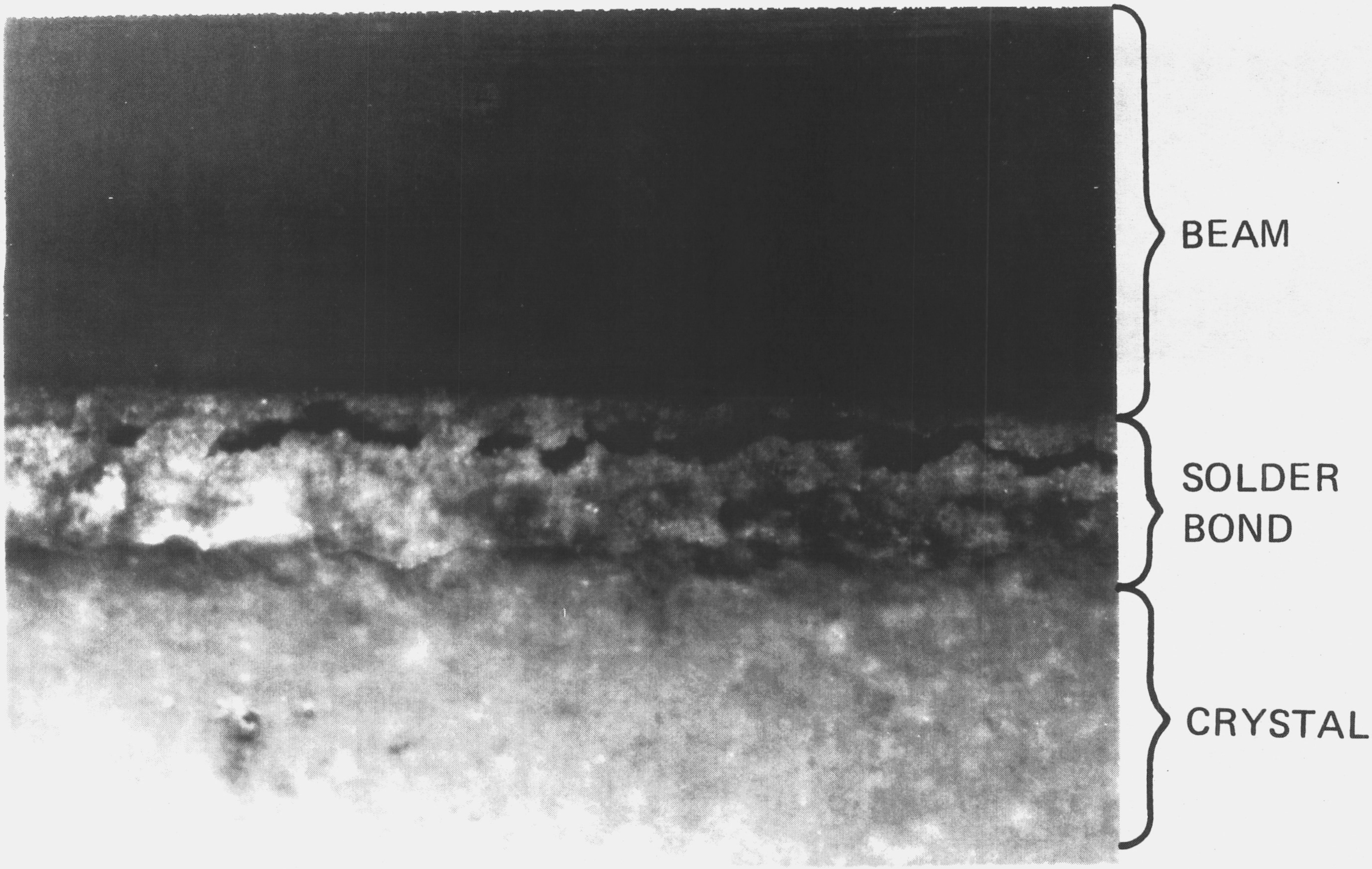
BEAM
SOLDER
BOND
CRYSTAL